International Scientific-Technical and Production Journal

The Paton WELDING JOURNAL

October 2008 # 10

English translation of the monthly «Avtomaticheskaya Svarka» (Automatic Welding) journal published in Russian since 1948

Founders: *E.O. Paton Electric Welding Institute of the NAS of Ukraine*
International Association «Welding»

Publisher: *International Association «Welding»*

Editor-in-Chief B.E.Paton

Editorial board:

Yu.S.Borisov I.A.Ryabtsev
A.Ya.Ishchenko V.F.Khorunov
B.V.Khitrovskaya I.V.Krivtsun
S.I.Kuchuk-Yatsenko
Yu.N.Lankin L.M.Lobanov
V.N.Lipodaev A.A.Mazur
V.I.Makhnenko I.K.Pokhodnya
O.K.Nazarenko K.A.Yushchenko
A.T.Zelnichenko

International editorial council:

N.P.Alyoshin (Russia)
U.Diltey (Germany)
Guan Qiao (China)
D. von Hofe (Germany)
V.I.Lysak (Russia)
N.I.Nikiforov (Russia)
B.E.Paton (Ukraine)
Ya.Pilarczyk (Poland)
P.Seyffarth (Germany)
G.A.Turichin (Russia)
Zhang Yanmin (China)
A.S.Zubchenko (Russia)

Promotion group:

V.N.Lipodaev, V.I.Lokteva
A.T.Zelnichenko (exec. director)
Translators:
I.N.Kutianova, T.K.Vasilenko,
V.F. Orets
PE «Melnik A.M.»
Editor
N.A.Dmitrieva
Electron galley:
I.S.Batasheva, T.Yu.Snegiryova

Address:
E.O. Paton Electric Welding Institute,
International Association «Welding»,
11, Bozhenko str., 03680, Kyiv, Ukraine
Tel.: (38044) 287 67 57
Fax: (38044) 528 04 86
E-mail: journal@paton.kiev.ua
http://www.nas.gov.ua/pwj

State Registration Certificate
KV 4790 of 09.01.2001

Subscriptions:
$324, 12 issues per year,
postage and packaging included.
Back issues available.

All rights reserved.
This publication and each of the articles contained herein are protected by copyright. Permission to reproduce material contained in this journal must be obtained in writing from the Publisher.
Copies of individual articles may be obtained from the Publisher.

CONTENTS

© PWI, International Association «Welding», 2008

50 YEARS OF ELECTRON BEAM WELDING AT THE E.O. PATON ELECTRIC WELDING INSTITUTE

Studies into the principles of building of the equipment for electron beam welding and capabilities of this welding method were started at the E.O. Paton Electric Welding Institute of the NAS of Ukraine in 1958 by the initiative and with the direct participation of Prof. Boris E. Paton. The first laboratory machine having a small vacuum chamber equipped with a diode gun with a filamentary cathode was built, and welding of various small pieces was performed at that time. As soon as in a year, the results of efforts of the Institute proved to be needed by the industry, first of all for the manufacture of liquid-propellant jet engines. Often it was required to build large vacuum chambers, the transportation of which to their operation site was difficult because of their big dimensions. At the same time, customers had the possibility to manufacture a vacuum chamber on their own. It was necessary just to equip the chamber with an electron beam welding power unit, consisting of a welding gun, high-voltage power source and control system. In this connection, in the 1960s the E.O. Paton Electric Welding Institute arranged mass production of the power units for electron beam welding of metals, primarily of medium and large thicknesses, on the base of a specialised Ukrainian enterprise, i.e. Sumy Factory for Electron Microscopes and Electric Automatic Devices (SELMI). Based on the initial technical documents of the Institute, the SELMI Company developed production documents and manufactured 72 sets of power units SP-30 (25 kV, 500 mA), 330 sets of power units U-250A (30 kV, 450 mA), and 320 sets of units ELA-60 (60 kV, 250, 500 and 1000 mA) and ELA-120 (120 kV, 1000 mA).

Prof. O. Nazarenko

After disintegration of the Soviet Union, the E.O. Paton Electric Welding Institute managed to preserve and further develop its research and production capabilities, and obtained foreign orders for the «turnkey» manufacture of industrial equipment. At present we can distinguish four main areas of activities of the Electron Beam Welding Department and Engineering Centre of the E.O. Paton Electric Welding Institute:

- development of technologies and processes for EBW of materials and parts with up to 200 mm thickness of the weld edges;
- upgrading of power units;
- design and manufacture of EBW machines in cooperation with partners;
- development of software for EBW machines.

Consider the most significant results, which have been achieved in these four areas for the last 10 years.

Technological developments. In view of an increasingly wide application of thick-walled structures from hard-to-weld aluminium alloys of series 7000, the work cycle was performed to study weldability of these alloys with a thickness of up to 150 mm. It was found that in this case the main defect of the welded joints is a network of fine hot cracks in the weld zone. It was shown that to prevent these cracks it is necessary to achieve a fine-grained structure of the base metal at least in the heat-affected zone, e.g. by processing the weld edges to a depth of 8–10 mm by friction stir welding. Decreasing width of the cast zone and increasing stability of the weld shape are also efficient in this respect. This can be provided by welding with the inclined beam and by oscillating the beam. High stability of maintaining the accelerating voltage and suppression of electric breakdowns make it possible to form a defect- and spiking-free weld in the fade-out region of a circumferential joint.

The technology and procedure for EBW of metal 200 mm thick were developed and optimised for the fabrication of structures from aluminium-magnesium alloys. These technology and procedure were mastered to advantage by two South Korean companies.

The technology was developed for simultaneous electron beam welding of 3 longitudinal welds on drill bits by using 3 welding guns. This technology proved to be very efficient. It provides a considerable reduction of residual welding distortions of drill bit bodies and increase in productivity of the welding process, which is confirmed by successful commercial operation of our machines in the USA and Russia.

The technology and procedure were developed for EBW with the deflecting beam (see the cover) and cosmetic smoothing of the root part of the welds in hard-to-reach areas by using the 90° deflecting electromagnetic system. Application of this technology is particularly efficient for the manufacture of high-frequency niobium resonators and aircraft engine pylons.

Power units. Until recently, the E.O. Paton Electric Welding Institute has used cathodes of lanthanum hexaboride LaB_6 in its electron guns. These cathodes are classed with high-efficiency hot cathodes with a low electronic work function and, hence, low working temperatures (1800–1900 °C) and low power consumption.

As long as the scopes of application of EBW for the manufacture of parts from titanium alloys and heat-resistant nickel alloys were relatively small, the industry accepted the phenomenon of decrease in the emissive ability of hexaboride cathodes caused by metallisation of their emitting surface with vapours of refractory components of the metals welded.

However, now it is a pressing problem to replace the lanthanum hexaboride cathodes by the cathodes with a working temperature of not less than 2800 °C. The main difficulty of using the high-temperature cathodes lies in ensuring the reliable fixation of a cathode in its holder with a minimal heat removal. The use of pins introduced into lateral holes of thick washer-type cathodes of melting guns is impossible for cathodes with a diameter of several millimetres, whereas welding of a rear end surface of the cathode to the holder in the form of a washer («Techmeta» design) leads to a huge consumption of power, i.e. up to 300 W, required to heat the cathode.

Thanks to application of the laser technology, we managed to develop the tungsten cathode fixation design that requires a much lower power for heating. For example, a power of about 70 W is needed to heat a 3 mm diameter cathode forming the beam with a current of up to 500 mA, while to heat a 4.2 mm diameter cathode forming the beam with a current of up to 1000 mA the power requirement is approximately 100 W. Such cathodes are already employed in some commercial machines.

For 40 years the E.O. Paton Electric Welding Institute has been using an electron tube as a linear transmission element in its electron beam power sources. And this design is still efficient for the 30–120 kW power sources. Currently, we are making the up to 18 kW power sources on the basis of high-frequency resonance generators using high-power insulated-gate bipolar transistors (IGBT). A low stored energy, i.e. 1–2 J/kW, hampers transformation of spark discharges in the accelerating gap into the arc ones, thus preventing operation of the current protection of a power source. The specific volume power (the ratio of total power of a power source to its unit volume) exceeds that of the traditional sources by a factor of 5 to 10. Unfortunately, a drooping character of the external characteristic of the high-frequency resonance-type power sources, depending upon the load, does not allow using them in a mode of pulse modulation of the beam current.

Quite often the industry needs the off-line power units for EBW to replace the obsolete or worn-out ones, as well as to complete the vacuum chambers independently made by the customers. Control racks of a power source, comprising an industrial computer and RASTR system for visualization of the welding zone by means of secondary electrons, can be made either in the form of a direct control rack, where an operator sets and edits the welding programs directly from this rack, or in the form of a remote control rack, where setting and editing of the welding programs are performed from the CNC panel of the EBW machine.

During the last 10 years we have commissioned 19 power units with a power of 1.2 to 60 kW at an accelerating voltage of 60 kV, and with a power of 6 to 120 kW at an accelerating voltage of 120 kV.

Industrial machines. Distinctive feature of the Paton Institute machines for EBW of large-size parts is, without doubt, the use of the inside-chamber electron guns, which can be moved within

a range of 12 m. This design allows the coefficient of utilization of the internal volume of a vacuum chamber to be increased to the maximum possible degree.

Having the facility with a floor area of 2000 m^2, equipped with the 30 t gantry, we can perform assembly and adjustment of our EBW machines with a capacity of the vacuum chambers amounting to 100 m^3. If dimensions or weight of a vacuum chamber exceed the transportation limits, this vacuum chamber is dismembered into several parts. The chambers are made in the form of two vacuum-tight and comparatively thin-walled (each 8–12 mm thick) shells joined to each other with stiffeners, i.e. ribs. Doors of the chambers are made on the same principle. The use of this box-like design of the walls and doors instead of the conventional T-shaped one provides a 2 times higher moment of inertia and, as a result, lower distortion of the walls in evacuation of the chamber.

During a period of 1998–2008, we introduced into commercial operation 27 complete sets of the EBW machines.

Software. Development of the so-called visual method for design of software programs for EBW of complex-configuration structures can be considered to be our key achievement in the field of program control of the electron beam welding process.

The EBW machines are controlled, as a rule, by using the distributed computer systems that include devices of the CNC and PLC types, which are connected to each other via interface busbars, but function independently of each other. Normally, the programs are stored in CNC in the G-codes, and constitute a sequence of blocks, where the coordinates of a point to which it is necessary to move, method and parameters of interpolation for performing a given movement, values of the welding, focusing, sweep and deflection currents, as well as the speed of movement in a given length are set for each length of the path. In the case where several coordinates are used simultaneously, when the final path is a complex space curve, the time of preparation of a program may range from a several hours to several days and even weeks, depending upon the complexity of the path.

Therefore, being internationally oriented to application of the high-accuracy CNC systems, the E.O. Paton Electric Welding Institute in collaboration with the Institute for Problems of Mathematical Machines and Systems of the NAS of Ukraine developed the software tools, which are built into the CNC systems, allowing an operator to use the so-called visual method for design of programs for EBW of complex-configuration structures. In addition to traditional computer systems that combine the CNC and PLC devices, we introduces a higher level of operator's interface for visual design of the work programs and control of the welding process, as well as an extra computer, which, independently of the other processor nodes, solves the problems of recognition of a seam from the workpiece surface image received from the RASTR observation equipment, and provides, together with the host computer, performance of the automatic teaching, correction and seam tracking functions. The visually designed welding program, when started for automatic run, with no assistance of an operator, is converted into the CNC executed sequence of the G-codes.

The results of this work were noted with the State Prize of Ukraine in the field of science and technology in 2006.

The Electron Beam Welding Department and Engineering Centre maintain constant contacts with Ukrainian and foreign industrial enterprises and companies, participate in international welding exhibitions, give consultations and reasoned conclusions, provide training and probation work for specialists, and support the website in Internet.

Prof. O. Nazarenko
E.O. Paton Electric Welding Institute, NASU, Kiev, Ukraine

PECULIARITIES OF IMPACT TOUGHNESS TESTS OF AUTOMATIC FLASH BUTT WELDED JOINTS ON PIPES

S.I. KUCHUK-YATSENKO[1], **V.I. KIRIAN**[1], **B.I. KAZYMOV**[1], **I.V. MIRZOV**[1] and **V.I. KHOMENKO**[2]
[1]E.O. Paton Electric Welding Institute, NASU, Kiev, Ukraine
[2]Open Joint Stock Company «Strojtransgaz», Moscow, Russia

The effect of mechanical heterogeneity of flash butt welded joints on values of impact toughness *KCV*, as well as of natural stress raisers in the form of the welding zone defects, resulting from violation of the welding technology, on fracture energy has been studied. It is shown that inadmissible welding defects act as softer stress raisers than a standard sharp notch. Also, it is shown that the *KCV* values of sound joints in the as-welded state reflect the level of their service properties and high operational reliability.

Keywords: *automatic flash butt welding, pipelines, mechanical heterogeneity, strength, impact toughness, fracture energy, mechanical notches, natural stress raisers, fractures*

Automatic flash butt welding (FBW) is a variety of pressure welding. It is widely applied in different industries [1–4], including power generation and construction of pipelines [5–8]. Many years' (over 30 years) practice of operation of different-application welded pipelines, including 1420 mm diameter high-capacity gas pipelines, showed high reliability of assembly circumferential joints made by the FBW method. Mechanical properties of the FBW joints (Table 1) meet requirements of the standards [9, 10] used for large-scale construction of main and field gas and oil pipelines.

Welded joints (Figure 1, *a*) produced by the FBW method under the set (optimal) conditions contain no defects that could negatively affect their mechanical properties [11–13]. As shown in studies [11, 14], high performance of the FBW joints under service conditions is guaranteed by the existing relationship between the stable welding conditions and quality of the joints, as well as by maintaining the process parameters at a set level for the entire welding process equipped with the integrated automated control and monitoring system. As a result of specific peculiarities of formation of a welded joint, the main of which are plastic deformation in upsetting at the final stage of welding and absence of cast metal in JZ, the joint contains no cracks and sharp stress raisers. Local regions with non-metallic inclusions which transferred from the pipe metal to JZ (Figure 1, *b*), or with microparticles which may form as a result of fracture of thin oxide films during upsetting, are not identified as defects. They are structural heterogeneities [11], which hardly have any effect on strength properties of the FBW joints. This was proved by the results of static loading tests of standard (flat) and large-scale specimens of the welded joints produced under conditions approved for welding of pipes in construction of main pipelines [15]. Surface area of the regions with structural heterogeneity in real joints on modern pipe steels is usually no more than 20 mm^2. Moreover, comprehensive evaluation of the effect of structural heterogeneity on properties of the joints was carried out on 6 mm diameter round specimens cut out from

Table 1. Mechanical properties of FBW joints on pipe steels

Strength group	Specimen cutting location	Tensile strength σ_t^*, MPa	Hardness *HV*
X70	Base metal	606–616 / 610	196–205 / 197
	Welded joint	600–612 / 604	194–200** / 196
X80	Base metal	612–626 / 620	201–212 / 209
	Welded joint	604–623 / 608	195–203** / 202

*Minimal and maximal values are given in numerator, and average value is given in denominator. ** — joining zone (JZ).

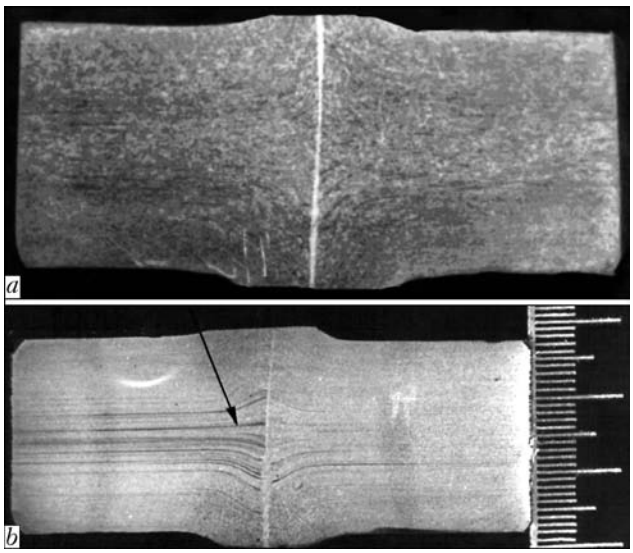

Figure 1. Macrosections of FBW joints on pipe steels with different contents of segregation inclusions: *a* — typical structure of modern pipe steels; *b* — structure with clearly pronounced segregation lines (shown by arrow)

© S.I. KUCHUK-YATSENKO, V.I. KIRIAN, B.I. KAZYMOV, I.V. MIRZOV and V.I. KHOMENKO, 2008

Table 2. Results of static tension tests of 6 mm diameter round specimens of steel of the X60 strength group with regions of structural heterogeneity in JZ

Specimen No.	Ratio of structural heterogeneity on fracture surface of specimen to its cross section area, %	Ratio of level of fracture stresses to rated mechanical properties of base metal, %	
		$\sigma_{0.2}$	σ_t
1	50	110	85
2	70	128	99
3	40	123	95
4	50	130	100
5	30	114	88

the welded joints on pipes made from steel X60 with a high content of segregation inclusions (see Figure 1, *b*). This made it possible to substantially increase the relative area of the regions with structural heterogeneity in a test specimen. The test results are given in Table 2. Despite the fact that regions with structural heterogeneity, having the relative area of 30 to 70 % of that of the cross section of a specimen, were detected on fracture surfaces of the specimens that fractured in JZ, the values of fracture stresses σ_f were higher than yield stress $\sigma_{0.2}$ of the pipe metal.

All of the above-said predetermines the many years' failure-free operation of the FBW joints. According to the common world-wide practice, to confirm the guaranty that the welded joints will not fracture under service conditions (independently of the welding method), they have to meet requirements for the certain values of toughness, which was determined by testing standard impact specimens with a sharp notch (*KCV*). The rated values of impact toughness are set from a condition of prevention of fractures of the welded joints containing the most probable defects of different types, including the crack-like ones. Therefore, to substantiate the level of impact toughness, the use is lately made of approaches and criteria of fracture mechanics [16], the initial postulate of which is based on the fact that fracture is always a result of initiation and propagation of cracks in structural members. It is well known that formation of such defects in welding of pipes is characteristic of the electric arc welding methods.

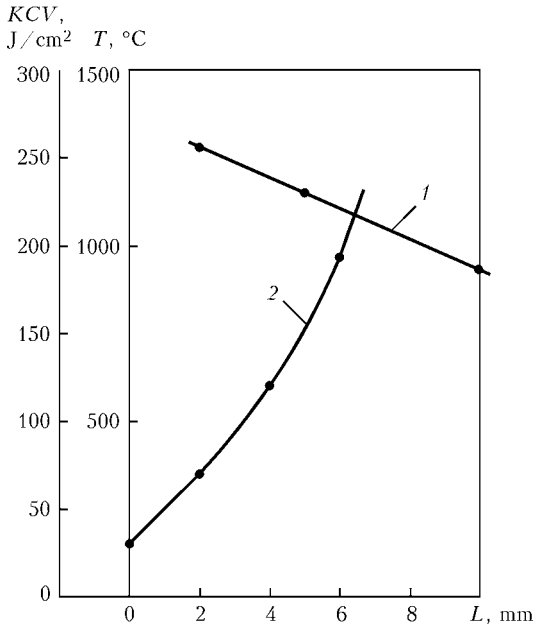

Figure 2. Variations in temperature *T* of pipe metal in the FBW zone (*1*) and impact toughness *KCV* of a welded joint with the stress raiser located at different distances *L* from the central section of JZ (*2*)

The purpose of this study was to investigate peculiarities of fracture of standard impact specimens cut out from the FBW joints containing different types of artificial (mechanical notches) and natural stress raisers (welding defects typical of the FBW technology), and to evaluate their effect on fracture energy of the joints.

We should emphasise one specific feature of a formed welded joint produced by the FBW method, which is of a fundamental importance for interpretation of test results. Such a welded joint is formed as a result of mutual compression of pieces being welded, which are heated to welding temperatures. The heated region on pipes along their generating lines has a non-uniform temperature field. The weld edges have temperature which amounts to the melting point of metal, and which gradually decreases with distance from the flashing surface. The temperature field gradient within the heating zone is determined by the time and intensity of flashing (Figure 2, curve *1*). Therefore, at the moment of mutual compression of the pipes in upsetting, the heat-affected zone metal is subjected to a differing degree of reduction. As a result, the thermomechanically strengthened zone (TMSZ) is formed on both sides of JZ, having different properties in different regions of the latter. The regions immediately adjoining JZ have the highest values of hardness. Hardness of the JZ metal is much lower (down to 30 %, depending upon the steel welded and welding conditions). However, as shown by testing standard specimens with a sharp notch in JZ, the *KCV* values are insufficient, compared with the rated ones set for the welded joints produced by the electric arc welding methods, allowing for a high probability of their cracking. So, the *KCV* values of sound joints on pipe steels of controlled rolling, belonging to the X70 strength group, are 14.3–56.3 J/cm^2 at 20 °C, the average value being 29.8 J/cm^2. Note that wide scattering of the *KCV* values is characteristic of all welded joints, independently of the welding method. Decrease in the *KCV* values is strongly affected by the presence of coarse grains formed under the influence of the thermal cycle of welding. The minimal required value for main pipelines operating at negative temperatures (T_{test} = −20 °C) should be 29.4 J/cm^2 (the average value should be not less than 34.4 J/cm^2) [9]. At 20 °C, the *KCV* value of pipe metal amounts to 300 J/cm^2.

Probable defects in the welded joints in the case of inadmissible deviations from the set FBW parameters are lacks of fusion, which may have the form of

unclosed craters and thick oxide films [8]. These defects are formed at a too low upsetting allowance. Formation of thick oxide films takes place in the case of inadmissible interruption of the flashing process prior to upsetting at a low upsetting allowance, whereas to produce the sound joint it is necessary to provide a stable intensity of flashing. If the flashing process is interrupted prior to upsetting, oxide films will be formed in JZ. At a sufficient upsetting, the thin films will be disrupted to form a strong metal bond in the disruption locations. As shown by investigations, in contrast to lacks of fusion in the form of thick oxide films, they cannot be identified as cracks, because fragments of such films also act as a connecting link between the pipes welded. In this case, metallic bond occurs through a film, which is provided by its composition, where lower oxides predominate, having the crystalline lattice identical in structure and close in size to that of α-iron [17]. It was established by tensile tests of large-scale 500 mm wide specimens cut out from the welded joints containing the above defects, that their critical sizes at T_{test} = = −60 °C are in excess of 70 mm^2 [11, 17]. The average *KCV* values of standard specimens cut from the joints with the defects under consideration are almost the same as those of the sound joints, however, with a wider scatter of the results (7–60 J/cm^2). Some specimens exhibit comparably high *KCV* values. For example, a specimen with such an abnormal structure of the surface area, constituting more than 60 % of the cross section area (Figure 3), had impact toughness of 60 J/cm^2.

It should be emphasised here that lacks of fusion and oxide films can be detected with the 100 % probability from the results of monitoring of the welding process parameters. Ultrasonic inspection [18, 19] and X-ray inspection, which is widely applied in construction of pipelines (Figure 4), provide the sufficiently high probability of detection of such defects. For this, one of the important conditions is removal of flash. In the case of detection of the above defects the welded joints should be discarded.

The data given served as a basis for the development of the test procedure for evaluation of toughness of the FBW joint metal and rating of its level.

Decrease in impact toughness of individual zones of a welded joint, compared with the pipe metal, takes place with all the welding methods accompanied by high-temperature transformations in the weld metal. In electric arc welding of longitudinal joints on pipes made from low-alloy steels of controlled rolling, the region of transition from the deposited to base metal is a local brittle zone, which in some cases is a cause of insufficient impact toughness. The special test procedure was developed for evaluation of fracture toughness of the welded joints with the local brittle zone, allowing for high reliability of such pipes under service conditions [20].

Finding solution to this problem is very important for the FBW joints. This can be done on the basis of the data on absence of cracks and sharp stress raisers in metal of the joints.

Figure 3. Appearance of typical fracture surface on standard specimen (*KCV* = 60 J/cm^2) with crushed oxide film (delineated region)

Decrease in the *KCV* values of metal of the FBW joints takes place only in the case of testing standard specimens with a notch in JZ (see Figure 2, curve *2*). The results of solving the elasto-plastic problem of the stress-strain state of such a specimen tested to 3-point bending by the finite element method show that the fragmented heterogeneity of metal of the joints, oriented strictly across the maximal tensile stresses, leads to localisation of development of the region of plastic strains (Figure 5), which precede fracture, in a narrow JZ with lower mechanical properties ($\sigma_{0.2}$), compared with TMSZ adjoining it. Boundary of the zone of plastic strains near a mechanical stress raiser (2 mm deep, with a rounding radius of 0.25 mm) located along the centre of JZ 0.6 mm wide was determined from the Mises–Henki condition:

$$\sigma_i = \frac{1}{\sqrt{2}} \sqrt{(\sigma_1 - \sigma_2)^2 + (\sigma_2 - \sigma_3)^2 + (\sigma_3 - \sigma_1)^2} = \sigma_y,$$

where σ_i is the stress intensity; σ_1–σ_3 are the principal stresses; and σ_y is the yield stress.

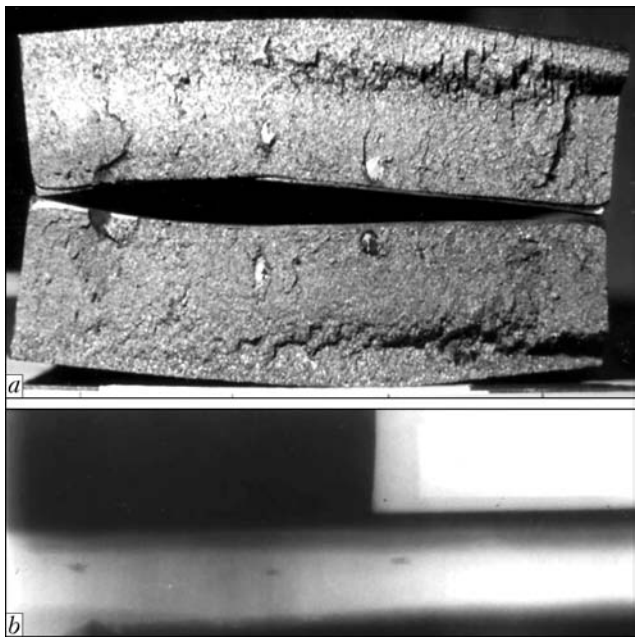

Figure 4. Fracture of the welded joint produced with inadmissible deviations of welding process parameters (*a*), and X-ray pattern of the joint before fracture (*b*)

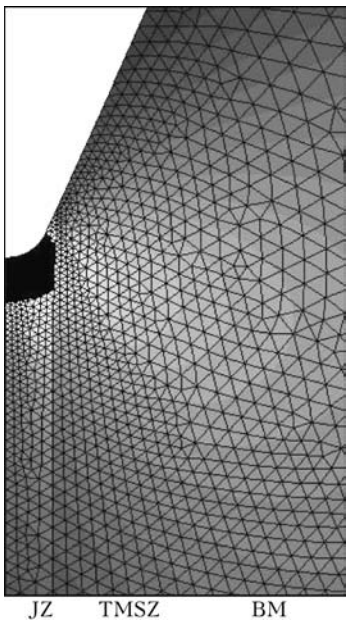

Figure 5. Localisation of the zone of plastic strains (blackened) in narrow (0.6 mm wide) JZ in testing of the $10 \times 10 \times 55$ mm standard specimen with a sharp mechanical notch in the central section of JZ to 3-point bending

As a result of substantial decrease in volume of the plastically deformed metal in the fracture region and lower mechanical properties of JZ ($\sigma_{0.2}$), compared with the base metal (BM) and TMSZ, here fracture becomes less energy-intensive, thus leading to decrease in the impact toughness values.

Under such test conditions with a limitation of plastic deformation of metal, the highly ductile pipe steel exhibited impact toughness values two times as low as those of standard specimens. Three batches of specimens with a standard V-shaped mechanical notch, 2 mm deep and with an apex radius of 0.25 mm, were made from steel X70 and tested to impact bending. Specimens of batch 1 (measuring $10 \times 10 \times 55$ mm) had a weakened section area of 0.8 cm^2 (Table 3). In batch 2, thickness of the specimens was decreased to 5 mm (cross section area of 0.4 cm^2). In batch 3, side recesses were made in the specimens of batch 1, which were similar in configuration to a standard notch, but had a depth of 2.5 mm, so that the weakened section area corresponded to

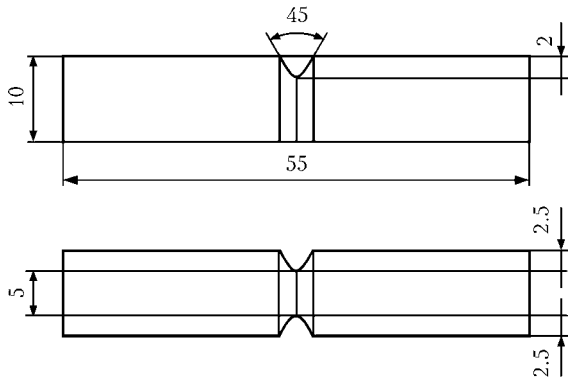

Figure 6. Schematic of the *KCV* impact toughness test specimen of a standard size with two additional side recesses similar to a standard notch 2.5 mm deep

Figure 7. Appearance of the specimen without mechanical notch, cut out from the sound FBW joint, after the test to 3-point impact bending

that of the specimens of batch 2 (Figure 6). Such side mechanical notches excluded the probability of formation of shrinkages on side surfaces of a specimen, thus creating a rigid stress-strain state within the fracture zone. Decrease in thickness of a specimen from 10 (batch 1) to 5 mm (batch 2) led to an insignificant increase in impact toughness due to some decrease, compared with thickness, of the volume of metal in middle sections of the specimen that was in the plane-deformed state ($\varepsilon_z = 0$). At the same time, transition of the entire section of the specimen to the above conditions due to making side recesses (batch 3) led to decrease in impact toughness (Table 3).

We think the data on the energy consumed for fracture of standard specimens with stress raisers in the form of inadmissible defects probable for FBW, such as lacks of fusion (unclosed craters and oxide films), are important for the development of the test procedure for welded joints to control their fitness for purpose. The first to be tested to impact bending were the specimens of a standard size ($10 \times 10 \times 55$ mm), cut out across the sound welded joint produced by the FBW method, with JZ in its central part, without a mechanical notch (Figure 7). None of them fractured at an energy content of a striker equal to 300 J. This is indicative of a high resistance of metal of the welded joins to crack initiation and fracture during operation.

Impact specimens of a standard size without artificial stress raisers were made from the joints, which were deliberately welded with admissible and inadmissible deviations of the welding process parameters, to reveal the extent of the effect of welding defects

Table 3. Results of impact tests of three batches of specimens made from microalloyed pipe steel of controlled rolling, belonging to X70 strength group, at room temperature

Specimen batch No.	*KV*, J	*KCV* (average value), J/cm^2
1	217.8–266.4 / 248.4	310.5
2	124.2–133.4 / 129.2	323.0
3	46.8–83.4 / 62.6	156.5

Minimal and maximal values are given in numerator, and average values are given in denominator.

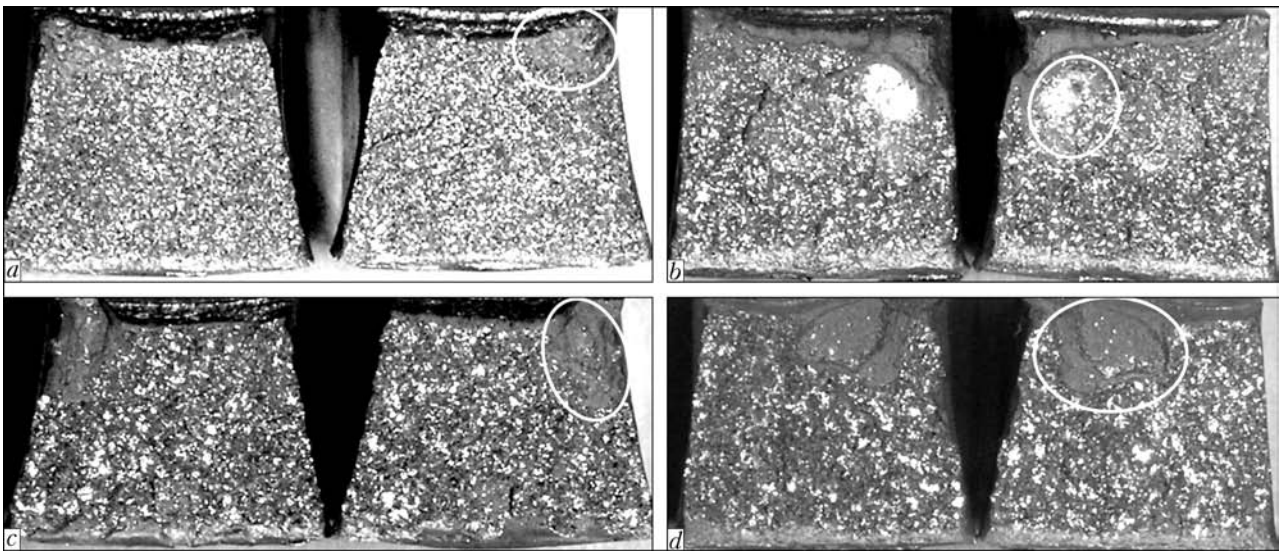

Figure 8. Fracture surfaces of impact test specimens containing defects, which are characteristic of the FBW technology: *a* — structural heterogeneity at the specimen surface (*KD* = 261 J); *b* — lack of fusion (inadmissible defect) inside JZ (*KD* = 278 J); *c, d* — same at the specimen surface at *KD* = 151 and 96 J, respectively

on the fracture energy. In this case, the fracture energy of a specimen without a mechanical notch, but containing natural defects typical of the used welding methods, is designated as *KD*, in analogy with the *KU* and *KV* designations reflecting the type of a mechanical notch.

Impact specimens, on the fracture surfaces of which the regions were detected with a structural heterogeneity having an area of 4 to 25 % of the specimen area, which are located immediately at the specimen surface (some of the specimens completely fractured after the impact tests), exhibited an impact energy of 153–261 J (Figure 8, *a*). Specimens with a structural heterogeneity, which did not escape to the surface even at its relatively large surface area, did not fracture, like the sound ones.

The presence of internal (not escaping to the specimen surface) inadmissible defects in JZ, i.e. lacks of fusion (Figure 8, *b*), also leads to fracture at high enough values of the absorbed energy. Despite a considerable size of the defects (with an area of up to 20 % of the cross section area of a specimen), the fracture energy was 202–278 J.

The role of inadmissible defects in decreasing the *KD* values grows, if they escape to the surface (Figure 8, *c, d*). In this case, the fracture energy depends not as mush on the area of a defect as on its linear size on the surface. For example, at a linear size of the surface defect equal to 2.3 mm, the impact energy was 151 J, whereas at a length of 4.4 mm it was 96 J. The results of tests of the specimens containing defects shows that a decisive factor decreasing the fracture energy is a relative value of the linear size of a surface defect. At the same time, it is evident that inadmissible defects in JZ, which are absent in commercial joints, act as softer stress raisers, compared with a standard mechanical notch 2 mm deep. It is important that this fact should be taken into account in assessment of fitness for purpose of the circumferential FBW joints, which have their specific peculiarities: on the one hand, it is a substantial mechanical fragmented heterogeneity in the welding zone, and on the other hand, it is the absence of crack-like defects and a low level of residual stresses.

Therefore, the standard test procedure for evaluation of impact toughness of the welded joints on pipes does not allow for the specific features of the joints made by the automatic FBW method. These features consisted in a marked fragmented heterogeneity of metal, strictly oriented with respect to JZ, and absence of conditions for the formation of cracks. This leads to inadequate evaluation of performance of the welded joints. In this connection, improvement of the test procedure for such joints to assess their fitness for purpose can be aimed at decreasing the stress concentration factor, compared with standard specimens, and at providing plastic deformation in the process of their fracture not only in narrow JZ, but also in TMSZ.

Investigation of peculiarities of fracture of standard impact specimens with different artificial and natural stress raisers in JZ shows that metal of the FBW joints is characterised by a sufficiently high resistance to brittle fracture. Probable defects in such joints in the form of structural heterogeneity have almost no effect on fracture energy of the specimens having no mechanical notch, while the lacks of fusion act as softer stress raisers compared with a standard V-notch. Hence, it is apparent that the obtained average value of impact toughness ($KCV = 29.8\ J/cm^2$) of sound joints in the as-welded state reflect the level of the service properties that ensure the absence of fracture of the joints under operation conditions. This is proved by a many years' (over 30 years) successful operation of pipelines, e.g. 1420 mm diameter gas pipelines, made by the automatic FBW method.

1. Kuchuk-Yatsenko, S.I. (1964) Continuous flash butt welding of rails. *Avtomatich. Svarka*, **4**, 55–62.
2. Kuchuk-Yatsenko, S.I., Didkovsky, A.V., Krivenko, V.G. et al. (2004) Flash butt welding of rails. Experience of appli-

cation and prospects of improvement. *Put i Putevoe Khozyajstvo*, **9**, 5–8.
3. Kuchuk-Yatsenko, S.I., Shvets, Yu.V., Dumchev, E.V. et al. (2005) Flash butt welding of rail frogs with rail ends using an intermediate insert. *The Paton Welding J.*, **1**, 2–4.
4. Lebedev, V.K., Tishura, V.I., Chernenko, I.A. et al. (1975) Mechanised line for assembly and welding of carters of high-capacity transport diesel blocks. *Avtomatich. Svarka*, **5**, 41–44.
5. Kazymov, B.I., Kuchuk-Yatsenko, S.I., Korsunov, V.M. et al. (1972) Flash butt welding of boiler pipes. *Ibid.*, **9**, 52–55.
6. Skulsky, Yu.V., Kazymov, B.I. (1981) Flash butt welding of increased-strength drill pipes. *Ibid.*, **2**, 59–61.
7. Paton, B.E., Lebedev, V.K., Kuchuk-Yatsenko, S.I. (1979) Complex «Sever-1» for flash butt position welding of large-diameter pipes. *Ibid.*, **11**, 41–45.
8. Kuchuk-Yatsenko, S.I., Krivenko, V.G., Sakharnov, V.A. (1986) *Flash butt welding of pipelines*. Kiev: Naukova Dumka.
9. *SP 105-34–96*: Rules. Performance of welding operations and quality control of welded joints. Introd. 01.06.96.
10. *API 1104*: Welding of pipelines and related facilities. ASME boiler and pressure vessel. Publ. 1999.
11. Kuchuk-Yatsenko, S.I., Kirian, V.I., Kazymov, B.I. et al. (2006) Methodology for control of fitness for purpose of flash butt welded joints in pipelines. *The Paton Welding J.*, **10**, 2–6.
12. Mazur, I.I., Serafin, O.M., Karpenko, M.P. (1989) Resistance welding of pipelines: ways of improvement. *Stroitelstvo Truboprovodov*, **4**, 8–11.
13. Makarenko, V.D., Izvekov, Yu.G., Shatilo, S.P. (1987) Brittle fracture resistance of resistance welded joints. *Ibid.*, **7**, 25–29.
14. Kuchuk-Yatsenko, S.I. (1976) *Continuous flash butt welding*. Kiev: Naukova Dumka.
15. Trufyakov, V.I., Mazur, V.G., Zhemchuzhnikov, G.V. et al. (1987) Influence of some defects on strength of flash butt welded joints. *Avtomatich. Svarka*, **2**, 7–9.
16. Girenko, V.S., Dyadin, V.P. (1986) Relationships between impact toughness and fracture mechanics criteria of structural materials and their welded joints. *Ibid.*, **10**, 61–62.
17. Kuchuk-Yatsenko, S.I. (1992) *Flash butt welding*. Kiev: Naukova Dumka.
18. Troitsky, V.A., Radko, V.P., Yushchak, P.T. et al. (1981) Ultrasonic quality control of flash butt welded joints. *Avtomatich. Svarka*, **4**, 38–40.
19. Kuchuk-Yatsenko, S.I., Kazymov, B.I., Radko, V.P. (1996) Integrated monitoring of joints made by automatic flash butt welding. *Tekhnich. Diagnostika i Nerazr. Kontrol*, **4**, 46–50.
20. Kirian, V.I., Semyonov, S.E. (1995) Assessment of fitness for purpose of welded joints on main pipelines made from microalloyed steels. *Avtomatich. Svarka*, **3**, 4–9.

ACCUMULATION OF FATIGUE DAMAGE IN TEE WELDED JOINTS OF 09G2S STEEL IN THE INITIAL CONDITION AND AFTER STRENGTHENING BY HIGH-FREQUENCY MECHANICAL PEENING

V.V. KNYSH, S.A. SOLOVEJ and **A.Z. KUZMENKO**
E.O. Paton Electric Welding Institute, NASU, Kiev, Ukraine

Criteria of fracture of welded T-joints on 09G2S steel in as-welded condition and after strengthening by the technology of high-frequency mechanical peening (HFMP) loaded in the decreasing, increasing and quasi-random loading modes, are considered in the context of the hypothesis of linear summation of fatigue damage. It is noted that the linear hypothesis of fatigue damage accumulation is well suitable for prediction of fatigue life of welded joints strengthened by the HFMP technology. For the as-welded joints, where accumulation of damage strongly depends upon the load history, the rule of summation of damage is suggested that decreases the scatter of total damage.

Keywords: *welded structures, low-alloyed steels, tee joints, fatigue damage accumulation, high-frequency mechanical peening, cyclic fatigue life*

In welded metal structures designed for long-term operation under the conditions of alternating loading, fatigue damage accumulates in the near-weld zones in the sites of maximum concentration of working and residual stresses. Solving the problems on evaluation and forecasting the fatigue life of such structures envisages alongside calculation of the stress-strain state of their elements also determination of the law of fatigue damage summation in the raiser zones. A lot of studies are devoted to experimental investigation of the regularities of fatigue damage accumulation in structural steels [1–3].

When solving the problems of evaluation of fatigue life for various non-stationary loading modes the most widely used is the hypothesis of linear summation of damage applied both for the base material and for the welded joints, which is attributable to its simplicity and absence of unknown parameters. This hypothesis was suggested for the first time by Palmgren in 1924 and was later developed by Meiner in 1945.

According to Palmgren–Meiner hypothesis damage fraction D_i at any i-th level of cycle stresses is directly proportional to the ratio of cycles of its action n_i to the number of fracture cycles on this level N_i. It is predicted that fracture will occur, if

$$\sum_{i=1}^{k} D_i = \sum_{i=1}^{k} \frac{n_i}{N_i} \geq 1. \qquad (1)$$

Results of experimental investigations derived at various kinds of loading for smooth samples and samples with stress raisers, not always are in a satisfactory agreement with Palmgren–Meiner linear hypothesis. Scatter of values of the sum of damage fractions at fracture of such samples varies approximately from

© V.V. KNYSH, S.A. SOLOVEJ and A.Z. KUZMENKO, 2008

0.1 to 5 [1–3]. It is noted that the sequence of load application has an essential influence on sample fatigue life. At loading modes when low stresses precede the high ones, so-called training takes place, and the total damage, as a rule, is greater than a unity. Training is manifested to the greatest extent when the initial stress range below the fatigue limit is slightly increased in several million cycle intervals. At loading modes when high stresses precede the low ones, so-called overload is in place and the total damage, as a rule, is below a unity. If various amplitudes of cyclic stresses alternate in a quasi-random fashion, the experimental value of the sum of damage fractions at the moment of fracture is close to a unity. As in many practical applications the stresses change in a quasi-random fashion, use of Palmgren–Meiner rule of linear summation of damage often turns out to be acceptable for fracture prediction. Sometimes, with the known loading spectra characteristic for a particular product, improvement of the correspondence of the predicted fatigue life to the experimentally established value is achieved by modification of Palmgren–Meiner linear hypothesis derived by replacement in expression (1) of the fracture criterion by value a differing from a unity. In publications there is no common opinion on the procedure of determination of a parameter. Most often its value is calculated experimentally at unchanged program loading of individual samples with averaging of testing results.

Such a modification of the linear hypothesis has an essential drawback of being valid for a strictly defined range of materials and loading conditions, and cannot be extrapolated to conditions going beyond the limits of the initial experiment.

As regards the welded joints, there is a much smaller number of works on investigation of the regularities of fatigue damage accumulation. In [4, 5] it is noted that in welded joints with high tensile residual stresses at one-time change of the maximum stresses of alternating loading cycle, damage accumulation essentially depends on the loading pattern. In addition, the total damage of welded joints experiencing a multi-step decreasing or increasing loading sequence depends on the loading pattern [6–8]. Scatter of the given values of total relative fatigue resistance varies approximately from 0.3 to 3. For other loading modes, in particular, at multi-block and two-step loading with multiple stress reversal, the hypothesis of linear summation of damage was confirmed experimentally. In [4] the validity of the linear hypothesis of fatigue damage accumulation was confirmed at multi-block loading of welded samples of VSt3 steel with high residual stresses. It is shown that starting with the ten-block two-step loading, the test results become practically independent on the pattern of the initial loading (transition from the upper level to the lower level or from the lower level to the upper level).

Over the recent years technologies of surface plastic deformation, in particular, high-frequency mechanical peening (HFMP), are becoming widely accepted to improve the cyclic fatigue life of welded components and elements of metal structures. The effectiveness of this technology application at the stage of product manufacturing at regular loading is well studied. However, experimental data on establishing the law of damage summation in HFMP strengthened welded joints are practically absent (note the only work [9]).

The purpose of this work is experimental verification of the applicability of the hypothesis of linear summation of damage for tee welded joints in the initial and HFMP strengthened condition at increasing, decreasing and quasi-random loading blocks.

Experimental investigations were conducted on samples of tee joints of 09G2S steel (σ_y = 370 MPa, σ_t = 540 MPa). Billets for samples of this steel were cut out of the rolled sheets so that the long side were oriented along the rolling stock direction. Transverse stiffeners were welded by fillet welds from both sides by manual electric arc welding with UONI-13/55 electrodes. The shape and geometrical dimensions of the sample are given in Figure 1. Sample thickness is due to a wide applicability of 12 mm thick rolled stock in welded structures, and the gauge width was selected proceeding from the testing equipment capacity. It is known that at sample width of 50 mm the levels of residual tensile stresses in the near-weld zone do not reach the limit value, but are equal, approximately, to $0.5\sigma_y$. However, as will be shown further on, this factor does not have any essential influence on the investigation results. At joint strengthening by HFMP technology surface plastic deformation was applied to a narrow zone of transition of weld metal to base metal. Fatigue testing of samples was conducted in URS 20 testing machine at uniaxial variable tension with cycle asymmetry $R_\sigma = 0$. All the samples were tested to complete fracture. S–N curves of tee joints on 09G2S steel in the initial and HFMP

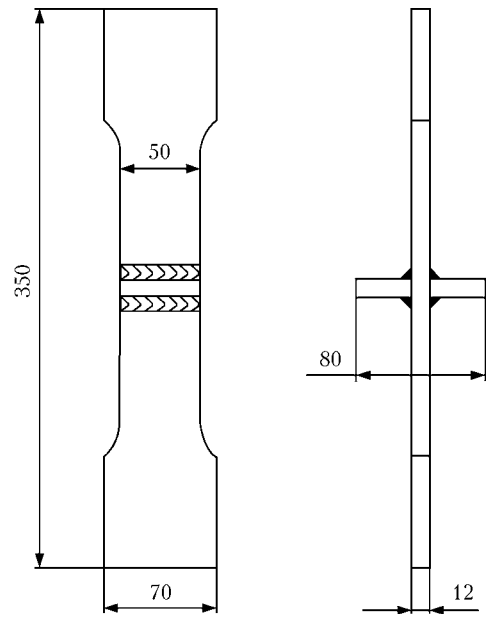

Figure 1. Schematic of a sample of 09G2S steel tee joint

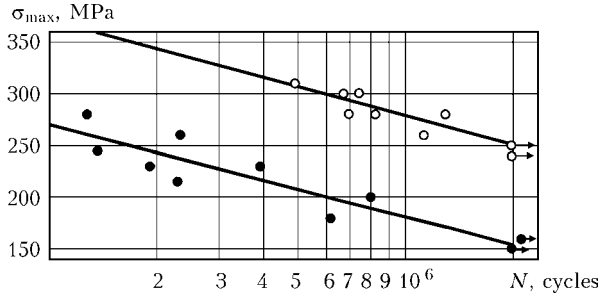

Figure 2. *S–N* curves of tee welded joints of low-alloyed steel 09G2S: ●, ○ — in the initial condition and after strengthening in as-welded condition, respectively

strengthened as-welded conditions were initially derived (Figure 2). To establish the fracture criterion (*a* value) in keeping with the linear hypothesis of fatigue damage accumulation six sample series were tested, namely three series for strengthened and unstrengthened welded joints, respectively. Each series consisted of three samples.

At fatigue testing of welded joints in the initial condition the block included five loading stages of the duration equivalent to 20 % of the fatigue life in each of them. The first series of samples was tested at the specified initial stress level of 180 MPa with subsequent increase up to 260 MPa with 20 MPa step (increasing loading mode). Samples of the second series were tested at the initial stress level of 260 MPa with subsequent decrease to 180 MPa also with 20 MPa step (decreasing loading mode). Samples of the third series were tested at the following five successive levels of the maximum cycle stresses of 220, 200, 240, 180, 260 MPa (quasi-random loading mode).

For welded joints strengthened by HFMP technology immediately after welding the welding block included four loading stages with the duration equivalent to 25 % of the fatigue life in each of them. The fourth sample series was tested at the specified initial stress level of 260 MPa with subsequent increase up to 305 MPa with 15 MPa step. Samples of the fifth series were tested at the initial stress level of 305 MPa with subsequent decrease to 260 MPa also with 15 MPa step. Samples of the sixth series were tested at the following four successive levels of maximum cycle stresses: 290, 275, 305, 260 MPa.

Results of testing welded joints in the initial and HFMP strengthened as-welded condition are presented in Tables 1 and 2, respectively. The established limit values of the sum of relative fatigue lives in fatigue testing of welded joints in the initial condition vary in the range from 0.32 up to 1.97. Here, the sequence of load application has an essential influence on the cyclic fatigue life of welded joints. Values of total damage obtained at testing three samples to fracture, in the increasing sequence of load application, are in the range from 0.32 to 0.56, in the decreasing sequence — from 1.48 to 1.97 and at quasi-random loading mode — from 0.84 to 1.25. These values of limit sums of damage fractions confirm that the pattern of load application in welded joints gives rise to

Table 1. Results of fatigue testing of tee welded joints of 09G2S steel at different kinds of loading block

Sample number	Kind of loading block	1st loading*		2nd loading			3rd loading		
		σ_{1max}, MPa	n_1, thou cycles	σ_{2max}, MPa	n_2, thou cycles	n_2/N_2, %	σ_{3max}, MPa	n_3, thou cycles	n_3/N_3, %
1	Increasing	180	208.8	200	119.9	20.0	220	55.9	15.6**
2		180	208.8	200	72.9	12.2**	–	–	–
3		180	208.8	200	119.9	20.0	220	13.4	3.7**
4	Decreasing	260	25.6	240	42.8	20.0	220	71.6	20.0
5		260	25.6	240	42.8	20.0	220	71.6	20.0
6		260	25.6	240	42.8	20.0	220	71.6	20.0
7	Quasi-random	220	71.6	200	119.9	20.0	240	42.8	20.0
8		220	71.6	200	119.9	20.0	240	42.8	20.0
9		220	71.6	200	119.9	20.0	240	42.8	20.0

Table 1 (cont.)

Sample number	Kind of loading block	4th loading			5th loading			$\sum \frac{n_i}{N_i}$, %
		σ_{4max}, MPa	n_4, thou cycles	n_4/N_4, %	σ_{5max}, MPa	n_5, thou cycles	n_5/N_5, %	
1	Increasing	–	–	–	–	–	–	55.6
2		–	–	–	–	–	–	32.2
3		–	–	–	–	–	–	43.7
4	Decreasing	200	119.9	20.0	180	1221.8	117.0**	197.0
5		200	119.9	20.0	180	710.7	68.1**	148.1
6		200	119.9	20.0	180	998.2	99.4**	179.4
7	Quasi-random	180	208.8	20.0	260	5.3	4.1**	84.1
8		180	208.8	20.0	260	57.2	44.7**	124.7
9		180	208.8	20.0	260	23.6	18.4**	98.4

*For the 1st loading n_1/N_1 = 20 %. **Sample failed.

Table 2. Results of fatigue testing of tee joints of 09G2S steel strengthened by HFMP technology at different kinds of loading blocks

Sample number	Kind of loading block	1st loading*		2nd loading*		3rd loading			4th loading			$\sum \frac{n_i}{N_i}$, %
		σ_{1max}, MPa	n_1, thou cycles	σ_{2max}, MPa	n_2, thou cycles	σ_{3max}, MPa	n_3, thou cycles	n_3/N_3, %	σ_{4max}, MPa	n_4, thou cycles	n_4/N_4, %	
1	Increasing	260	387.2	275	261.8	290	185.7	25.0	305	82.4	16.0**	91.0
2		260	387.2	275	261.8	290	185.7	25.0	305	120.3	23.4**	98.4
3		260	387.2	275	261.8	290	185.7	25.0	305	109.7	21.3**	96.3
4	Decreasing	305	128.6	290	185.7	275	248.9	23.8**				73.8
5		305	128.6	290	185.7	275	155.8	14.9**				64.9
6		305	128.6	290	185.7	275	205.3	19.6**				69.6
7	Quasi-random	290	185.7	275	261.8	305	128.6	25.0	260	503.7	32.5**	107.5
8		290	185.7	275	261.8	305	118.3	23.0**				73.0
9		290	185.7	275	261.8	305	128.6	25.0	260	287.2	18.5	93.5

*For the 1st and 2nd loading n_1/N_1 and n_2/N_2 = 25 %. **Sample failed.

a reverse effect in the regularities of fatigue damage accumulation when a linear hypothesis is used compared to structural steels [4].

Experimentally established limit values of the sum of relative fatigue lives in fatigue testing of all the samples of welded joints strengthened by HFMP technology in as-welded condition, fall within narrower limits from 0.65 to 1.08. Scatter of values of the total damage for the increasing sequence of the applied loads is in the range from 0.91 to 0.98, for the decreasing sequence — from 0.65 to 0.74, and for the quasi-random loading mode — from 0.73 to 1.08, respectively. Therefore, for HFMP strengthened tee welded joints the applied load sequence does not have any significant influence on the cyclic fatigue life of the joints.

The established regularities of fatigue damage accumulation in the studied welded joints reflect their specific features compared to the base metal, such as presence of residual welding stresses and geometrical stress raiser α_σ, due to the joint shape. It is known that as a result of interaction of the residual stresses with the stress of alternating loading cycle, a new cycle of stresses of the same range as the initial one, but of another asymmetry, forms in the welded joint raiser zone. At unchanged parameters of cyclic loading applied to welded joints in the initial condition (R_σ = = 0) with high residual tensile stresses in the raiser zone, maximum σ^k_{max} and minimum σ^k_{min} cycle stresses are found from the following relationship [10]:

$$\sigma^k_{max} = \sigma_y, \quad (2)$$

$$\sigma^k_{min} = \sigma^y_{res} = \sigma_y - \alpha_\sigma\, 2\sigma_a, \quad (3)$$

where σ_y is the material yield point; σ^y_{res} are the steady-state residual stresses; σ_a is the stress amplitude of the alternating loading cycle.

Relationships (2) and (3) are written for an ideally elastoplastic material.

It is assumed that the properties of 09G2S steel are close to the ideally elastoplastic properties. Therefore, at plotting of an *S–N* curve (Figure 2) of the tee welded joints in the initial condition with residual tensile stresses $\sigma_{res} \approx 0.5\sigma_y$ a limit stress cycle of the respective range, in which σ^k_{max} reach the material yield point, is realized in the entire range of applied external loads in the raiser zone (α_σ = 1.5). In view of the above, increase of sample width (increase of the residual stress level) will not lead to a change in the stress cycle realized in the raiser zone, and, therefore, will not have any influence on the test results.

In the loading blocks maximum stress of the first level of applied loading has the determinant role in the regularity of fatigue damage accumulation by the welded joint. It is known that already after the first cycles of the initial loading stage a steady-state level of residual stresses σ^y_{res} which can be both tensile and compressive, forms in the raiser zone. These are exactly the stresses which will determine maximum σ^k_{max} and minimum σ^k_{min} cycle stresses in the raiser zone at the subsequent loading stage:

$$\sigma^k_{max} = \sigma^y_{res} + \alpha_\sigma 2\sigma_a, \quad (4)$$

$$\sigma^k_{min} = \sigma^y_{res}. \quad (5)$$

Similarly, the stress level of the previous loading stage will influence formation of alternating loading cycle of the next stage in the raiser zone. It should be noted that σ^k_{max} determined by ratio (4) cannot exceed the value equal to the material yield point, as proceeding from the model of an ideally elastoplastic material, it will only induce plastic deformations in the raiser zone.

Using relationships (2)–(5) let us consider in greater detail the alternating loading cycles which form in the stress raiser zone of a tee joint allowing for the influence of residual stresses and stress concentration factor at the impact of the above loading sequences. For welded joints in the initial condition at the increasing loading block (Figure 3, *a*) at each of its stages limit stress cycles ($\sigma^k_{max} = \sigma_y$) are implemented in the raiser zone, which are identical to those found when plotting the *S–N* curve. The influence of the residual stresses during loading leads to development of plastic deformations in the raiser zone at each

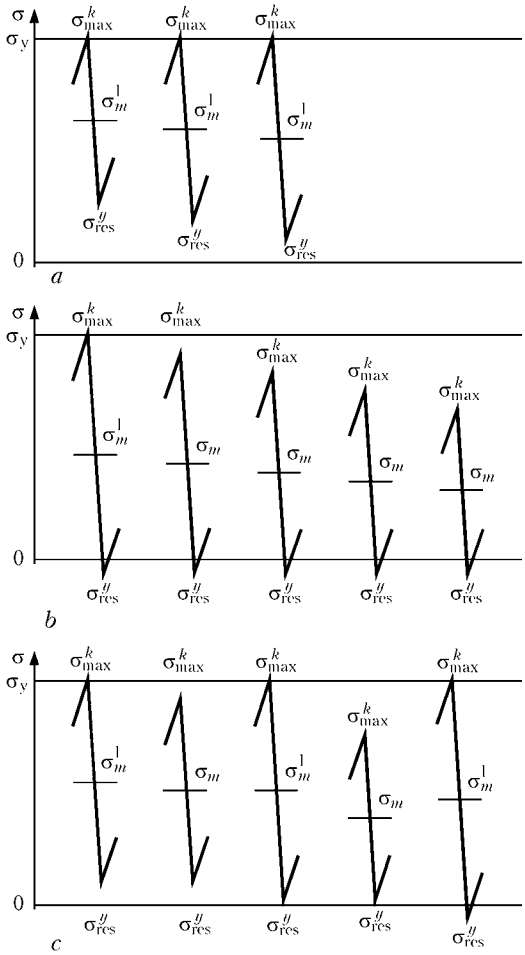

Figure 3. Schematic of stress ranges in the zone of welded joint raiser in as-welded condition at increasing (*a*), decreasing (*b*) and quasi-random (*c*) loading blocks

of its stages. At the decreasing loading block in the raiser zone (Figure 3, *b*) stress cycles are implemented, which are different from the limit ones, starting from the second loading stage. Their damaging ability is lower than that of the limit stress cycles which are realized at the same levels of external alternating loading when plotting *S–N* curve of welded joints in the initial condition. With a quasi-random loading block both limit and different from them stress cycles are realized in the raiser zone (Figure 3, *c*). Thus, at the same level of external loading the raiser zone develops a stress cycle of the same range, but with the stress cycle asymmetry dependent on the sequence of load application, the stresses being exactly what determines its damaging ability. Therefore, it is incorrect to calculate the damage fraction of the welded joints for the decreasing and quasi-random loading blocks by the *S–N* curve, in the plotting of which only the limit stress cycles are realized in the raiser zone. For these cases it is suggested to determine the total damage from the following formula:

$$D = \frac{n_1}{N_1} + \sum_{i=2}^{k} \frac{n_i}{N_i} \left(\frac{\sigma_{mi}}{\sigma_{mi}^{l}} \right), \qquad (6)$$

where σ_{mi} is the mean cycle stress in the raiser zone corresponding to *i*-th level of external alternating loading; σ_{mi}^{l} is the mean limit cycle stress in the raiser zone, corresponding to *i*-th level of external alternating loading.

Values of total damage of welded joints in the initial condition obtained from formula (6) are within the following ranges: with the rising sequence of load application — from 0.32 to 0.56, with decreasing sequence — from 0.96 to 1.20 and at quasi-random loading mode — from 0.80 to 1.15, respectively. As is seen, use of relationship (6) decreases the scatter of values of the limit sums of fatigue life fractions from the range of 0.33–1.97 to 0.33–1.20, while average values of total damage at decreasing and quasi-random loading blocks are close to a unity (1.10 and 0.95, respectively), which confirms the rationality of using this formula in calculation of the fatigue life of welded joints at different loading modes. A quite broad scatter range of total damage after application of relationship (6) is indicative of the fact that the processes occurring in the zone of weld transition to the base metal, are quite complicated and are not reduced just to allowance for residual stresses. Therefore, experimentally established from expression (6) average values of the limit sum of accumulated damage fractions for the studied kinds of loading should be assumed as the criteria of fatigue fracture of tee welded joints of 09G2S steel, as even for the base material it is not possible to establish the general regularity of fatigue damage accumulation depending on the load variation modes [1–3].

In welded joints strengthened by HFMP technology in as-welded condition, residual compressive stresses are induced in the concentrator zone, which may reach values close to the base material yield point. Therefore, when plotting the *S–N* curve of tee welded joints in the strengthened condition in the entire range of applied external loads a cycle of alternating stresses in which the maximum $\sigma_{\max}^{k}$ and minimum $\sigma_{\min}^{k}$ stresses are determined by relationships (4) and (5) is realized in the raiser zone. In the loading blocks the stress cycles realized in the raiser zone, are identical to those which occur when plotting the *S–N* curve of welded joints in the strengthened condition and are independent on the level and pattern of applied stresses (this is schematically shown in Figure 4). Average values of limit summary damage derived by the linear hypothesis of fatigue damage accumulation (for the increasing sequence of applied loads — 0.95, decreasing — 0.69 and for quasi-random loading — 0.91) are indicative of a weak sensitivity of strengthened joints to loading sequence. For the studied loading modes these values should be taken as the criteria of fatigue damage of tee welded joints of 09G2S steel strengthened by HFMP technology. However, in view of their slight difference from the strengthened welded joints, application of Palmgren–Meiner hypothesis is quite justified (1). Differences in the regularities of fatigue damage accumulation and in scatter of values

of limit sums of fatigue life fractions of welded joints in the initial (0.33–1.20) and HFMP strengthened as-welded conditions (0.65–1.07), respectively, are due to their specific features, namely different coefficients of stress concentration and residual stress levels; difference of plastic deformations in the zone of transition of the weld to base metal; different condition of the surfaces, etc.

CONCLUSIONS

1. *S–N* curves of tee joints of 09G2S steel in the initial and HFMP strengthened as-welded condition have been established.

2. Within the hypothesis of linear summation of fatigue damage fracture criteria of tee welded joints of 09G2S steel in the initial and HFMP strengthened as-welded condition were established at the increasing, decreasing and quasi-random loading blocks. It is confirmed that the sequence of load application has an essential influence on fatigue damage accumulation in the welded joints in the initial condition.

3. It is experimentally established that the regularities of fatigue damage accumulation at the increasing, decreasing and quasi-random blocks of loading tee welded joints strengthened by HFMP in as-welded condition, are in good agreement with Palmgren–Meiner linear hypothesis.

4. A relationship is proposed for fatigue damage accumulation in unstrengthened welded joints allowing for the influence of residual welding stresses and stress concentration factor of the joints which essentially reduces the scatter of limit damage sums irrespective of the applied load pattern.

1. Manson, S.S., Halford, G.R. (1986) Re-examination of cumulative fatigue damage analysis — an engineering perspective. *Eng. Frac. Mech.*, **25**, 539–571.
2. Troshchenko, V.T., Sosnovsky, L.A. (1987) *Fatigue resistance of metals and alloys*: Refer. Book. Part 1. Kiev: Naukova Dumka.
3. Collins, J. (1984) *Damage of materials in structures. Analysis, prediction, prevention*. Moscow: Mir.
4. (1990) *Strength of welded joints under alternating loads*. Ed. by V.I. Trufyakov. Kiev: Naukova Dumka.
5. Trufyakov, V.I. (1973) *Fatigue of welded joints*. Kiev: Naukova Dumka.
6. Gurney, T.R. (1979) *Fatigue of welded structures*. Cambridge: Cambridge Univ. Press.
7. Blom, A.F. (1998) Spectrum fatigue behaviour of welded joints. *Int. J. Fatigue*, **17**, 485–491.
8. Sonsino, C.M., Lagoda, T., Demofonti, G. (2004) Damage accumulation under variable amplitude loading of welded medium- and high-strength steels. *Ibid.*, **26**, 487–495.

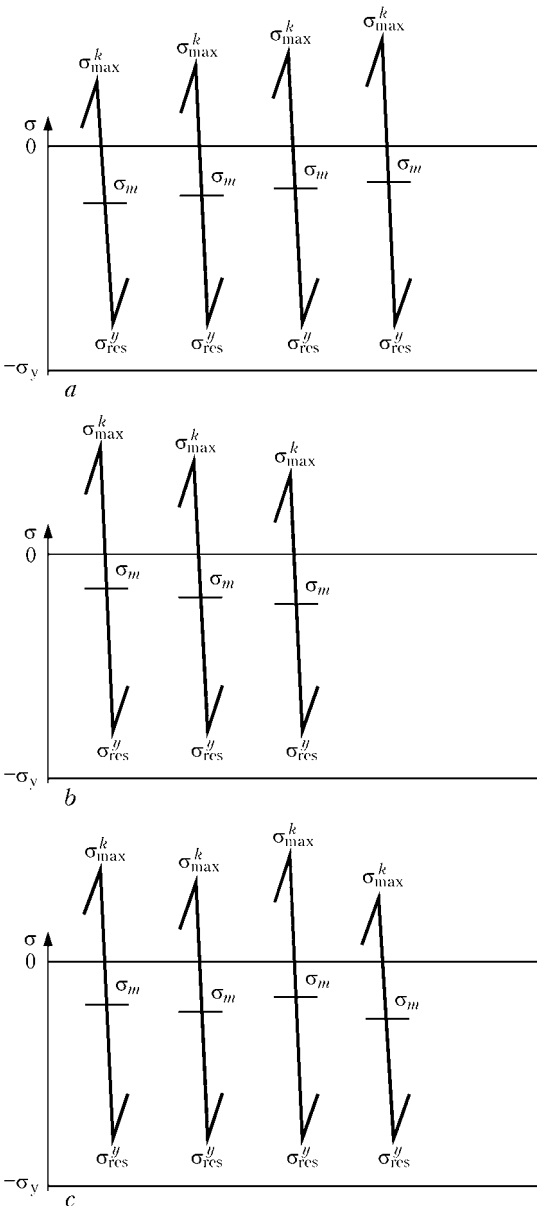

Figure 4. Schematic of stress ranges in the raiser zone of a welded joint strengthened by HFMP at an increasing (*a*), decreasing (*c*) and qausi-random loading blocks

9. Huo, L., Wang, D., Zhang, Y. (2005) Investigation of the fatigue behaviour of the welded joints treated by TIG dressing and ultrasonic peening under variable amplitude load. *Ibid.*, **27**, 95–101.
10. Trufyakov, V.I., Kudryavtsev, Yu.F., Mikheev, P.P. (1988) About influence of residual stresses on fatigue resistance of welded joints. *Avtomatich. Svarka*, **2**, 1–4.

MODELLING OF THE PROCESSES OF EVAPORATION OF METAL AND GAS DYNAMICS OF METAL VAPOUR INSIDE A KEYHOLE IN LASER WELDING

I.V. KRIVTSUN[1], **S.B. SUKHORUKOV**[1], **V.N. SIDORETS**[1] and **O.B. KOVALEV**[2]
[1]E.O. Paton Electric Welding Institute, NASU, Kiev, Ukraine
[2]S.A. Khristianovich Institute of Theoretical and Applied Mechanics, RAS Siberian Division, Novosibirsk, Russia

Self-consistent mathematical models are suggested to describe processes of metal evaporation, surface condensation and gas dynamics of metal vapour inside a keyhole formed in molten metal in deep-penetration laser welding. Numerical analysis of thermal and gas-dynamic characteristics of the flow of vapour inside the keyhole in laser welding of steel has been conducted. The effect of the gas-dynamic processes on the state of vapour in the keyhole, its pressure on the keyhole wall and heat exchange in the molten pool induced by the processes of evaporation and condensation on its free surface has been studied.

Keywords: *laser welding, keyhole, evaporation, surface condensation, gas dynamics, metal vapour, mathematical model*

Materials joining and treatment processes involving high-density energy sources have been attracting an increasing attention of researchers. One of such processes is laser welding of metals performed in the deep (or keyhole) penetration mode. To implement this process, the required radiation power density should be not less than $1 \cdot 10^5$ W/cm^2 [1]. Affected by such a concentrated energy source, the metal welded is not only melted, but also locally overheated to temperatures that exceed its boiling point. This heating induces intensive evaporation of the metal and spread of the vapour, which is accompanied by formation of a reactive force causing distortion of the melt surface [1, 2]. As a result, a deep and narrow channel filled with the metal vapour, which is called a keyhole, is formed in the weld pool.

Technical literature abounds with publications describing theoretical research and mathematical modelling of physical phenomena occurring in deep-penetration laser welding [3, 4], and investigations of the mechanisms of formation of the keyhole [5–7] and its stability [8, 9], determining stability of the welding process. At the same time, while describing evaporation of metal and gas-dynamic processes in the flow of the metal vapour, governing the pressure on the melt surface and, eventually, shape and size of the keyhole, the majority of the said publications use very rough approximations, namely: either the vapour inside the keyhole is assumed to be equilibrium (saturated) [3, 8], or its velocity near the evaporating surface is assumed to be equal to a local velocity of sound [7]. Such approximations do not allow correct calculation of gas-dynamic characteristics of the vapour flow inside the keyhole and, hence, distribution of the overall (including reactive) vapour pressure on the keyhole wall. Moreover, authors of the said studies do not consider the possibility of condensation of the metal vapour on some part of the keyhole surface, which, combined with intensive evaporation of the rest of the melt surface, may have a substantial effect on the local energy balance of this surface.

Main objectives of the present study were to develop a self-consistent mathematical model of the processes of metal evaporation, surface condensation and gas dynamics of the metal vapour inside the keyhole of a preset shape, as well as to conduct numerical analysis of gas-dynamic and thermal characteristics of the vapour flow. An important peculiarity of such a model should be allowance for non-equilibrium of the vapour, related to the probability of its outflow from the molten metal surface (by way of evaporation) or inflow to it (by way of condensation), movement of the vapour along the keyhole, and its subsequent effusion to the external gas environment.

The mathematical model suggested is based on approximation of the actual keyhole to a corresponding axisymmetric deepening in the melt (Figure 1), whose free surface in the cylindrical coordinate system is set by relationship $r = R(z)$, where $R(z)$ is the local value of the keyhole radius, which is assumed to vary slowly in depth H of the keyhole. The model uses the effective axisymmetric distribution of temperature of the keyhole wall, $T_s(z)$, instead of the known (determined from solution of the equation of heat transfer in the metal welded) spatial distribution of temperature of the free surface of the melt. The probability of bulk condensation of the metal vapour inside the keyhole and formation of microdrops are neglected. And, finally, it is assumed that the vapour filling the keyhole is non-ionised, which is a good approximation for laser welding using short-wave solid-state lasers.

Dependence of pressure p_s of the saturated vapour near the surface of the molten metal upon its temperature can be determined by using the Clapeyron–Clausius equation written down, e.g. as follows [1]:

© I.V. KRIVTSUN, S.B. SUKHORUKOV, V.N. SIDORETS and O.B. KOVALEV, 2008

$$p_s = p_0 \exp\left[\frac{\lambda}{k}\left(\frac{1}{T_b} - \frac{1}{T_s}\right)\right], \quad (1)$$

where p_0 is the atmospheric pressure; λ is the atomic work function of the melt; k is the Boltzmann constant; and T_b is the metal boiling temperature, at which the saturated vapour pressure is equal to the atmospheric pressure. To allow for impact by non-equilibrium of the vapour formed in the convective mode of evaporation or surface condensation on characteristics of the metal vapour near the keyhole wall, the use is made of an approach suggested in study [10] to describe the process of rapid surface evaporation of metals under conditions of the intensive laser effect, and generalised in [11] for a case of surface condensation. The point of this approach consists in regarding a thin Knudsen layer formed in the vapour phase near the interface with the molten layer as a gas-dynamic discontinuity (with certain assumptions on the kind of functions of distribution of vapour particles at boundaries of this layer), as well as in using balance relationships derived by means of the laws of conservation of the flows of particles and their momentum and energy flows.

To substantiate appropriateness of employing this approach, it should be taken into account that thickness of the Knudsen layer equal to several lengths of the free path of the vapour particles ($L_K \le 1 \cdot 10^{-2}$ mm) is much smaller than radius of the keyhole ($R \le 1$ mm) under the deep-penetration laser welding conditions. This means that the Knudsen layer can be considered flat and locally unidimensional, and boundary of the gas-dynamic region of the vapour flow in the keyhole can be conditionally superposed with the keyhole wall.

In the context of this consideration, we can derive a system of algebraic equations to find the distributions of temperature $\overline{T}(z)$, mass density $\overline{\rho}(z)$ (or pressure $\overline{p}(z)$) of the metal vapour along the length of the keyhole at the Knudsen layer and gas-dynamic flow region interface [10, 11]:

$$\frac{\overline{T}}{T_s} = 1 + \frac{\overline{m}^2\pi}{32}\left(1 - \frac{8}{\overline{m}\sqrt{\pi}}\sqrt{1 + \frac{\overline{m}^2\pi}{64}}\right);$$

$$\frac{\overline{\rho}}{\rho_s} = \left\{\left(\overline{m}^2 + \frac{1}{2}\right)\exp(\overline{m}^2)\,[1 - \Phi(\overline{m})] - \frac{\overline{m}}{\sqrt{\pi}}\right\}\frac{T_s^{1/2}}{T^{1/2}} + \quad (2)$$

$$+ \frac{1}{2}\left\{1 - \overline{m}\sqrt{\pi}\exp(\overline{m}^2)\,[1 - \Phi(\overline{m})]\right\}\frac{T_s}{\overline{T}},$$

where $\overline{m}(z) = \overline{v}\left(\frac{M}{2k\overline{T}}\right)^{1/2}$; M is the mass of atom of the vapour; $\overline{v}(z)$ is the local value of the mean-mass velocity of its movement in a direction normal to the melt surface ($\overline{v} > 0$ corresponds to evaporation, and $\overline{v} < 0$ — to condensation); $\rho_s(z) = p_s M/kT_s$ is the saturated vapour density corresponding to a given value of $T_s(z)$; and $\Phi(x) = \frac{2}{\sqrt{\pi}}\int_0^x \exp(-\xi^2)d\xi$ is the probability integral. Here and below all the values relating to the boundary of the gas-dynamic flow region are marked with a line over a letter.

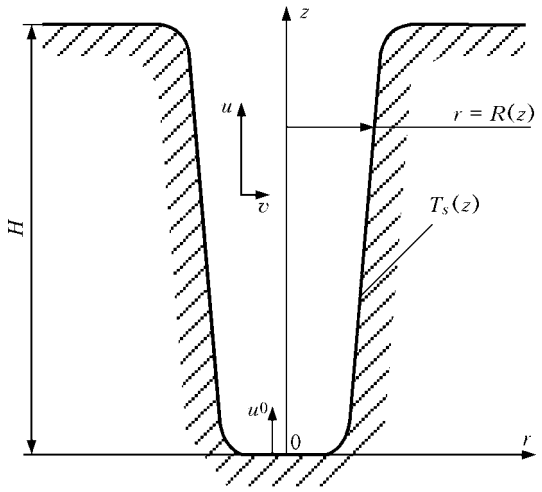

Figure 1. Approximation of keyhole to axisymmetric deepening in the melt (see designations in the text)

If the metal vapour is regarded as a monatomic ideal gas, its residual pressure at the said boundary can be determined from the following known relationship:

$$\overline{p} = \frac{\overline{\rho}k\overline{T}}{M}, \quad (3)$$

and the distribution of overall pressure $P(z)$ (allowing for the reactive component) exerted by a moving (expanding or condensed) vapour on the keyhole surface — from the following expression [1]:

$$P = \overline{p}\left(1 + \frac{5}{3}\overline{\mathrm{M}}^2\right), \quad (4)$$

where $\overline{\mathrm{M}}(z) \equiv \overline{v}/\overline{s}$ is the value of the Mach number at the boundary of the gas-dynamic region of the Knudsen layer; and $\overline{s} = \sqrt{5k\overline{T}/3M}$ is the local velocity of sound. It should be noted that the velocity of the vapour at this boundary should be limited by the $\overline{\mathrm{M}} \le 1$ condition [10].

The calculated values of dimensionless parameters $\overline{\rho}/\rho_s$, $\overline{T}/T_s$, $\overline{p}/p_s$, as well as P/p_s characterising the pressure on the molten metal surface, depending upon the Mach number of the vapour flow through the boundary of the gas-dynamic region are given in the Table. As follows from the data presented, with increase in the velocity of outflow of the vapour from the evaporating surface its gas-static pressure and pressure on the said surface become much lower than the corresponding pressure of the saturated vapour. As to $\overline{p}/p_s$ and P/p_s in condensation of the vapour on the melt surface, their values may be much in excess of p_s.

Analysis of the Knudsen layer near the keyhole surface gives no information on $\overline{\mathrm{M}}$ values of the vapour flow through the gas-dynamic flow region. In other words, here the velocity of the vapour normal

Characteristics of vapour near the melt surface in convective evaporation and surface condensation

$\bar{M}$		$\bar{T}/T_s$		$\bar{\rho}/\rho_s$		$\bar{p}/p_s$		P/p_s	
0		1		1		1		1	
0.05	−0.05	0.980	1.021	0.927	1.081	0.908	1.104	0.912	1.108
0.10	−0.10	0.960	1.041	0.861	1.171	0.827	1.219	0.841	1.240
0.20	−0.20	0.922	1.084	0.748	1.384	0.690	1.501	0.736	1.602
0.40	−0.40	0.851	1.175	0.576	1.985	0.490	2.333	0.621	2.956
0.60	−0.60	0.785	1.274	0.457	2.693	0.358	3.774	0.573	6.039
0.80	−0.80	0.725	1.380	0.371	4.619	0.269	6.376	0.556	13.181
1.00	−1.00	0.669	1.495	0.308	7.531	0.206	11.256	0.549	30.023

to the melt surface in transition through the Knudsen layer can be arbitrarily chosen without any violation of the laws of conservation of mass, momentum and energy [10]. This result is not unusual, as the same is also true for the Rankin–Hugonio conditions for shock waves [12]. Distribution of the $\bar{v}$ (or $\bar{M}$) values along the keyhole surface should be determined only on the basis of solving the gas-dynamic equations describing the vapour flow in this keyhole.

For modelling of gas dynamics and thermal state of the metal vapour in the considered axisymmetric keyhole (see Figure 1), we make use of the system of equations describing a laminar motion of the compressed gas [12]. Assuming that the axial (along the keyhole axis) component of the vapour flow velocity, $u(r, z)$, is much higher than the radial component, $v(r, z)$, and considering that changes of all the values are most significant in the radial direction, this system of equations can be written down in an approximation of the boundary layer for internal axisymmetric flows [13]:

$$\frac{1}{r}\frac{\partial}{\partial r}(r\rho v) + \frac{\partial}{\partial z}(r\rho u) = 0; \tag{5}$$

$$\rho\left(v\frac{\partial u}{\partial r} + u\frac{\partial u}{\partial z}\right) = \frac{1}{r}\frac{\partial}{\partial r}\left(r\eta\frac{\partial u}{\partial r}\right) - \frac{d\bar{p}}{dz}; \tag{6}$$

$$\rho C_p\left(v\frac{\partial T}{\partial r} + u\frac{\partial T}{\partial z}\right) = \frac{1}{r}\frac{\partial}{\partial r}\left(r\chi\frac{\partial T}{\partial r}\right) + u\frac{d\bar{p}}{dz} + \eta\left(\frac{\partial u}{\partial r}\right)^2. \tag{7}$$

Here $\rho(T, \bar{p})$ is the mass density; $\eta(T)$ is the dynamic viscosity factor; $\chi(T)$ is the coefficient of thermal conductivity of the vapour; C_p is its specific heat under a constant pressure; and $T(r, z)$ is the spatial distribution of temperature in the vapour flow. As within the framework of approximation of the boundary layer the pressure across its section is assumed to be constant [13], these equations use a corresponding value of the gas-static pressure of the vapour near the keyhole wall, $\bar{p}(z)$.

The distribution of values $d\bar{p}/dz$ and, hence, vapour pressure $\bar{p}$ along the keyhole length can be found from an integral condition of balance of the vapour mass flow through a cross section of the keyhole [14], allowing for the inflow of the vapour to the gas-dynamic region (due to evaporation of the wall), or its outflow (due to condensation on the keyhole wall):

$$G(z) \equiv 2\pi\int_0^{R(z)} r\rho(r, z)u(r, z)dr = \\ = G(0) + 2\pi\int_0^z R(r)\bar{\rho}(z)\bar{v}(z)dz. \tag{8}$$

Here $G(0)$ is the mass flow of the vapour at the initial section of the keyhole (at $z = 0$); value $\bar{p}(z)$ is expressed in terms of density $p_s(z)$ of the saturated vapour corresponding to the preset temperature of the keyhole, $T_s(z)$, and vapour velocity $\bar{v}(z)$ determined in each section of the keyhole by using equations (2) and relationship (3), with the found value of $\bar{p}(z)$ substituted into it.

To close the system of equations (5) through (7), it is necessary to determine dependencies of the density, specific heat and coefficients of transfer of the metal vapour upon the temperature and pressure. Allowing for the above assumption that vapour is an ideal monatomic gas, in analogy with (3) we can write down that

$$\rho = \frac{\bar{p}M}{kT}, \tag{9}$$

and determine its heat capacity under a constant pressure as follows [15]:

$$C_p = \frac{5}{2}\frac{k}{M}. \tag{10}$$

As to the coefficients of viscosity and thermal conductivity of the metal vapour, within the framework of the model of hard elastic spheres, for example, these values can be calculated as follows [16]:

$$\chi = \frac{75}{64}\frac{\sqrt{k^3T}}{\sqrt{\pi M}r_0^2}; \quad \eta = \frac{5}{16}\frac{\sqrt{kTM}}{\sqrt{\pi}r_0^2}, \tag{11}$$

where r_0 is the effective radius of the metal atom.

To solve the system of differential equations (5) through (7), it is also necessary to set the corresponding edge and initial (input) conditions for the boundaries of the calculation region $\{0 \le r \le R(z);\ 0 \le z \le H\}$ (see Figure 1). Boundary conditions on the keyhole axis are selected from the considerations that the vapour flow is characterised by a cylindrical symmetry

$$\frac{\partial u}{\partial r} = 0;\ v = 0;\quad \frac{\partial T}{\partial r} = 0 \quad \text{at} \quad r = 0. \qquad (12)$$

It is assumed that tangent to the surface of the vapour velocity component is equal to zero on the side surface of the keyhole or, to be more exact, on the external boundary of the Knudsen layer, and its temperature is chosen to be equal to the corresponding value of temperature at the boundary of the gas-dynamic region, which is determined from the known values of $T_s(z)$ and using the first equation from (2), i.e.

$$u = 0;\quad T(z) = \overline{T}(z) \quad \text{at} \quad r = R(z). \qquad (13)$$

Input conditions at the keyhole bottom are set on the basis of an assumption that here there is a certain velocity of vapour, u_0, which is directed along axis Oz, and is constant across the keyhole section:

$$u(r) = u^0;\ v(r) = 0;\ T(r) = \overline{T}(0) \quad \text{at} \quad z = 0. \qquad (14)$$

Here the $\overline{T}(0)$ values, like above, can be found by using the first equation from (2), with $T_s(0)$ and $\overline{v}(0) = u^0$ substituted into it. The chosen conditions make it possible to determine the mass flow of the vapour at the initial section of the keyhole, which is part of integral balance (8):

$$G(0) = \pi R^2(0)\overline{\rho}(0)u^0, \qquad (15)$$

where $\overline{\rho}(0)$ is the value of the density of the metal vapour corresponding to the above values of its temperature and velocity. Also, they make it possible to calculate the pressure of the vapour near the keyhole bottom, $\overline{p}(0)$, which can be found by using relationship (3). And, finally, to find unknown parameter u^0, it is possible to use the following integral condition:

$$\overline{p}(H) = \overline{p}(0) + \int_0^H \frac{d\overline{p}}{dz}\, dz, \qquad (16)$$

where $\overline{p}(H)$ is the pressure of the metal vapour at exit from the keyhole, equal to pressure in the external gas environment.

This concludes description of the self-consistent mathematical model of the processes of evaporation of metal, surface condensation and gas dynamics of the metal vapour in the axisymmetric keyhole.

The system of non-linear differential equations (5) through (7) was solved by the finite difference method using the basic difference scheme for integration of the boundary layer equations [17]. Second-order equations (6) and (7) were approximated by the implicit two-layer six-point difference scheme, while first-order equation (5) — by the explicit four-point one. The resulting algebraic system of difference equations was solved by the sweep method using iterations.

The corresponding software was developed, and detailed numerical analysis of thermal and gas-dynamic characteristics of the metal (iron) vapour flow in the keyhole of a preset shape was conducted on the basis of the described calculation scheme. The calculations were made by using the relationships of temperature of the melt surface, $T_s(z)$, and radius of the keyhole, $R(z)$, determined by means of the mathematical model [3] for the conditions of laser welding of low-carbon steel (laser beam power — 2.5 kW, beam radius in the focal plane — 0.25 mm, lens focal distance — 150 mm, welding speed — 0.8 cm/s, shielding gas — helium, and pressure in the external environment — atmospheric). The shape and size of such a keyhole are shown in Figure 2.

Radial distributions of the velocity and temperature of the metal vapour in reference sections of the keyhole considered are shown in Figure 3. As follows from the given calculation data, the axial component of the vapour velocity in all the sections of the keyhole has the highest value on its axis, and decreases to zero with distance to the keyhole wall (Figure 3, *a*). Its profile is similar to the profile of velocity of the Poiseuille's flow [12]. The maximal vapour velocity at exit from the keyhole (at $z = H = 6.9$ mm) amounts to about 150 m/s.

The calculated values of the radial velocity component are much lower (Figure 3, *b*), which allows the use of approximation of the boundary layer to be fully justified. At the same time, the vapour flow in the radial direction has a very complex structure. Near the keyhole bottom (at $z = 1$ mm) the radial velocity is practically equal to zero, except for a small region adjoining the side wall of the keyhole, where it has negative values. This corresponds to movement of the vapour from the evaporating surface to the keyhole axis (curve *1* in Figure 3, *b*). At $z = 3$ mm, the values of the radial velocity become positive across the entire section of the keyhole (curve *2*), this meaning transition from wall evaporation to surface condensation

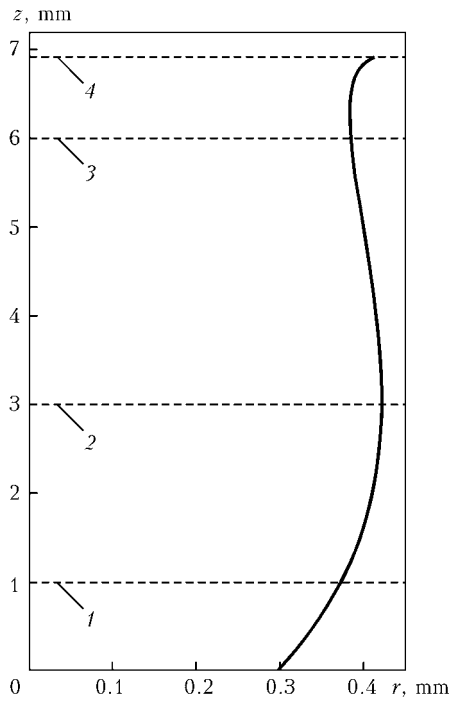

Figure 2. Shape and size of the keyhole used for calculations: *1–4* — reference sections of the keyhole

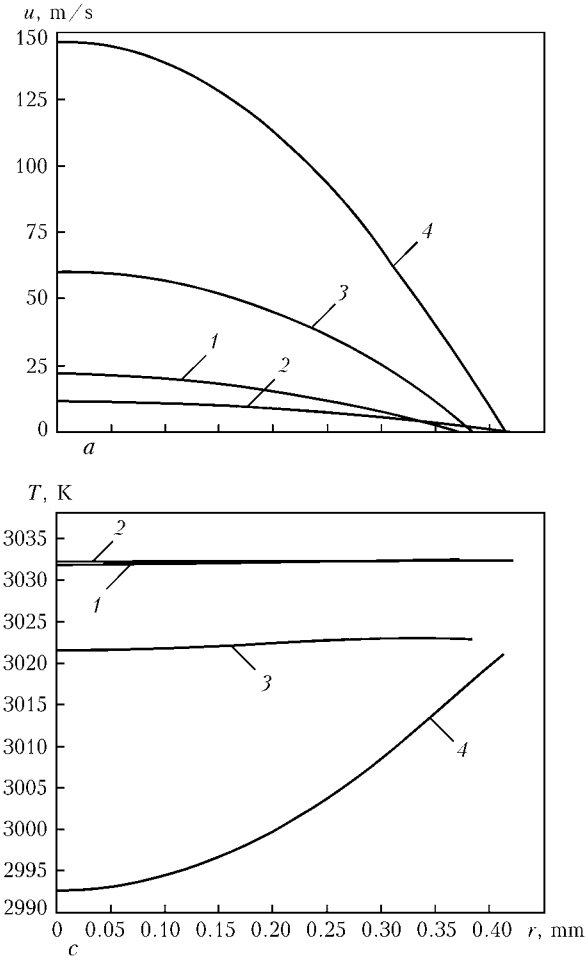

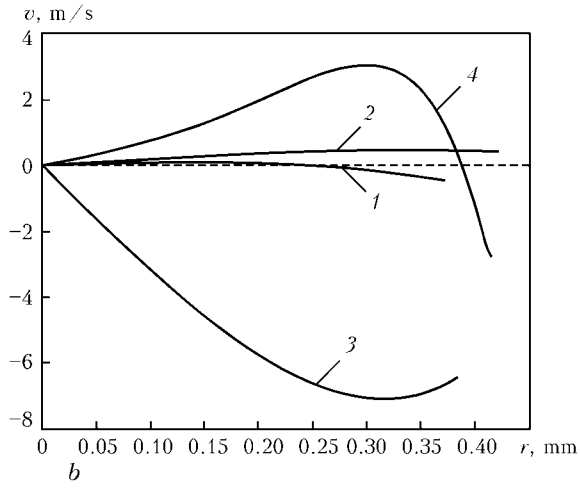

Figure 3. Radial distributions of axial (*a*) and radial (*b*) components of velocity v of the metal vapour and its temperature T (*c*) in sections of the keyhole: *1–4* — see Figure 2

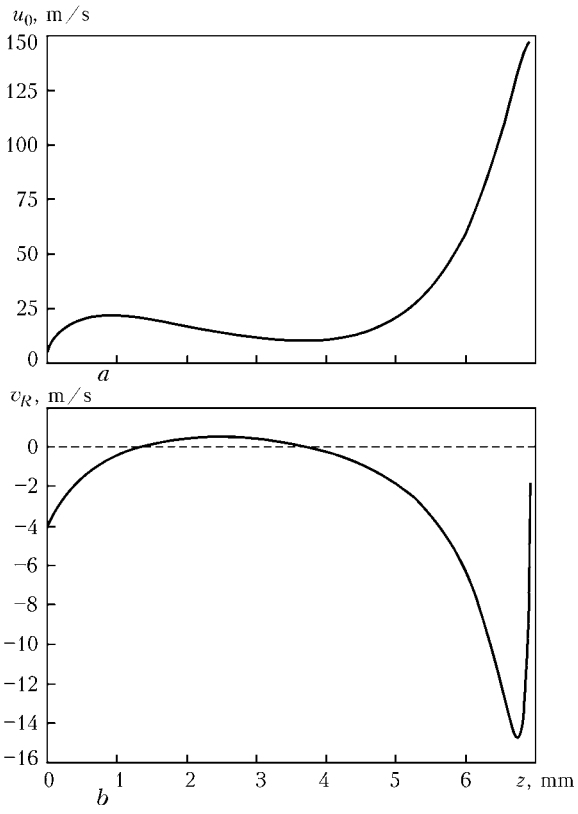

Figure 4. Distribution of axial velocity u_0 of the metal vapour along the keyhole axis (*a*), and radial velocity v_R of the vapour near the melt surface (*b*) in depth of the keyhole

of the vapour. Then, at z = 6 mm, the vapour again becomes directed from the evaporating wall to the keyhole axis (curve *3*), and, finally, at the exit section (z = 6.9 mm) the vapour in the near-axis zone of the keyhole moves to the wall, and in the near-wall zone — to the keyhole axis (curve *4*).

As shown by the calculation of temperature of the metal vapour, the lowest temperature in any section of the keyhole is exhibited by the vapour located in the near-axis zone of the keyhole, the temperature distribution non-uniformity increasing with distance to the exit section of the keyhole (Figure 3, *c*). This is associated with the known effect of cooling of the vapour in its expansion [12, 15].

The distributions of the vapour velocity on the axis, $u_0(z) \equiv u(O, z)$, and near the keyhole wall, $v_R(z) \equiv v(R, z) = -\bar{v}(z)$, in depth of the keyhole, are shown in Figure 4. As follows from Figure 4, *a*, movement of the metal vapour along the keyhole first speeds up, then slows down a bit, and then speeds up again. This is related to variations in its mass flow through the keyhole section because of the processes of evaporation and surface condensation on the keyhole wall. Indeed, the radial velocity of the vapour near the keyhole wall (at the gas-dynamic region boundary) is negative near the keyhole bottom (see Figure 4, *b*), i.e. the vapour flows into the keyhole, this corresponding to the evaporation region. Then, at z > 1.4 mm, it becomes positive, this corresponding

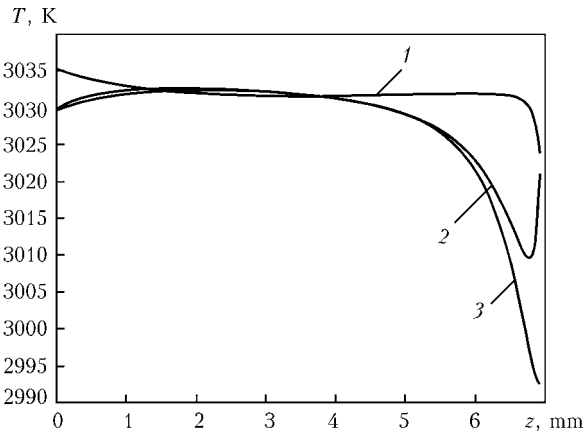

Figure 5. Distribution of temperature of the melt surface (*1*), metal vapour near this surface (*2*), and on the keyhole axis (*3*)

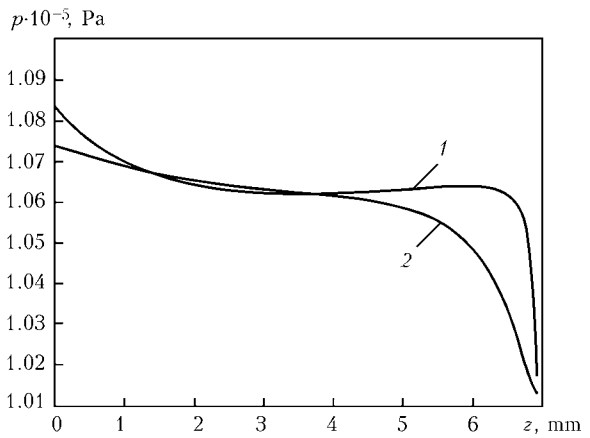

Figure 6. Distribution of pressure p in depth of the keyhole: *1* — pressure of saturated vapour corresponding to a given value of the keyhole surface temperature; *2* — pressure of metal vapour determined as a result of solving the gas-dynamic problem

to the surface condensation region, and, as a result, to decrease of the G and u_0 values. At last, at $z > 3.7$ mm, the surface condensation again changes into the wall evaporation, this parameter reaching its maximal value, i.e. about 15 m/s, near the exit section (Figure 4, *b*).

The presence of the vapour surface condensation region can be well seen in Figures 5 and 6, which show the distribution of the vapour temperature and pressure along the length of the keyhole. As follows from the calculated data shown in these Figures, the vapour temperature and pressure near the keyhole wall in a region of 1.4 mm $< z <$ 3.7 mm exceed the corresponding values of T_s and p_s (curves *1* and *2* in Figures 5 and 6), i.e. this is the case of condensation of the metal vapour on the keyhole surface. As to the values of pressure of the vapour and its overall pressure (including the reactive pressure) on the keyhole wall, these values, e.g. near the keyhole exit section, may be almost $5 \cdot 10^3$ Pa lower than in the case of using the saturated vapour model (Figure 6). Therefore, when determining the shape of the keyhole and, hence, distribution of the laser radiation power absorbed by the free surface of the melt, it is necessary to take into account the gas dynamics of the vapour inside the keyhole.

Another factor which may be essential for consideration of energy balance on the keyhole surface is heat exchange induced by the processes of evaporation and surface condensation of the metal vapour on the keyhole wall. Figure 7 shows distribution q of the heat flow transferred by the metal vapour through the keyhole surface in depth of the keyhole:

$$q(z) = \frac{\overline{\rho}(z)}{M}\,\overline{v}(z)\left[\lambda + \frac{5}{2}\,k\overline{T}(z) + \frac{1}{2}\,\overline{Mv^2}(z)\right]. \qquad (17)$$

As follows from the calculated data shown in this Figure, the keyhole surface can be subdivided into three regions. The region of a positive heat flow directed towards the keyhole wall (heating through surface condensation of the vapour and energy of the atomic bond in the melt released in this case) separates the two regions, where the vapour removes the energy (cooling of the melt surface as a result of evaporation). The maximal absolute value of the heat flow carried by the vapour from the keyhole surface is achieved near the keyhole exit and amounts to about $3 \cdot 10^7$ W/m^2. These values of the heat flow, substantial as they are, are indicative of the need to take it into account in analysis of the heat exchange processes occurring on the surface of the weld pool for conditions of deep-penetration laser welding.

To characterise the state of the metal vapour filling the keyhole, it is possible to use dimensionless parameter θ, which determines the extent of overcooling of the vapour [18]:

$$\theta = \frac{T_p - T}{T_p}, \qquad (18)$$

where T_p is the temperature of the saturated vapour at the preset density; and T is the actual temperature of the vapour. At this setting of the overcooling extent, condition $\theta > 0$ corresponds to the oversaturated (overcooled) vapour, and $\theta < 0$ — to the overheated one (in the first case the vapour may condense in the bulk of the keyhole to form the condensate particles that scatter laser radiation). As shown by the calculations, the keyhole under consideration can be subdivided into three zones, based on

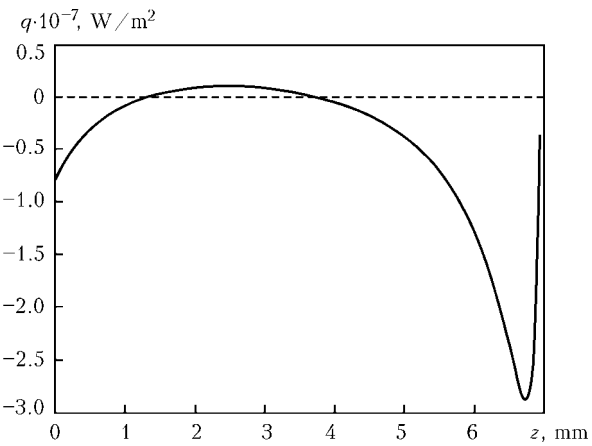

Figure 7. Distribution q of heat flow transferred by the vapour through its surface in depth of the keyhole

the state of the vapour. The vapour is oversaturated in the zone where evaporation of the keyhole wall takes place, this corresponding to the data of study [2]. And it is overheated in the zone where surface condensation occurs. The extent of overcooling of the metal vapour in the keyhole investigated is low and equals just a few percent, this justifying neglect of the bulk condensation of the vapour.

The authors express their appreciation to Prof. G.A. Turichin for providing the calculated data on the shape, size and temperature of the surface of the keyhole in laser welding of low-carbon steel.

The study performed under integrated project 2.10 «Laser Treatment of Materials. Scientific Principles of Application of High-Density Energy Sources for Welding of Metals and Alloys» was supported by the National Academy of Sciences of Ukraine and Siberian Division of the Russian Academy of Sciences.

1. Arutyunyan, R.V., Baranov, V.Yu., Bolshov, L.A. et al. (1989) *Effect of laser radiation on materials*. Moscow: Nauka.
2. Anisimov, S.I., Imas, Ya.A., Romanov, G.S. et al. (1970) *Effect of high power radiation on metals*. Moscow: Nauka.
3. Lopota, V.A., Sukhov, Yu.T., Turichin, G.A. (1997) Model of deep-penetration laser welding for application in technology. *Izvestiya AN SSSR. Series Physics*, 61(**8**), 1613–1618.
4. Rai, R., Elmer, J.W., Palmer, T.A. et al. (2007) Heat transfer and fluid flow during keyhole mode laser welding of tantalum, Ti–6Al–4V, 304L stainless steel and vanadium. *J. Phys. D: Appl. Phys.*, **40**, 5733–5766.
5. Kaplan, A. (1994) A model of deep penetration laser welding based on calculation of the keyhole profile. *Ibid.*, **27**, 1805–1814.
6. Semak, V.V., Bragg, W.D., Damkroger, B. et al. (1999) Transition model for the keyhole during laser welding. *Ibid.*, **32**, 61–64.
7. Amara, E.H., Fabbro, R., Bendib, A. (2003) Modeling of the compressible flow induced in a keyhole during laser welding. *J. Appl. Phys.*, 93(**7**), 4289–4296.
8. Turichin, G.A. (1996) Hydrodynamic aspects of stability of the keyhole in beam welding methods. *Fizika i Khimiya Obrab. Materialov*, **4**, 74–82.
9. Lee, J.Y., Ko, S.H., Farson, D.F. et al. (2002) Mechanism of keyhole formation and stability in stationary laser welding. *J. Phys. D: Appl. Phys.*, **35**, 1570–1576.
10. Knight, Ch.J. (1979) Theoretical modelling of rapid surface vaporization with back pressure. *AIAA J.*, 17(**5**), 519–523.
11. Demchenko, V.F., Krivtsun, I.V., Nesterenkov, V.M. (2004) Model of evaporation-condensation processes occurring on a flat surface. *Dopovidi Nats. Akad. Nauk Ukrainy*, **1**, 90–94.
12. Landau, L.D., Lifshits, E.M. (1986) *Theoretical physics*. Vol. 6: Hydrodynamics. Moscow: Nauka.
13. Lojtsyansky, L.G. (1962) *Laminar boundary layer*. Moscow: Fizmatgiz.
14. Anderson, D., Tannekhill, J., Pletcher, R. (1990) *Computational hydromechanics and heat exchange*. Vol. 1. Moscow: Mir.
15. Landau, L.D., Lifshits, E.M. (1976) *Theoretical physics*. Vol. 5: Statistical physics. Moscow: Nauka.
16. Smirnov, B.M. (1978) *Physics of low-ionized gas*. Moscow: Nauka.
17. Paskonov, V.M., Polezhaev, V.I., Chudov, L.A. (1984) *Numerical modelling of heat and mass exchange processes*. Moscow: Nauka.
18. Zeldovich, Ya.B., Rajzer, Yu.P. (1966) *Physics of shock waves and high-temperature hydrodynamic phenomena*. Moscow: Nauka.

INFLUENCE OF FRICTION STIR WELDING PROCESS PARAMETERS ON WELD FORMATION IN WELDED JOINTS OF ALUMINIUM ALLOYS 1.8–2.5 mm THICK

A.G. POKLYATSKY, A.Ya. ISHCHENKO and **S.V. PODIELNIKOV**
E.O. Paton Electric Welding Institute, NASU, Kiev, Ukraine

Geometrical dimensions of working surfaces of tools, requirements to edge preparation of butt joints on aluminium alloys, and desired accuracy of their assembly and fixation, have been experimentally det ermined. The ranges of variation of process parameters, providing defect-free welded joints, have been established.

Keywords: *friction stir welding, aluminium alloys, process parameters, weld formation, faultlessness*

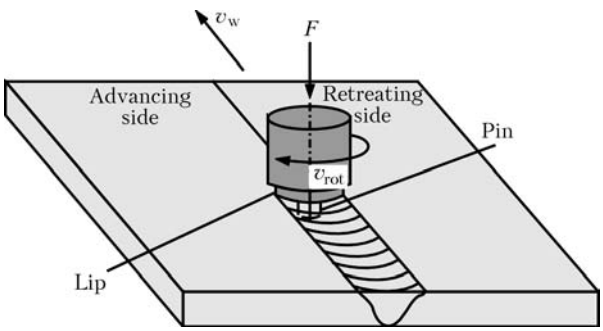

Figure 1. Block-diagram of FSW process

The last decade has witnessed rapid development of friction stir welding (FSW) and widening of its application in shipbuilding, automotive, carriage-building, aircraft and aerospace industry [1–3].

The principle of producing welds in FSW is based on metal heating in the joint zone up to a plastic state as a result of friction forces, its displacement and plastic deformation in a closed volume, limited by working surfaces of the tool and backing (Figure 1). The metal is not heated up to the melting temperature, which results in a much lower degree of structural-phase transformations than in fusion welding. Improved physico-mechanical properties of such joints ensure high performance of structures made with FSW [4–7]. However, as with any welding process, sound joints at FSW can only be obtained at certain process parameters.

© A.G. POKLYATSKY, A.Ya. ISHCHENKO and S.V. PODIELNIKOV, 2008

The purpose of this work is investigation of the main parameters of FSW process and process factors influencing formation of sound joints of aluminium alloys 1.8–2.5 mm thick.

Investigations were performed using sheets from mass-produced aluminium alloys of different alloying systems (AMts, AD31, AMg2, AMg6, V95, 1420 and 1460). Before welding they were cleaned from lubrication, and then chemical etching was performed by the standard procedure. No preliminary mechanical cleaning of the surfaces was performed, as the oxide film breaks up during welding, is refined through dispersion and uniformly distributed through the entire volume of the weld by the rotating tool.

Experimental results showed that the quality of weld formation in FSW of aluminium alloys 1.8–2.5 mm thick mainly depends on such process parameters as size and configuration of the tool lip and pin working surfaces, force of tool clamping to sheet surfaces and depth of its immersion into the metal being welded, tool rotation frequency and welding speed.

The tool should ensure metal heating in the welding zone up to the plastic state, its stirring along the entire thickness of edges being welded and displacement in a closed volume at excess pressure. The main quantity of heat Q evolves in the contact area as a result of lip friction and is found from the following formula [5]:

$$Q = 2/3\ \pi\mu P N(r_l^3 - r_p^3),$$

where μ is the coefficient of friction; P is the pressure applied by the tool to the sheets being welded, Pa; N is the tool rotation frequency, rps; r_l, r_p are the outer radius of the lip and pin, respectively.

When FSW is performed using a tool with a small diameter of the lip, the plasticized metal volume can be insufficient for complete filling of the space freed behind the tool, which may lead to formation of defects in welds of the type of lacks-of-fusion. A too large diameter of the lip promotes formation of a wide weld face, pronounced distortion of the welded joints and defect formation as a result of metal overheating in the welding zone. It is established that for FSW of aluminium alloys 1.8–2.5 mm thick, the optimum outer diameter of the tool lip should be in the range of 10–12 mm. In addition, in order to ensure a stable weld formation a small circular recess should be made on the lip end face, ensuring a smooth and continuous displacement of plasticized metal and formation of a sound weld face. However, its size should be such that at a shallow immersion of the tool lip, the displaced metal always was at an excess pressure.

Metal stirring across the entire thickness of edges being welded occurs due to its displacement by the rotating tool pin. Conducted research revealed that in welding of aluminium alloys 1.8–2.5 mm thick sound welded joints can be produced when using the tool pin in the form of a simple truncated cone. To ensure the pin performance under the conditions of the action of high bending forces, torque and friction forces, its diameter near the lip end face should be equal to 3.2–3.6 mm, and 2.4–2.6 mm at its tip, respectively. To prevent lacks-of-fusion in the weld root part, the pin length should be (0.90–0.95)δ. Smooth and uniform displacement of plasticized metal during welding is ensured owing to a high finish of the tool working surfaces. Any burrs, protrusions, dents or tears on these surfaces of the tool lip and pin, cause periodical changes of the trajectory, speed and amount of displaced metal, disturbing the stability of formation and quality of welds.

Drawings of some of the developed tool designs are given in Figure 2. It is recommended to make the tool from tool or stainless martensitic steels [8]. Therefore, welding was performed using a tool made of R6M5 tool steel with high strength properties at increased (about 600 °C) temperatures.

Weak pressing of the tool to part surfaces during welding or insufficient immersion of the tool lip into the metal being welded leads to an increases of the volume to be filled by plasticized metal at weld formation, and, therefore, to lowering of excess pressure and formation of discontinuities in welds. During experimental investigations it was established that for-

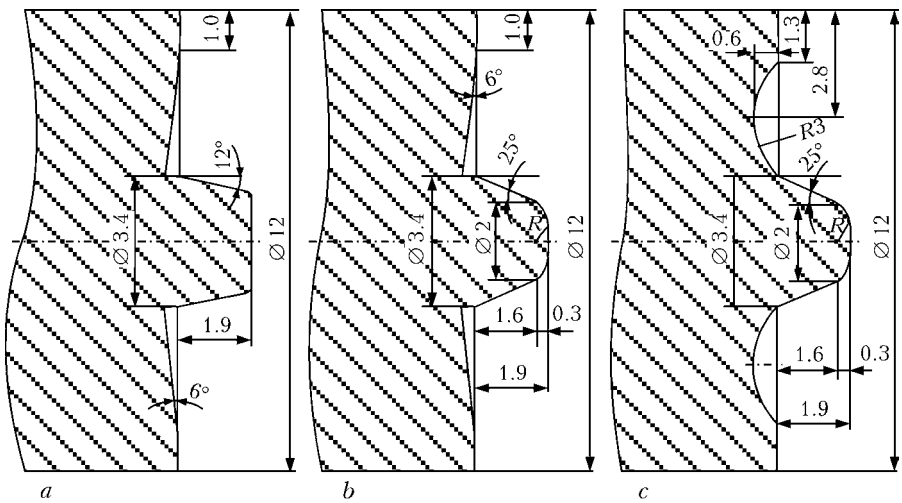

Figure 2. Drawings of the working parts of tools with the conical (*a, b*) and semispherical (*c*) grooves on the lip working surface and different shape of pins for FSW of aluminium alloys 2 mm thick

Figure 3. Appearance of the face surface of welds produced by FSW of aluminium alloy 1420 2 mm thick at excess (*a*) and insufficient (*b*) immersion of the lip into the metal being welded (×2)

mation of sound welds is provided at the forces of tool pressing of 5–10 kN and depends on the grade of the alloy being welded. Tool lip should be immersed into the metal being welded to the depth of 0.1–0.2 mm. Its excessive immersion leads to metal overheating and formation of defects in the form of tears on the weld face (Figure 3, *a*). At shallow immersion of the tool into the metal being welded the amount of heat evolving in the welding zone is insufficient to achieve the required level of plasticizing of the metal volume, necessary for a sound weld formation. Therefore, in such cases defects of the type of lacks-of-fusion, form on the weld face (Figure 3, *b*). Moreover, welding should be performed by «backward inclined tool» at tool inclination angle of 2–3°. The rotating lip applies additional pressure on the metal being welded by its rear edge, thus making the weld metal denser.

Tool rotation frequency and welding speed have an essential influence on weld formation. Heat evolution in the welding zone increases with increase of the number of tool rotations or lowering of the speed of its displacement along the butt. At a certain ratio of tool rotation frequency and welding speed for a given alloy, the amount of heat evolved due to friction, can be insufficient for plasticizing the metal volume required for filling the entire cavity formed by the tool pin. This disturbs the discontinuity of the flow of the metal moving along a complex trajectory,

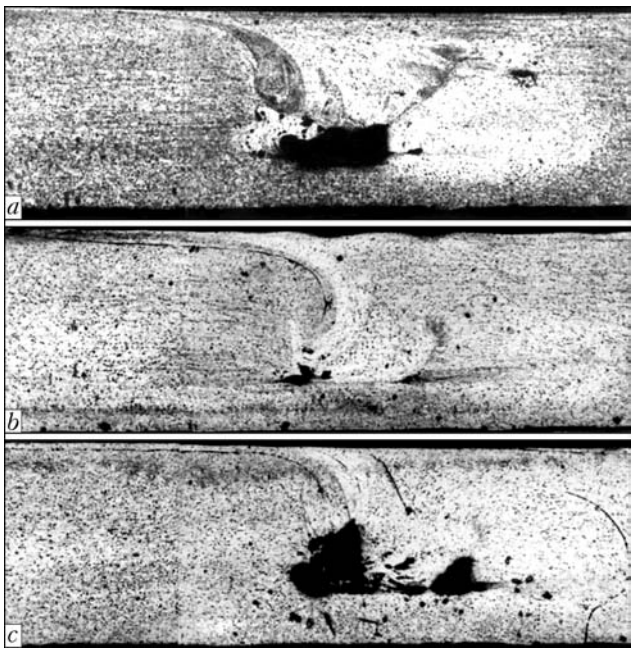

Figure 4. Transverse macrosections of welded joints of AMg6 alloy 2 mm thick obtained at FSW at a constant frequency of tool rotation of 2880 rpm and different welding speed: *a* — v_w = 38; *b* — 20; *c* — 8 m/h (×20)

and the weld develops inner cavities unfilled with metal (Figure 4, *a*). At preservation of the same speed of tool rotation and lowering of the speed of its displacement, the amount of plasticized metal increases, resulting in improvement of weld quality (Figure 4, *b*). However, excessive lowering of welding speed leads to excess heat evolution, leading to melting of low-melting eutectics on intergranular boundaries and formation of inner defects in the form of cavities and discontinuities (Figure 4, *c*).

Experimental results showed that ductile low-alloyed alloys (AMts, AMg2, AD31, etc.) are joined successfully by FSW in a broad range of welding speed variation (6–40 m/h) at tool rotation frequency of 1420 or 2880 rpm. High-strength complex alloys (AMg6, 1460, V95, etc.) should be welded at a lower (1420 rpm) frequency of tool rotation and lower (6–14 m/h) welding speeds.

Accuracy of the butt fit-up for welding and close contact between the edges and backing in the welding

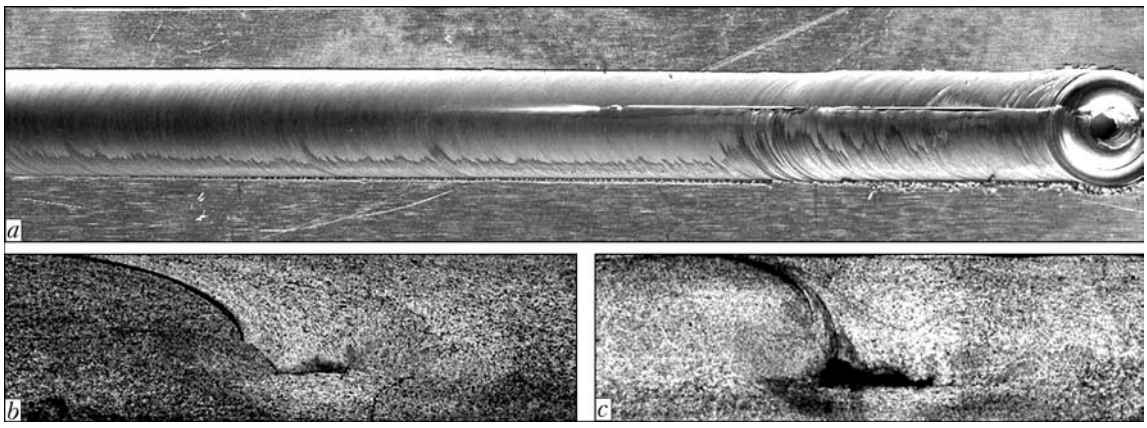

Figure 5. Appearance of the face of a weld (*a* — ×1.4) produced by FSW at assembly of the butt with a variable gap (0.2–1.2 mm) between the edges, and transverse macrosections of welded joints of AMg2 alloy 2 mm thick at the gap of 0.3 (*b*) and 0.5 (*c*) mm

zone are very important for producing sound joints. Investigations of transverse macrosections of welds made by FSW of AMg6 alloy 2 mm thick showed that for sound welds the gap between the edges being welded should be not more than 15 % of the thickness of metal being welded (Figure 5). Warping of the edges being welded has a significant influence on the quality of weld formation. The warping results from inaccuracy of edge fit-up and assembly, unreliable fastening of the blanks on the backing or change of thermophysical conditions during welding. At too high edge from the tool retreating side (where the vectors of the tool direction and displacement are opposite in direction), part of plasticized metal is pressed out during welding in the form of flash on the weld face (Figure 6). Therefore, in order to ensure a sound weld formation edge warping should not exceed 5 % of welded metal thickness.

As tools with very thin pins are used for FSW of aluminium alloys 1.8–2.5 mm thick, even their slight deviation from the butt axis can lead to violation of weld quality. Investigations of macrosections of welds on AMg6 alloy 1.8 mm thick showed that the admissible deviation of the tool from the weld axis should not exceed 0.5 mm. Their greater displacement may lead to formation of defects of the type of lacks-of-fusion, as weld formation across the entire depth of edges being welded occurs not in the butt center.

CONCLUSIONS

1. Conducted research resulted in determination of optimum dimensions and shapes of working surfaces of the tool lips and pins, ranges of the change of the main process parameters and requirements to assembly and fixation of the edges to produce sound joints of typical aluminium alloys 1.8–2.5 mm thick.

2. Welding should be performed at backward inclination of the tool of 2–3° at constant pressing and immersion of the tool lip to 0.1–0.2 mm into the metal being welded. The admissible deviations of the tool and butt axes are not more than 0.5 mm, the gap between the edges being welded is not more than 15 %, and edge misalignment is not more than 5 % of the welded metal thickness.

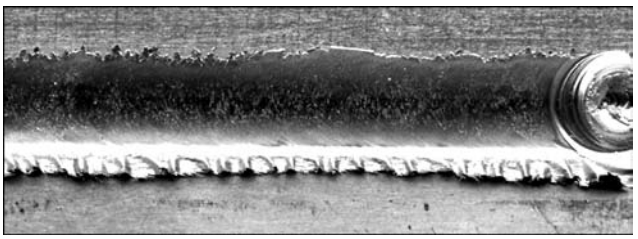

Figure 6. Appearance of the face of a weld produced by FSW of 1420 alloy 2 mm thick at excess height of an edge on the tool retreating side (×2)

3. Sound welds in FSW of ductile low alloys can be produced by FSW in a wide range of variation of rotation frequency of 1420–2880 rpm and speed of tool displacement of 6–40 m/h. For high-strength complex alloys a lower tool rotation frequency (1420 rpm) and welding speed (6–14 m/h) are recommended.

1. Thomas, W.M., Nicholas, E.D., Needham, J.C. et al. *Friction stir butt welding.* Pat. 5460317 US. Publ. 1995.
2. Arbegast, W.J. (2006) Friction stir welding. After a decade of development. *Welding J.*, 85(**3**), 28–35.
3. Enomoto, M. (2003) Friction stir welding: research and industrial application. *Welding Int.*, 17(**5**), 341–345.
4. Defalco, J. (2006) Friction stir welding vs. fusion welding. *Welding J.*, 85(**3**), 42–44.
5. Hassan, Kh.A.A., Prangnell, P.B., Norman, A.F. et al. (2003) Effect of welding parameters on nugget zone microstructure and properties in high strength aluminium alloy friction stir welds. *Sci. and Technol. of Welding and Joining*, 8(**4**), 257–268.
6. Tretyak, N.G. (2002) Friction stir welding of aluminium alloys (Review). *The Paton Welding J.*, **7**, 10–18.
7. Poklyatsky, A.G., Ishchenko, A.Ya., Yavorskaya, M.R. (2007) Strength of joints on sheet aluminium alloys produced by friction stir welding. *Ibid.*, **9**, 42–45.
8. Tokisue, H., Shinoda, T. (1999) Applications of friction stir welding into light metals. *J. Jap. Institute of Light Metals*, 49(**6**), 258–262.

DETERMINATION OF PARAMETERS OF SIMPLIFIED STATIC CORROSION CRACK RESISTANCE DIAGRAM FOR PIPE STEELS IN SOIL CORROSION

V.I. MAKHNENKO, V.M. SHEKERA and **E.M. ONOPRIENKO**
E.O. Paton Electric Welding Institute, NASU, Kiev, Ukraine

Procedure for determination of parameters of a simplified static corrosion crack resistance diagram for pipe steels in soil water solution environment is described. The possibility of plotting simplified diagrams using small-sized Charpy-type specimens with a pre-induced fatigue crack is shown. The use of acoustic emission for fixation of crack growth steps allows the test time to be reduced to 5–7 days.

Keywords: *static corrosion crack resistance diagram, main pipelines, acoustic emission, stress intensity factor, crack growth rate*

The guaranteed safe service life provided by an adequate response to the results of regular technical diagnostics of the state of a pipeline and, first of all, to various material discontinuity defects revealed by the technical diagnostics, among which the most dangerous defects are corrosion cracks, is of high importance for modern main pipelines (MP). According to the «prediction and prevention» ideology («fitness for service» [1]), this adequate response provides for prediction of behaviour of a revealed defect over a specified service time and working out of recommendations for prevention of its unfavourable manifestations (failures), right up to the necessity of repair.

Prediction of behaviour of a detected corrosion crack of a certain shape and size in the known field of static mechanical stresses, as well as under the known temperature conditions and corrosive environment, is implemented on the basis of the static corrosion crack resistance diagram (SCCRD) for a given material (Figure 1).

Such a diagram for pipe steels relates crack growth rate v at a certain point of its profile, θ (Figure 2), to stress intensity factor $K_I(\theta)$ at this point. SCCRD has three characteristic zones: I — $0 < K_I < K_{ISCC}$, where the mechanism of electrochemical corrosion and rates $v(K_I)$, which are close to those for uniform corrosion, prevail; II — $K_{ISCC} < K_I < K_{IC}$, where the mechanism of hydrogen-induced embrittlement prevails [1, 2], and crack growth rate $v(K_I)$ is much higher than in zone I; and III — $K_I > K_{IC}$, where a spontaneous crack growth corresponds to brittle fracture.

In a general case, plotting SCCRD is time-consuming, the major portion of time being consumed to derive dependence $v - K_I$ in zone I. For practical predictive calculations related to estimation of the risk of failure due to a specific corrosion crack in the MP wall, it is enough to know the value of K_{ISCC} and dependence $v - K_I$ in zone II at $K_I << K_{IC}$, i.e. it is possible to use the simplified form of SCCRD determined by the following relationships:

$$v = 0 \text{ at } K_I < K_{ISCC};$$
$$v = QK_I^n \text{ at } K_{ISCC} < K_I << K_{IC}, \quad (1)$$

where K_{ISCC}, Q and n are the experimentally determined parameters.

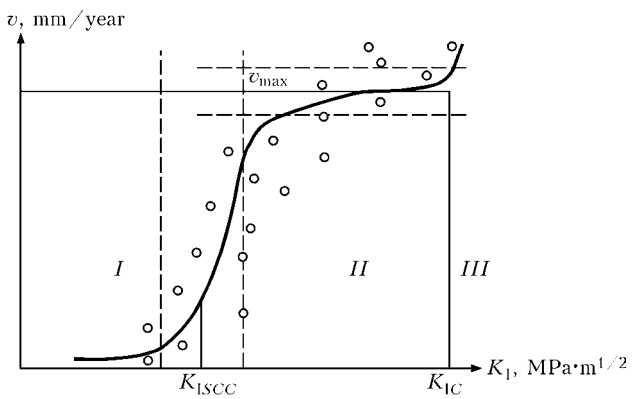

Figure 1. Static corrosion crack resistance diagram: see *I–III* and rest of designations in the text

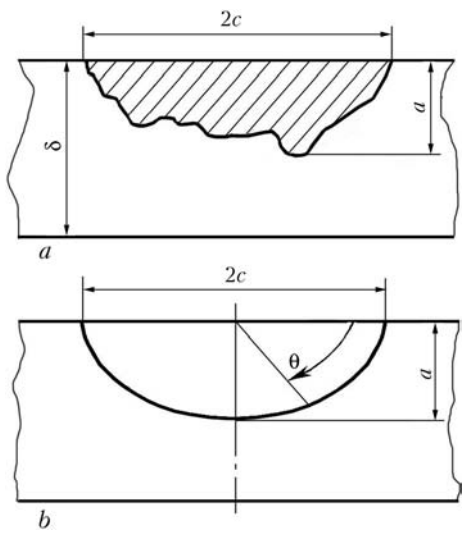

Figure 2. Schematic of a surface crack in pipe wall (*a*), and its description by a semi-elliptical crack with size $a \times 2c$ (*b*)

© V.I. MAKHNENKO, V.M. SHEKERA and E.M. ONOPRIENKO, 2008

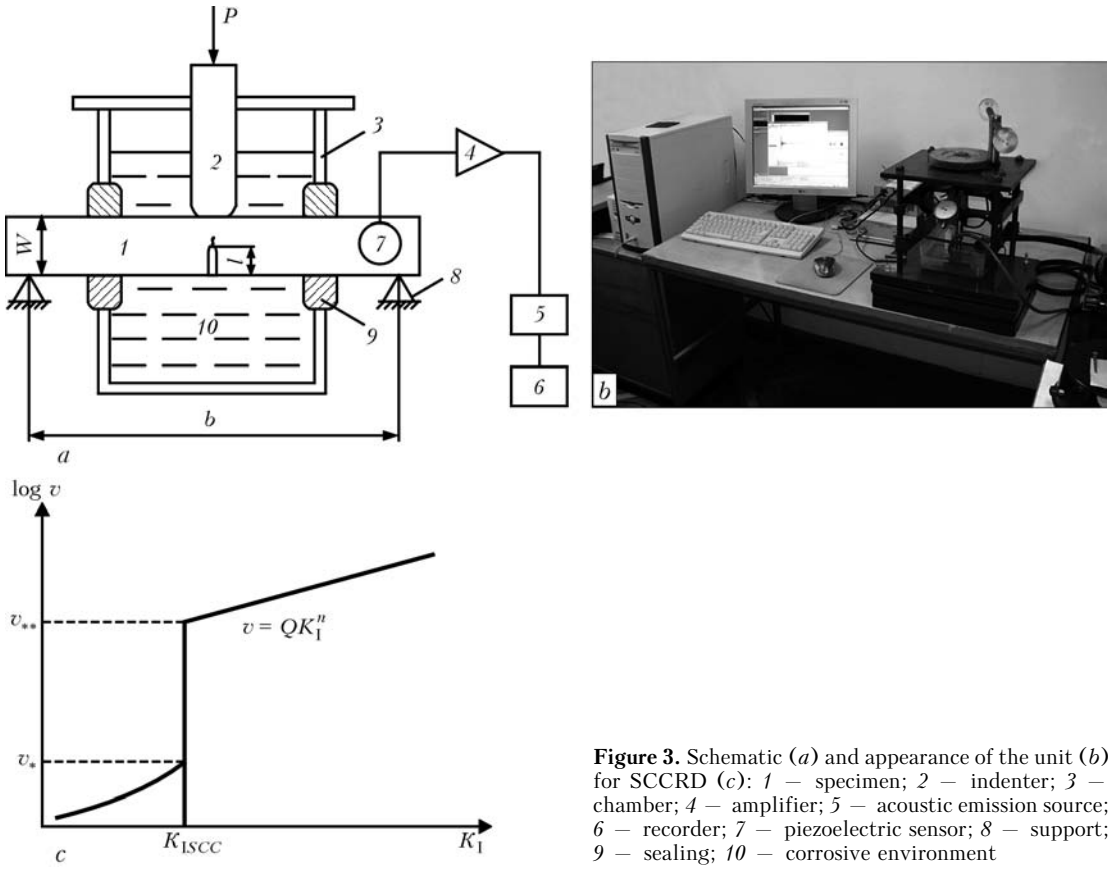

Figure 3. Schematic (*a*) and appearance of the unit (*b*) for SCCRD (*c*): *1* — specimen; *2* — indenter; *3* — chamber; *4* — amplifier; *5* — acoustic emission source; *6* — recorder; *7* — piezoelectric sensor; *8* — support; *9* — sealing; *10* — corrosive environment

The size of specimens is an important parameter for operational conditions of plotting simplified SCCRD (considering the limited (10–20 mm) thickness of MP), which makes measuring the kinetics of growth of a corrosion crack in tests much more difficult.

Given the above-said, the authors used the method described in [2] to generate experimental data for simplified SCCRD as applied to MP. According to this method, geometric measurements of growth of a crack during experiment are replaced to a considerable extent by listening to its growth using acoustic emission. Schematic of such an experiment is shown in Figure 3, *a*, and appearance of the PWI experimental unit for operation with the Charpy-type specimens containing a preliminarily grown fatigue crack at an aggressive environment (soil corrosion) temperature of 10–60 °C is shown in Figure 3, *b*.

The values of force P at the indenter are set with the help of a screw jack via a strain-gauge clip, and monitored during the test process following preset program P–t.

The value of stress intensity factor K_I is related to such parameters as distance b between supports, length l of the crack, height W and thickness B of a specimen (Figure 3), as well as force P, using the following dependence [3]:

$$K_I(l) = \frac{6P\sqrt{l}}{BW}\left\{1.93 - 3.07\left(\frac{l}{W}\right) + 14.53\left(\frac{l}{W}\right)^2 - 25.11\left(\frac{l}{W}\right)^3 + 25.8\left(\frac{l}{W}\right)^4\right\}. \quad (2)$$

For this the use is made of the known assumption that the crack grows in a stepwise manner, l, at $K_I > K_{ISCC}$, and the values of steps, Δl, are proportional to K_I^2, i.e.

$$\Delta l = \alpha K_I^2, \quad (3)$$

where α is the coefficient of proportionality, which does not depend upon the force conditions, but depends only upon the properties of a material and corrosive environment.

As a crack step is accompanied by a sound, time intervals Δt between the neighbouring crack growth steps are measured according to the schematic shown in Figure 3, *a*, instead of measurements of small increments of Δl (small section of a specimen) with time. Only the initial size of the crack, l_1, and its size l_N at the end of the test, after $n = 1, 2, \ldots, N$ steps fixed by the corresponding equipment (see Figure 3), are subject to the geometric measurements.

To find the required solution, the use is made of equations (2) and (3), combined with the following relationships:

$$l_n = l_{n-1} + \alpha K_I^2(l_n), \quad (4)$$

$$\alpha = \frac{l_N - l_1}{\sum_{n=1}^{N} K_I^2(l_n)}, \quad (5)$$

$$v_n = \Delta l_n / \Delta t_n \quad (n = 1, 2, \ldots, N). \quad (6)$$

Figure 4. Microstructure of 17G1S steel specimen with corrosion crack

The tests begin at high values of K_I from a region of $K_{ISCC} < K^I < K_{IC}$, where K_{ISCC} and K_{IC} are set on the basis of the experiment. With accumulation of signals corresponding to the crack growth steps, the values of P and, accordingly, K_I decrease to the minimal ones, at which no signals are fixed for a period of 20–40 h. The corresponding value of K_I is assumed to be K_{ISCC}. As the time of the tests is 1 to 4 weeks, at the mean growth rates that are not in excess of 10–20 mm/year, a change in $l_N - l_1$ is less than 1 mm. Hence, it needs to be carefully measured. Electron microscope «Cam-Scan» with ×80 magnification is employed for these purposes.

Figure 4 shows microstructure of the 17G1S steel specimen containing a corrosion crack (l_1 — at the beginning, and l_N — at the end) formed in tensile tests in 3 % NaCl solution. The accuracy of measurements of $l_N - l_1$ is not lower than 0.005 mm.

Figure 5 shows the experimental data obtained with the same specimen tested in 3 % NaCl solution for three weeks (Figure 6) at a temperature of about

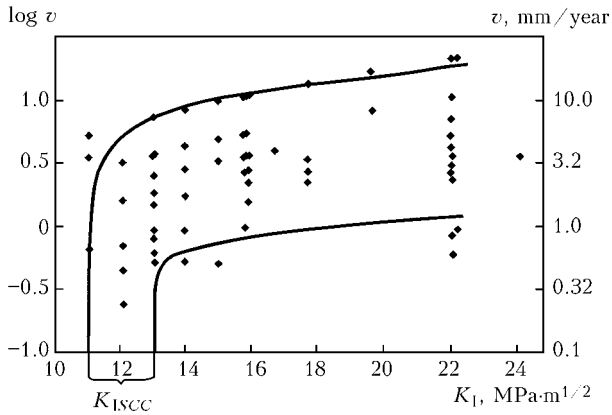

Figure 5. SCCRD plotted on the basis of the results of testing the 17G1S steel specimen in 3 % NaCl solution at $15 < T < 25$ °C for three weeks

15–25 °C (at the absence of temperature regulator). Chemical composition of steel 17G1S is as follows, wt.%: 97.11 Fe, 0.40 Ni, 0.06 Cr, 0.038 Co, 1.6 Mn, 0.04 Cu, 0.02 Ti, 0.57 Si, 0.15 Al, and 0.18 C.

It can be seen from Figure 6 that the real crack growth rate calculated on the basis of the acoustic emission signals is characterised by a rather wide scatter of values (mean rate $v_{mean} = 3.2$ mm/year), which is caused to a considerable degree by the neglected fluctuations in day and night temperatures. In addition, it should be taken into account that Δl determined by relationship (3) is not uniform in specimen thickness B, i.e. the fixed acoustic emission peaks correspond to local increments in length of the crack. This process is very chaotic. However, it reflects the crack growth rate depending upon the values of K_I and mean value of the crack growth rate, v_{mean}, on the basis of difference $l_N - l_1$ and total test time. As seen from Figure 5, the threshold value of K_{ISCC} is 11–13 MPa·m$^{1/2}$. The data presented in Figures 5 and 6 can be utilised with a certain conditionality to estimate the static corrosion crack resistance of pipe steel 17G1S in sea water. To estimate soil corrosion, obviously it will be necessary to carry out tests in the corresponding corrosive environment.

Allowing for a wide variety of soil compositions, a comprehensive program was worked out to conduct this type of investigations. Figure 7 shows SCCRD plotted for a case where an aqueous extract of soil taken from a region of the town of Borodyanka (soil No. 1) was used as a corrosive environment.

To prepare the aqueous extract, the soil was preliminarily dried and screened, and then poured with tap water for extraction for 24 h with a very intensive stirring. The extract solution held for several hours was filtered. In the finished state, it had a density of 0.997 g/cm^3 and pH 8.2. Chemical composition of the extract studied by evaporation of a certain volume until a solid residue is produced, by using Philips analytical X-ray spectrometer, was as follows, wt.%: 4.6 Na_2O, 6.8 SiO_2, 15.9 SO_3, 6.9 NaCl, 55.1 CaO, 0.02 TiO_2, 0.07 CuO, 6.9 MgO, 0.36 Al_2O_3, 0.46 P_2O_5, 0.23 Fe_2O_3, 0.027 NiO, 0.06 ZnO, 0.13 SrO, and 2.3 K_2O.

It can be seen from the above data that the aqueous extract of soil No. 1 markedly differs in composition from the 3 % NaCl solution, which has pH 7.0, and in which the corrosion crack growth rate is approximately 1.5 times higher. In other words, in analogy with uniform corrosion [4], it can be stated that the composition of the soil does have a certain effect on the crack growth rate, along with such factors as temperature and level of stresses in metal of a specimen. Therefore, the operational determination of SCCRD for the specific pipe–soil combinations is very important for estimation of the risk of damage of the anticorrosion insulation of MP. Consider a simple example to show it.

Most main pipelines are made from the longitudinally welded pipes. Damage of the insulation in the

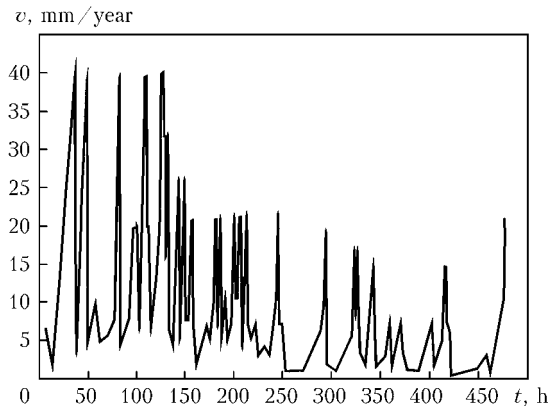

Figure 6. Kinetics of variations in corrosion crack growth rate in the specimen tested according to Figure 5

longitudinal weld region involves a high risk of development of a local surface corrosion. This is a very slow process controlled by the electrochemical mechanism of corrosion of pipe steel, the rate of development of which depends upon the degree of geometrical and physical heterogeneity within the weld zone (the latter depends to a certain degree upon the manufacturing company that supplies pipes).

Unless the corrosion process is stopped (by repairing the damaged insulation) at a proper time, the groove-like defect [1] of continuity of a material will form within the longitudinal weld zone. In this case, the high probability exists of initiation of a stress corrosion crack on the bottom of the above defect in the presence of effective circumferential stresses (allowing for the stress concentration). Such a crack will propagate primarily by the mechanism of electrochemical corrosion until its size, in the presence of circumferential stresses $\sigma_{\beta\beta}$, creates conditions for predominance of the mechanism of hydrogen-induced embrittlement. This will take place when the K_I values on the crack profile exceed the threshold ones, i.e. at $K_I > K_{ISCC}$. It can be shown that at $K_{ISCC} \approx 10$–13 MPa·m$^{1/2}$, and at circumferential stresses $\sigma_{\beta\beta}$ = = 260–350 MPa in the pipe wall, crack size $a \times 2c$ (see Figure 2) along the weld will be very small.

To calculate the K_I values, it is possible to use the recommendations of study [5] given in study [6]. In these recommendations, at $a/c < 0.2$ (the crack extends along the weld) the K_I values at $\theta = \pi/2$ (see Figure 2) can be determined from the following simple relationship:

$$K_I\left(\theta = \frac{\pi}{2}\right) = \sigma_{\beta\beta}\sqrt{\pi\frac{a}{1000}}\,M_K\,f(\alpha/\delta)\ [\text{MPa}\cdot\text{m}^{1/2}], \quad (7)$$

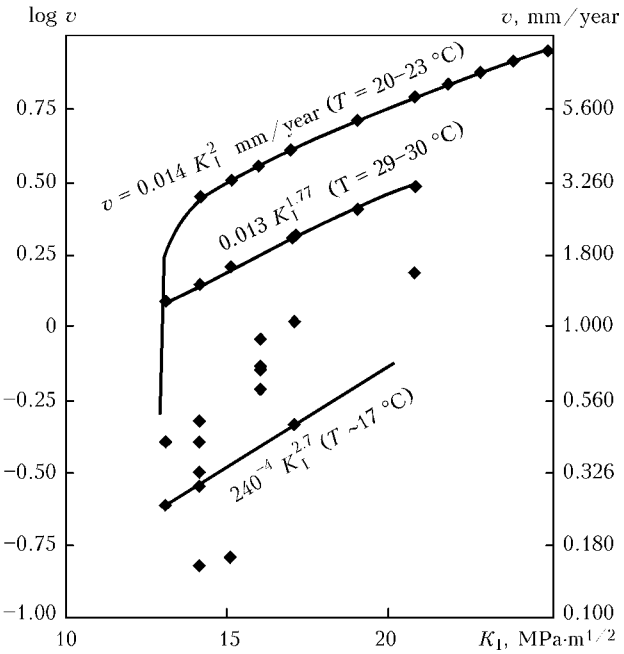

Figure 7. SCCRD for the 17G1S steel specimen tested under soil corrosion conditions

where

$$f(\alpha/\delta) \approx \frac{1.12 + 5(\alpha/\delta)^4}{1 - \alpha/\delta} \text{ at } \alpha/\delta \le 0.55;$$

$$f(\alpha/\delta) \approx \frac{0.303\left(1 + 3.03\,\dfrac{a}{\delta}\right)^4}{\sqrt{a/\delta\,(1 - a/\delta)^3}} \text{ at } \alpha/\delta > 0.55;$$

M_K allows for the concentration of stresses within the weld zone, and, according to [5],

at $L < 2\delta$ and $\alpha/\delta < 0.05\ (L/\delta)^{0.55}$

$$M_K = 0.51(L/\delta)^{0.27}(\alpha/\delta)^{-0.31} \ge 1.0; \quad (8)$$

at $\alpha/\delta > 0.05(L/\delta)^{0.55}$

$$M_K = 0.83(\alpha/\delta)^{-0.13(L/\delta)^{-0.45}}. \quad (9)$$

The data given in the Table, which are the results of calculation of $K_I(\pi/2)$ from (7) and (8) for a pipe wall thickness of δ = 20 mm at L = 30 mm, and $\sigma_{\beta\beta}$ = = 260 and 360 MPa, depending upon depth a (at $a/c < 0.2$) of the crack formed within the longitudinal weld zone and in a smooth part of the pipe, show that at K_{ISCC} = 10–13 MPa·m$^{1/2}$ the conditions for the crack growth by the mechanism of hydrogen-in-

Results of calculation of K_I (MPa·m$^{1/2}$) according to (7) and M_K according to (8) at δ = 20 mm, L/δ = 1.5 and different crack depths

Calculation results	$\sigma_{\beta\beta}$, MPa	a, mm						
		0.1	0.2	0.3	0.4	0.5	1.0	2.0
K_I in longitudinal weld zone	260	15.2	15.8	16.7	17.6	18.4	21.0	22.6
	360	21.1	22.1	23.2	24.4	25.4	29.0	31.4
K_I in smooth part of pipe	260	5.2	6.4	7.9	9.2	10.3	14.6	20.5
	360	12.2	11.6	11.0	12.8	14.2	20.1	28.5
M_K	–	2.94	2.37	2.10	1.91	1.78	1.44	1.1

duced embrittlement are created within the longitudinal weld zone at a = 0.1 mm and $\sigma_{\beta\beta}$ = 260 MPa, while in the smooth part of the pipe these conditions are created at a > 0.5 mm.

SCCRD shown in Figure 7, in a case it corresponds to the soil conditions, can be used to determine the kinetics of further growth of the crack with time until the risk is run of formation of a through defect, or transition to the stage of a spontaneous growth (see Figure 1, zone *III*).

The Table gives the values of M_K (8), which show the extent of the effect on K_I by the geometric heterogeneity within the weld zone. It can be seen from the Table that this effect dramatically diminishes with increase in the crack depth, and at a > 2 mm (δ = = 20 mm) the M_K values become close to 1. It follows from this that at the preset values of K_{ISCC} the decrease in membrane stresses shifts occurrence of the conditions of the crack growth by the mechanism of hydrogen-induced embrittlement to the zone of deeper cracks, where the effect of geometric heterogeneity within the weld zone dramatically decreases.

Therefore, the circumferential welds are mainly in more favourable conditions than the longitudinal ones, the corrosion protection of which requires great care.

CONCLUSIONS

1. To predict development of corrosion cracks in MP of Ukraine, it is necessary to have SCCRD for pipe steels under corresponding soil environments.

2. Considering a wide variety of probable combinations of the above factors, as well as the fact that for the given problem it is most important to know development of a corrosion crack at the K_I values above the K_{ISCC} ones, this study suggests using an approach based on listening to the crack growth rate by the acoustic emission method.

3. The required static corrosion crack resistance diagrams for specific conditions can be quickly plotted with small-size specimens.

1. (2000) *Fitness-for-service*: Recommended practice 579. Washington: American Petroleum Institute.
2. (2001) *Fracture mechanics and strength of materials*: Refer. Book. Vol. 5: Non-destructive testing and technical diagnostics. Lviv: G.V. Karpenko MPhI.
3. (1988) *Fracture mechanics and strength of materials*: Refer. Book. Vol. 2: Stress intensity factors in bodies with cracks. Kiev: Naukova Dumka.
4. Marchenko, A.F. (1995) Soil corrosion of pipeline steel and main pipelines. *Stroitelstvo Truboprovodov*, **1**, 29–34.
5. (1996) Recommendations for fatigue design of welded joints and components. *IIW Doc. XIII-1539–96/XV-845–96*.
6. Makhnenko, V.I. (2006) *Safe service life of welded joints and connections of modern welded structures*. Kiev: Naukova Dumka.

DATABANK OF WELDING PARAMETERS

The databank contains information on parameters of CO_2, submerged-arc (with one or two wires) and inert-gas shielded welding of structural steels in different spatial positions depending upon the thickness of base metal, type of a welded joint, groove shape and welding wire diameter. Recommendations on the number of passes for welding the root, filling and decorative beads are given for a case of multipass welding. The recommended welding parameters provide quality weld formation and required amount of deposited metal to ensure structural strength of a welded joint. At the given development stage, the database contains more than two thousand entries of welding conditions.

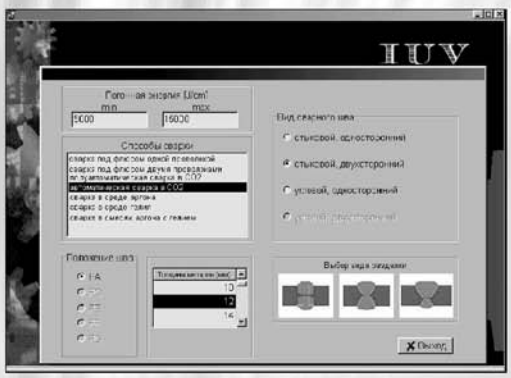

Figure 1. Selection of welding method, type of welded joint, spatial position and groove shape

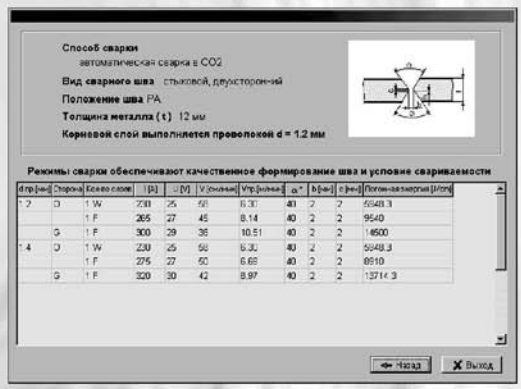

Figure 2. Information on CO_2 welding of butt joint

Application. The databank can be used at machine building enterprises for arrangement of computerised work place of a welding production engineer.

Contacts: Prof. Makhnenko V.I.
E-mail: d34@paton.kiev.ua

UP-TO-DATE EQUIPMENT OF THE E.O. PATON ELECTRIC WELDING INSTITUTE FOR ELECTRON BEAM WELDING

O.K. NAZARENKO
E.O. Paton Electric Welding Institute, NASU, Kiev, Ukraine

The paper presents the main results of the E.O. Paton Electric Welding Institute activities on development of electron beam welding equipment over the last 15 years. Technical data of the developed range of power units (gun–power source–control system), as well as of some of the electron beam welding machines, are given.

Keywords: *electron beam welding, electron beam gun, accelerating voltage source, setting, computer control*

Starting from 1990s, «Elektromekhanika» Plant (Rzhev, RF), Plant of «Istok» Research Institute (Kaliningrad, RF), Sumy Plant of Electron Microscopes and Electrics (Ukraine) stopped batch production of electron beam welding equipment in the post-Soviet space. Many creative teams focused on development and improvement of the equipment, development and industrial acceptance of electron beam welding technology, dissolved. Only the E.O. Paton Electric Welding Institute and NIKIMT, head organization of RF on welding in nuclear engineering and industry [1], managed to not only preserve, but also enhance the research and production capabilities, as well as attract orders from Russian enterprises and foreign countries outside CIS.

Over the last 15 years PWI, alongside various technological research, developed and manufactured new generation production equipment. These are new power units consisting of the welding gun–high- and low-voltage circuit power source–system of control of electron beam parameters in the electron beam welding machines.

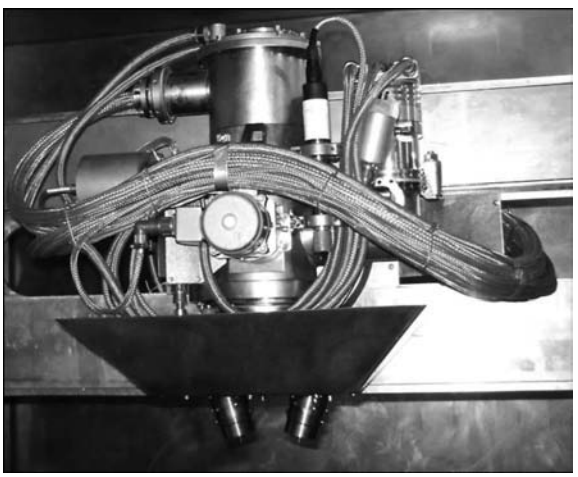

Figure 1. Appearance of in-chamber welding electron beam gun with 60 kV accelerating voltage and 60 kW beam power

Improvement of welding electron beam guns and power sources. PWI welding guns are designed for operation with two levels of accelerating voltages of 60 and 120 V. A feature of their design is the capability of using the gun both outside and inside the vacuum chamber (Figure 1).

Gun emission system is cut off from the transit channel by a gate valve and is pumped down by a self-sufficient turbomolecular pump, the exhaust from which is discharged into the vacuum chamber through a system of gate valves. Due to that the vacuum in the emission system area practically does not deteriorate during welding, thus promoting prevention of breakdowns in the gun. Inside the chamber the gun moves along three linear and two angular coordinates, which requires quite extended (up to 40 m) cable and water supply lines laid into flexible channels — cable ducts.

Electric breakdown of vacuum insulation in the gun leads to dramatic consequences in the case of a high cost of the item being welded and impossibility of weld repair after disturbance of its formation. A rational design of the electronic-optical system and of the electron beam gun improved the electric strength of accelerating gap vacuum insulation. Application of massive disc cathodes heated by electron bombardment, allowed avoiding violation of emitting surface

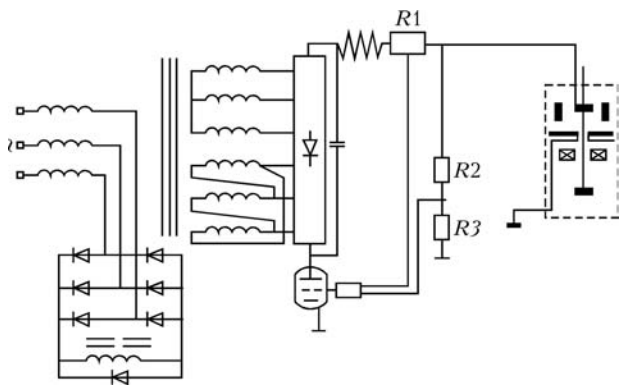

Figure 2. Simplified block-diagram of the gun and accelerating voltage source ELA-60 fitted with a transmission tube PP-2 (filter capacity of $15 \cdot 10^{-9}$ F)

© O.K. NAZARENKO, 2008

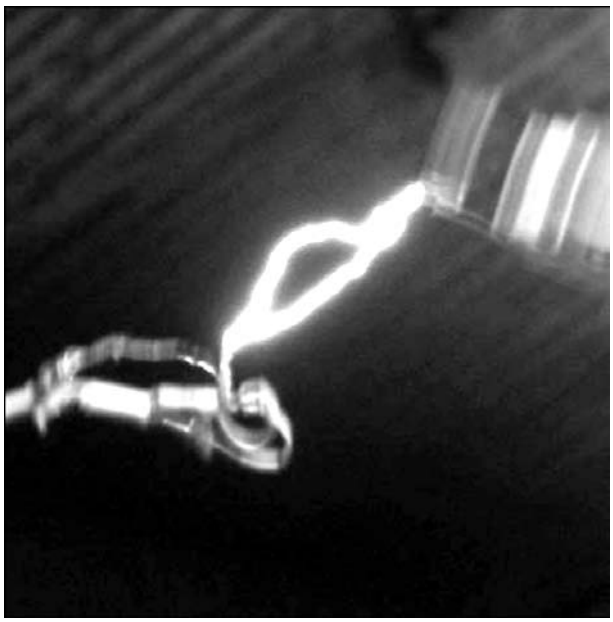

Figure 3. Checking the functioning of the system of automatic restarting of the power source by its loading by a grounded rod

geometry inherent to filamentery cathodes, the associated breakdowns and spot erring over the item surface. However, the possibility of breakdown development still remains, and, therefore, further improvement of accelerating voltage sources is important.

The electron tube connected as a linear transmission element (Figure 2) already at the initial stage of an anomalous non-stationary process «takes up» the accelerating voltage [2]. The electric strength of the emission system and gun accelerating voltage are restored within several milliseconds.

Power source is not switched off by electrical protection even at simulation of vacuum breakdown by short-circuiting to the high-voltage output ground (Figure 3).

The smoothing filter discharge is effectively interrupted by the transmission tube and the energy released during the breakdown is commensurate with such in the case of application of high-frequency sources of the same power [3]. High stability of maintaining the accelerating voltage and ability to prevent electric breakdowns provide formation of a sound weld in the most critical section of closing the circumferential weld made on thick-walled steel structures (Figure 4).

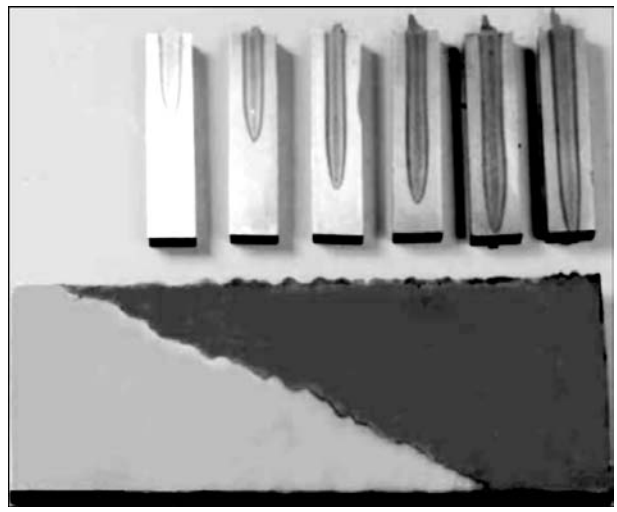

Figure 4. Macrosections of transverse (*top*) and longitudinal (*bottom*) sections of the cast zone, produced at closing of a circumferential weld on heat-resistant steel 130 mm thick [4]

High-frequency power sources differ favourably from the traditional ones operating at industrial frequency of 50 Hz, by their much smaller dimensions, and wide range of accelerating voltage adjustment. They do not require application of protective linear elements as they have a small energy store.

However, high-frequency power sources feature a much softer load characteristic and are not designed to operate in the mode of beam current pulsed modulation, as they cannot provide the required stability of accelerating voltage (Figure 5). On the other hand, beam current pulsed modulation is an effective technique and is widely used in electron beam welding not only of sheet materials, but also of thick metals.

The effectiveness of application of high-frequency power sources at up to 18 kW beam power and absence of stringent requirements on pulsed variation of beam current has been confirmed in practice. Electron beam welding of continuous band blanks, including those of such dissimilar metals as tool + carbon steels is an example of it. Ten sets of computer-controlled power units of 120 and 60 kW power for the respective machines have been developed and put into operation (Figure 6). Given below are the main technical characteristics of production power units.

Production machines. Due to the availability of a machine with 400 m^3 vacuum chamber at PWI, it

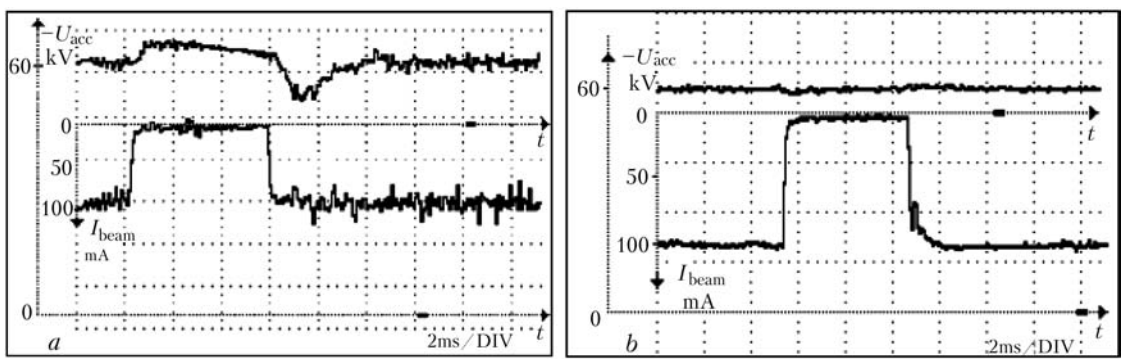

Figure 5. Dependence of accelerating voltage on pulsed variation of beam current in the high-frequency resonance power source (*a*) and power source with the transmission tube (*b*)

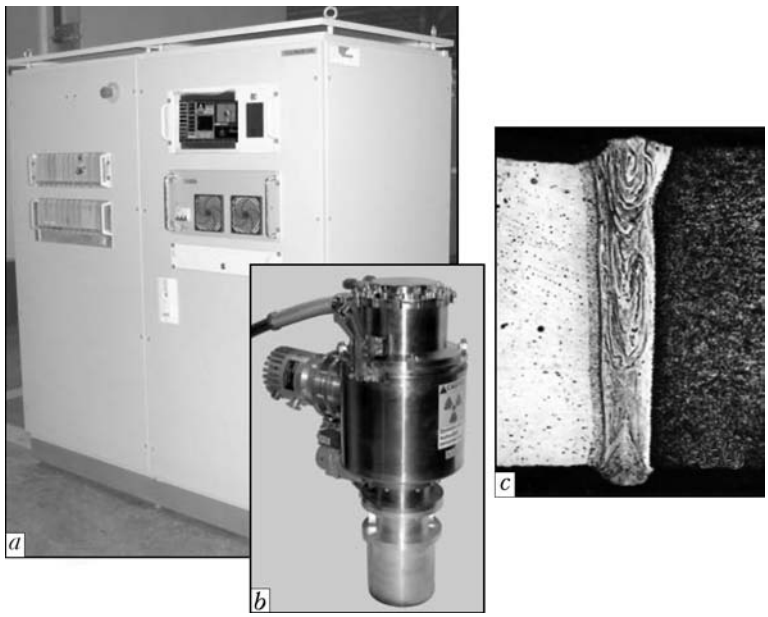

Figure 6. ELA-120/6 power source (*a*), welding gun with the removed X-ray protection (*b*) and macrostructure of the welded joint of R6M5 + 50KhFA steels 1.35 mm thick (*c*) at welding speed of 7.8 m/min; accelerating voltage of 120 kV; beam current of 12.5 mA; cast zone width in the weld upper and root part of 0.35 and 0.25 mm, respectively

is possible to apply electron beam welding for manufacturing vacuum chambers of production machines. In this case finish machining of the mated surfaces is not required.

Production machines of the following three types are in greatest demand.

The first type are machines with vacuum chambers of a relatively small (from 0.2 to 3.5 m^3) capacity fitted with a stationary welding gun or gun sliding along one of the walls (Figures 7 and 8).

Machines of the second, so-called cycle type, are used, in particular, for welding transmission gear blocks (Figure 9). Highly-efficient machine for welding drill bit cases (Figure 10), which is fitted with three welding guns powered from one accelerating voltage source, can be also included into this type. Welding of three longitudinal welds is performed simultaneously, thus minimizing welding deformations and improving the welding efficiency. Welding process is displayed in real time, the beam of each of the three guns being automatically aligned with the respective butt using «Rastr» system of second-electron surface imaging [5]. Welding process lasts less than one minute. For this reason, the under-roller areas with lubrication and sealing collars are not heated up to critical temperature before the welded bit immersion into the cooling liquid. Cycle time of welded drill bit output is less than 5 min. Overall dimensions of the vacuum chamber allow welding drill bits of all the type-sizes, just replacing the welding-assembly module.

The third type are large-sized all-purpose machines, featuring in-chamber electron beam guns moving in the range of 12 m at the maximum speed of 120 m/h with ±0.05 mm positioning accuracy. Such a solution allows maximizing the coefficient of utilization of the vacuum chamber inner volume. The guides, along which the welding gun moves, are fixed

Main technical characteristics of power units

Main parameters	Based on HF generators				Based on transmission tube				
	ELA-60/1.2	ELA-60/6	ELA-120/6	ELA-120/18	ELA-60/15	ELA-60/30	ELA-60/60	ELA-120/60	ELA-120/120
Maximum beam power, kW	1.2	6	6	18	15	30	60	60	120
Accelerating voltage, kV	60	60	120	120	60	60	60	120	120
Weight, kg:									
electron beam gun	55	55	60	60	55	55	55	60	60
gun radiation protection	–	–	130	130	–	–	–	–	130
power source	185	460	735	735	2500	2750	3000	5000	6000
«Rastr» system operating mode:									
before and after welding	+	+	+	+	+	+	+	+	+
in real time	–	–	–	–	+	+	+	+	+
Penetration depth, mm:									
steels	3	12	15	60	50	75	100	130	250
titanium alloys	3.5	15	20	100	80	110	150	220	400
aluminium alloys	5	30	35	140	120	150	200	240	450

Figure 7. SV-112 machine for welding small-sized items (seven such machines are now operating in industry)

Figure 8. UL-178M machine for welding heat exchanger components (I.I. Afrikantov DB, Nizhnij Novgorod, RF)

Figure 9. Cycle machine UL-157 for welding gear modules (AVTOZAZ Plant, Melitopol, Ukraine))

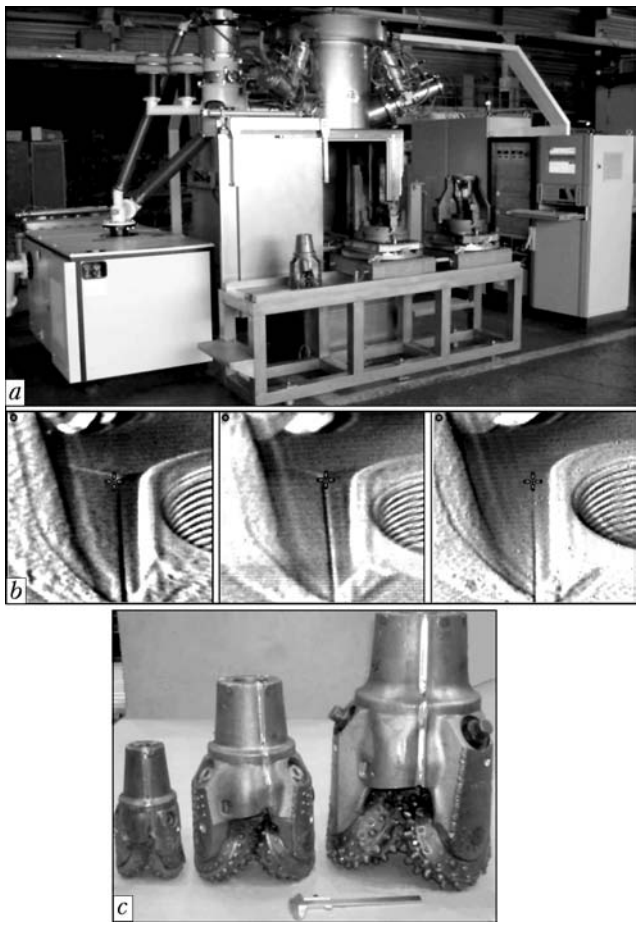

Figure 10. Three-gun machine for welding drill bits (*a*), butt image (*b*) obtained in secondary electrons on the display, and general view of welded drill bits of three type-sizes (*c*) (machines operate at «Volgaburmash» Association, Samara, RF; «Smith Tolls», Ponka City, USA)

directly on the vacuum chamber walls. Therefore, for minimum wall deformations during pumping-down, the chamber is made in the form of two vacuum-tight comparatively thin-walled (thickness of each of them is 8 to 12 mm) shells connected to each other by stiffeners — frame rings [6]. Application of such a box-like structure of the walls and doors instead of the standard tee structure allows increasing the moment of inertia 2 times, and, consequently, reducing the sagging at chamber pumping down. Elimination of external stiffeners allowed improvement of cham-

Figure 11. KL-132 machine with seven-coordinate system of welding displacements for making aerospace products

ber appearance (Figure 11) and preventing dust accumulation on its outer walls, this being particularly important under the shop conditions.

For structures of complex three-dimensional configuration a seven-coordinate system of welding displacements has been implemented: of the gun along three linear and two angular coordinates, and of the item to be welded — along two angular coordinates (rotation and inclination). Commercial system with a developed interface CNC + PLC [7] is used for synchronous control of displacements and parameters of the welding beam.

1. Khavanov, V.A., Bratchuk, S.D., Serioznov, V.A. et al. (2006) Electron beam equipment of NIKIMT. *Svarochn. Proizvodstvo*, **9**, 25–31.
2. Nazarenko, O.K., Kajdalov, A.A., Kovbasenko, S.N. et al. (1987) *Electron beam welding*. Ed. by B.E. Paton. Kiev: Naukova Dumka.
3. Nazarenko, O.K., Lokshin, V.E. (2005) Dynamic characteristics of high-voltage power sources for electron beam welding. *The Paton Welding J.*, **1**, 31–33.
4. Nesterenkov, V.M. (1990) Technology and equipment for electron beam welding of power engineering components. In: *Proc. of Conf. on Power Beam Technology* (Stratford-upon-Avon, UK, Sept. 23–26, 1990). Abington, Cambridge: TWI, 171–179.
5. Nazarenko, O.K., Shapoval, V.I., Loskutov, G.A. et al. (1993) Survey of electron beam welding process and automatic seam tracking. *Avtomatich. Svarka*, **5**, 35–38.
6. Nazarenko, O.K., Nesterenkov, V.M., Neporozhny, Yu.V. (2001) Design and electron beam welding of vacuum chambers. *The Paton Welding J.*, **6**, 40–42.
7. Paton, B.E., Nazarenko, O.K., Nesterenkov, V.M. et al. (2004) Computer control of electron beam welding with multi-coordinate displacements of the gun and workpiece. *Ibid.*, **5**, 2–5.

CYCLE TYPE MACHINE FOR EBW OF GEAR COMPONENTS FOR THE AUTOMOTIVE INDUSTRY MODEL UL-157

An extremely high power density at the focus of the beam, narrow welds and heat-affected zones with little distortion of the toothed gear wheels due to the high welding speed.

PLC of all machine systems.

Visualization of the weld zone by VCU system on the basis of secondary electron emission (×10-magnification).

High stability power source with electron tube flashless system.

Machine design

- 6-component positioning rotary table with pneumatic-lift for up-down moving of the workpiece lower chamber;
- workpiece upper chamber with the rotation mechanism;
- vacuum evacuation system;
- high-voltage source 15 kW, 60 kV;
- control system on Siemens PLC;
- video control unit.

The EB gun can slide transversely relative to the upper work chamber shifting the beam axis to the respective positions when welding seams of different diameters.

The entire working sequence, including evacuating, rotating the workpiece, welding and changing the workpiece is carried out automatically according to a preset program and with a high degree of reproducibility of the set welding parameters.

Contacts: Prof. Nazarenko O.K.
E-mail: nazarenko@technobeam.com.ua
http://www.nas.gov.ua/pwj/beam
http://paton.kiev.ua/eng/inst/ntkstructure/deplist/571.html

AGGLOMERATED FLUXES — NEW PRODUCTS OF OJSC «ZAPOROZHSTEKLOFLYUS»

V.V. GOLOVKO[1], **V.I. GALINICH**[1], **I.A. GONCHAROV**[1], **N.Ya. OSIPOV**[2], **V.I. NETYAGA**[2] and **N.N. OLEJNIK**[2]
[1]E.O. Paton Electric Welding Institute, NASU, Kiev, Ukraine
[2]OJSC «Zaporozhstekloflyus», Zaporozhie, Ukraine

Advantages and disadvantages of application of fused and agglomerated fluxes for arc welding are considered. The features of the new synergetic technology of manufacturing agglomerated fluxes in the city of Zaporozhie are noted.

Keywords: *arc welding, high-strength low-alloyed steels, agglomerated flux, pipe production, technology of flux manufacturing, welded joint properties*

Steels remain the most widely used structural material in fabrication of welded structures, apparatuses and products. However, their range in the local industry has noticeably changed over the recent years. While earlier most of the welds were made on low-carbon steels, and steels of grades 09G2S and 10KhSND (σ_t = = 400–550 MPa) were the most widely spread of the low-alloyed steels, at present a continuous increase of the volumes of consumption of the high-strength low-alloyed (HSLA) steels ($\sigma_t \geq 620$ MPa) is observed. They feature not only increased strength characteristics, but also higher toughness and ductility as a result of lowering of impurity content, microalloying and application of special modes of thermomechanical treatment.

A new generation of steels required new welding consumables. So, for instance during the very first efforts on mastering the technology of welded structure fabrication from HSLA steels it was established that fused fluxes of manganese-silicate type (AN-348A, OSTs-45, AN-60) which have been the most widely applied so far, cannot ensure production of weld metals close in their characteristics to base metal properties. Fluxes of these grades are ousted from production by agglomerated fluxes of aluminate-basic or aluminate-rutile types, as they, as a rule, have higher basicity compared to manganese-silicate fluxes. But, on the other hand, why are not they replaced by fused fluxes of a higher basicity? In order to reply to this question it is necessary to get a more detailed insight into the features of welding using agglomerated fluxes.

Differences in the manufacturing technology determine the advantages and disadvantages of each of the two main kinds of welding fluxes — fused and unfused. Fused fluxes during their manufacture are brought to the melting condition in the open gas or electric arc furnaces with subsequent heat and mechanical treatment of the produced material. Unfused (agglomerated or ceramic fluxes) are not subjected to heat treatment during fabrication at temperatures equal to or exceeding the melting temperature of the charge component mixture.

Fused fluxes feature a high homogeneity of grain composition, increased wear resistance and low moisture sorption capability during transportation, storage and utilization, but have limited capabilities of affecting the metallurgical processes in the arcing zone and in the weld pool.

Compared to fused fluxes, the unfused fluxes are characterized by broader capabilities of influencing the development of metallurgical processes in submerged-arc welding, but have two major drawbacks: increased wear susceptibility and high susceptibility to moisture sorption from the ambient air.

The above drawbacks of unfused fluxes are determined by the fact that joining individual charge components in the flux grains occurs due to adhesion properties of special binders, the mechanical properties and atmospheric moisture sorption capabilities of which differ essentially from the fused products.

In the case of welding using agglomerated flux, oxygen content in the arcing zone, with other conditions being equal, is higher compared to the fused flux, which is due to absence of the process of charge component melting during flux manufacture. In addition, presence of a dry residue in the liquid-glass binder in the agglomerated flux composition, promotes an increase arcing stability and its elongation, which results in a longer time of electrode metal drops staying in the gas phase. Oxygen content in the drop metal can greatly exceed its maximum solubility in iron. Increase of the content of such a surfactant as oxygen in the molten metal promotes a change of the direction of metal flows in the pool from the centrifugal to centripedal, thus changing the weld metal shape [1]. Practical application of agglomerated fluxes showed that in welding with them the depth of base metal penetration is approximately 20 % higher than in the case of using fused fluxes, this allowing reduction of the process heat input. Transition to welding large-diameter pipes in the shop from fused to agglomerated fluxes allowed 25–30 % reduction of weld width and welding wire consumption.

Slag composition of agglomerated fluxes, usually, differs from the eutectic one, characteristic for fused

© V.V. GOLOVKO, V.I. GALINICH, I.A. GONCHAROV, N.Ya. OSIPOV, V.I. NETYAGA and N.N. OLEJNIK, 2008

fluxes, so that they are characterized by a higher melting temperature and higher rate of toughness increase at temperature lowering. The data given in Figure 1 show that by their capability to form a weld, agglomerated fluxes of aluminate-basic type (AB) are close to fused fluxes of manganese-silicate (MS) and aluminate-silicate (AS) types, being on the same level with fused fluxes of fluorite-basic type (FB) as to basicity index.

Flux softening and melting temperatures determine another important characteristic — admissible current load (admissible current density in the welding electrode). This index very directly influences the process efficiency, its effectiveness and ability to use multiarc welding. Arc pressure increases at increase of welding current, so that preservation of a slag cavern around the arcing zone requires the flux to have certain characteristics: bulk weight, temperature dependence of slag melt viscosity and thickness of slag cavern walls. The first of these values is determined by the granulometric composition of the flux and is independent on temperature. The second was considered above, while the third is determined by temperature of softening T_s and melting T_m of the fluxes. Figure 2 shows the experimentally established dependence of the admissible current load on T_s and T_m.

Increased melting temperature of the agglomerated flux promotes its lower consumption for slag crust formation and it is 15–20 % lower than that of fused fluxes. Welding aerosol evolution decreases, accordingly.

Absence of melting processes in the technology of agglomerated flux manufacturing predetermines, primarily, their higher oxygen potential compared to fused fluxes, and, secondly, heterogeneity (presence of the crystalline and glass-like phase) of the slag. It should be noted that while at application of fused fluxes their oxidizing ability is associated predominantly with silica content (fluxes of CS, MS, ZS, RS, AS types), agglomerated fluxes are capable of providing the required level of oxygen potential as a result of adding higher metal oxides, carbonates or other readily dissociating components to their composition. Use of the above ingredients at formation of the agglomerated flux composition provides a good separability of the slag crust from the weld metal surface in welding with fluxes of a higher basicity [3].

At present large-diameter pipe manufacture is the area of the widest application of welding fluxes. In connection with the transition of pipe-welding plants of Ukraine and Russia to production of pipes from HSLA steels the volume of consumption of agglomerated fluxes of aluminate-basic or aluminate-rutile types supplied by foreign welding consumables manufacturers (OP 132, OP 192, OK.10.74, etc.), increased. Manufacturing of welding fluxes in Chelyabinsk, Zaporozhie, Nikopol, Novomoskovsk has more than 50 year history, and, quite naturally, this experience should be used in further improvement of technologies available in these plants. Not surprisingly, it

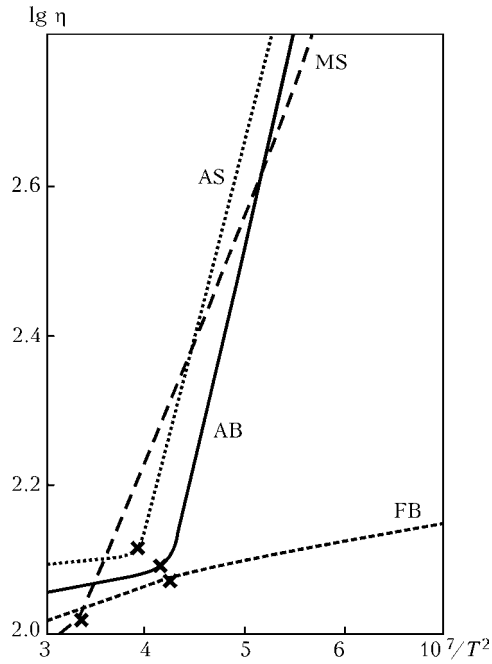

Figure 1. Temperature dependence of flux viscosity

was exactly in the Chelyabinsk pipe rolling mill that Russia's first process line for agglomerated flux manufacturing was installed, its products being oriented, primarily, for their own pipe production needs. Zaporozhie plant of welding fluxes and glassware at some time was established as and still remains to be the largest manufacturer of welding fluxes in Europe. The staff of this plant has long-standing well-established contacts with the users of their products, and conduct continuous monitoring of the market. Zaporozhie plant management took a decision to set up in their own facility a production section on manufacturing high-quality agglomerated fluxes with the capacity of 4 thou t per year.

During discussion with PWI specialists of various technologies of welding flux manufacturing all the advantages and disadvantages of both the open gas and arc processes and sintering were considered in detail. This led to the idea of development of a process, which allows combining the advantages, inherent to the technology of manufacturing fused fluxes with

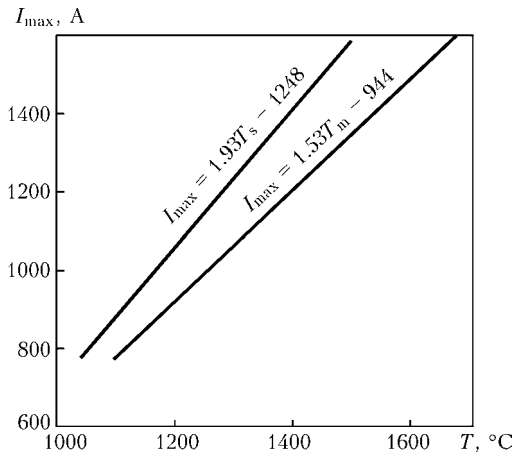

Figure 2. Dependence of the admissible current load on softening and melting temperatures of welding fluxes [2]

Results of evaluation of hygienic characteristics of toxic substance content in welding aersol evolving in welding using flux

Flux grade	Aerosol gross evolutions, mg/min	Fluorides, %		Bifluorides, % (II)	Manganese compounds, % (II)
		Soluble (II)	Insoluble (III)		
ANKS-28	11.8	12.5	2.1	–	4.4
AN-60	13.5	19.0	1.3	11.4	7.6
AN-348A	15.8	17.1	2.5	12.3	11.5

Note. Hazard class is given in the brackets: II — high hazard substances; III — moderately hazardous.

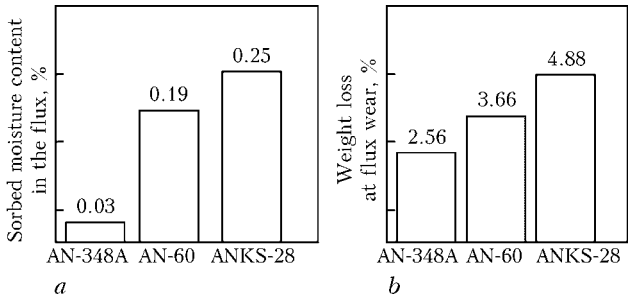

Figure 3. Flux susceptibility to moisture sorption from the environment (*a*) and wear in flux suction systems (*b*)

those characteristic of sintered flux manufacturing (so-called synergetic effect).

It is known that fused fluxes are characterized by a high resistance to grain breaking up during transportation, storage and use, as well as a low susceptibility to atmospheric moisture sorption. On the other hand, welding with sintered fluxes, as a result of their higher metallurgical activity, ensures an increased content of manganese, lower content of silicon in the deposited metal, as well as improvement of welding-technological properties compared to fused fluxes of a comparable composition. Combination of three technologies of flux manufacturing (open gas and arc melting, as well sintering) in one process enabled an essential improvement of the quality of the final product as a result of the synergetic effect of combining the advantages of each of them.

Addition of fused slag particles to the flux composition allowed lowering the granule (grain) susceptibility to mechanical breaking during transportation, storage and application, as well as reducing the flux susceptibility to atmospheric moisture sorption, while the technology of flux sintering at the final stage of their manufacturing allows development of metallurgical processes characteristic for unfused fluxes.

At present the Zaporozhie plant has mastered commercial production of sintered fluxes of ANKS type using the synergetic technology of their manufacturing. The Table and Figures 3–5 give the results of comparison of agglomerated flux ANKS-28 manufactured by the synergetic technology with fused fluxes AN-348A and AN-60.

The Table gives the data obtained during testing made at PWI and Zaporozhie plant together with the Institute of Labour Medicine of the AMS of Ukraine. To determine the susceptibility to moisture sorption from ambient air, flux samples after drying were soaked for seven days in the exiccator with the relative humidity of 78.8 % at the temperature of 20 °C. The susceptibility of flux granules to wear at transportation through the flux suction system was determined by PWI procedure [4]. Deposited metal samples for impact toughness determination were produced by single-arc welding with 4 mm wire of Sv-07G1NMA grade. During these tests relative flux consumption was also measured.

The given data show that by its service characteristics (susceptibility to moisture sorption, wear resistance, relative consumption) agglomerated flux ANKS-28 is close to fused flux AN-60, and by its sanitary-hygienic indices it has marked advantages compared to fused fluxes. ANKS-28 flux provides the deposited metal impact toughness higher than 60 J/cm^2 at testing temperature down to −70 °C.

In view of the above results, as well as the fact that the cost of flux manufacturing by the synergetic technology is lower compared to fluxes which are manufactured using fusion processes, Zaporozhie plant of welding fluxes and glassware together with PWI

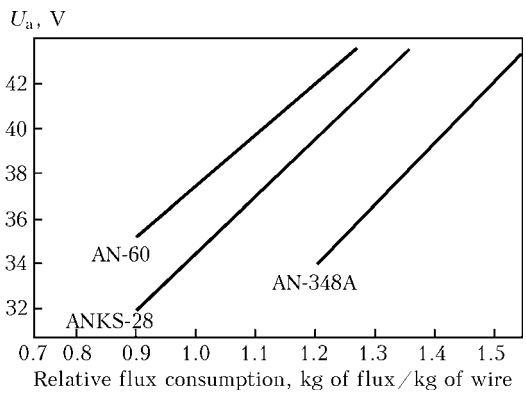

Figure 4. Relative consumption of fluxes in welding with 4 mm diameter

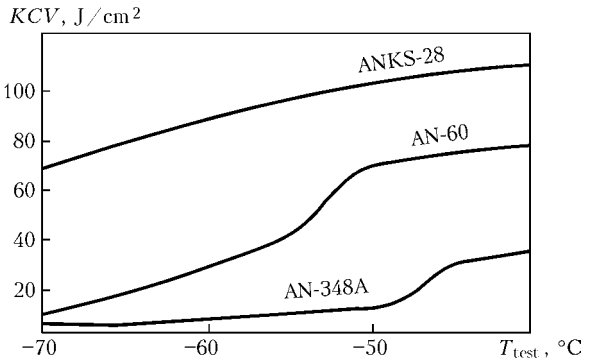

Figure 5. Impact toughness of deposited metal in welding with Sv-07G1NMA wire of 5 mm diameter using different fluxes

are recommending to the users a new generation flux ANKS-28 as a worthy replacement of AN-348A and AN-60 fluxes.

1. Golovko, V.V. (1994) Influence of physico-chemical properties of flux on liquid metal movement in the weld pool. *Avtomatich. Svarka*, **9/10**, 20–23.
2. Davis, M.L., Bailey, N. (1979) Have we the right ideas about fluxes. In: *Proc. of Int. Conf. on Trends in Steel and Consumables for Welding* (London, 14–16 Nov. 1978). Vol. 6. Abington, 231–247.
3. Pokhodnya, I.K., Golovko, V.V., Kushnarev, D.M. (1983) Investigation of detachability of slag crust in welding using ceramic fluxes of aluminate type. In: *Abst. of Pap. of All-Union Conf. on Welding Consumables* (Cherepovets, 10–14 Oct. 1983). Kiev: PWI, 30–31.
4. Kushnarev, D.M., Golovko, V.V. (1984) Method of quantitative evaluation of resistance of flux granules to abrasion. In: *Inform. Documents No. 1 of CMEA on problem «Welding»*. Kiev: PWI, 76–77.

EXPERIENCE AND PROSPECTS OF USING EQUIPMENT FOR WELDING OF RAILS IN PEOPLES REPUBLIC OF CHINA

P. MA[1] and **A.V. BONDARUK**[2]
[1]NTTU «Kiev Polytechnic Institute», Kiev, Ukraine
[2]Company «Elektrostyk», Kiev, Ukraine

Some indices of macroeconomics of China are presented. Plans of development of the country transport system are shown. Main welding technologies used for construction of a railway bed are described. Resistance welding equipment and its main technical-economic characteristics are given. The focus is on innovation technologies for construction of high-speed railroads. Potential demand for new equipment is estimated on basis of rough calculations. Main lines of the technological potential development in the field of equipment for welding of rails are determined.

Keywords: *resistance welding, welding equipment, industry of China, transportation infrastructure, trunk railways, prospects of development*

Economy of Peoples Republic of China (hereinafter China) is one of leading in the world as to indices of macroeconomic development. From 1978 to 2003 annual growth of GNP of the country was about 9.3 % (Figure 1).

Let us consider dynamics of the country's economy development using as an example transportation infrastructure. Length of motorways within this period increased by 36.9 %, while that of the railways just by 1.4 %. According to statistical data, share of the cargo railway haulage constitutes about 25 % of general world volume, whereby length of the trunk railways constitutes just 6 % of the world ones.

For liquidation of the unbalance Ministry of State Construction of China developed Program for construction of new railways for the period from 2006 through 2020. According to this program at the stage of implementation of the XI five-year plan (2006–2010) 18 thou km of new trunk railways have to be built. Capital investments into the construction should constitute 167 billions USD. Within the period from 2011 to 2020 it is planned to build 10 thou km railways more. In addition, in recent years large-scale construction of new subway lines in main megalopolises of the country (Beijing, Shanghai, Guanzhou, Shenzhen) is carried out, investments into which are not part of the Program (http://www.cin.gov.cn).

Let us briefly consider technological process of construction of trunk railways from the viewpoint of volumes of works, connected with welding of rails.

From metallurgical plants rails of 25 m length are supplied to stationary rail-welding enterprises, where they are welded into sections of up to 500 m length and then laid into the track and welded between themselves by the K-922 mobile field complexes. To produce one section of 500 m length it is necessary to perform 20 welding operations, i.e. 1 km of a single-track way needs 80 welding operations. Usually state-of-the-art truck railways have minimum two tracks plus side tracks at stations for ensuring a common schedule for movement of trains of different speed categories. That's why in preliminary calculations of necessary amount of the rails (for a detailed design) length of the truck railway is tripled.

For fulfillment of the whole complex of works, connected with welding and laying of rails in all sections of a railway track, four groups of equipment are used:

• stationary equipment for resistance welding, designed for making rail sections of up to 500 m length at rail-welding enterprises. Available for this purpose

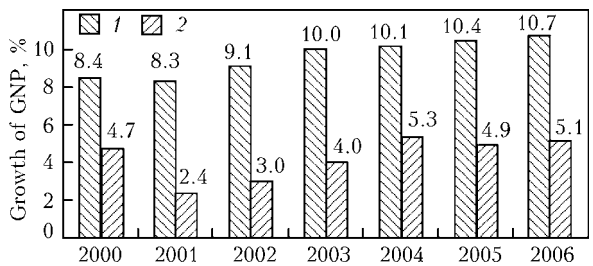

Figure 1. Comparative indices of GNP growth in China (*1*) and in the world (*2*)

© P. MA and A.V. BONDARUK, 2008

Figure 2. K-1000 stationary machine

Figure 4. K-992 mobile machine

stock of the equipment includes four K-190 and three K-100 machines (Figure 2) (developed in the E.O. Paton EWI and manufactured at Kakhovka Plant of Electric Welding Equipment (KZESO), Ukraine), and twenty two GAAS-80 machines (Figure 3) (Schlatter, Switzerland). It should be noted that from 22 Swiss machines 8 have been operating for more than 6 years, all K-190 machines have been working for more than 10 years and need overhaul repair and modification or replacement for new ones;

• mobile equipment for resistance welding, used for connection of railway sections into the tracks. These are mobile rail-welding complexes on basis of the K-922 welding heads (16 pcs) (Figure 4). Welding heads were developed and manufactured in Ukraine (the E.O. Paton EWI and KZESO) and control systems and mobile units — jointly by the USA, Canada, and China. All complexes started to work in 2006–2007. Rail-welding enterprises also have K-920 and more old K-900 machines;

• equipment for gas pressure welding of rails under field conditions. These are, as a rule, outdated machines of Japanese production and their analogues manufactured in China, technical-economic parameters of which can not compete with new machines for resistance butt welding;

• equipment for aluminothermic welding under field conditions (Figure 5). For this purpose a complex of consumable welding materials is used (for each welding operation one package is used). Mainly these are welding materials of the REILTEC company production (Australia, France). This technology is mainly used for connection of rails of the main track with switches at stations and in the places, which are inaccessible for mobile welding machines. Share of aluminothermic welding in general volume of welding operations under China conditions is negligently small.

Big share of new railways being built are planned as high-speed trunk railways (with speed of movement of trains over main track up to 380 km/h), that's why higher than usually requirements are established for quality of welded joints of the rails. These requirements may be met only in case of using the most state-of-the-art welding equipment with computer control of the welding cycle (Figure 6), minimization of the human factor effect, and automated recording of the process parameters and conclusion about quality of each produced welded joint.

According to assessments of the authors, such equipment at present are only state-of-the-art machines of the K-1000 type for welding under stationary plant conditions and complexes on basis of the K-922 and K-920 machines under field conditions.

It should be also noted that machines of the K-922 type (Figure 7) at present have no analogues in the world and are the only equipment that allows performing welding of final butts of rail sections, due to which so called velvet track is produced for high-speed trunk railways, operating under climatic conditions with big difference between summer and winter temperatures.

Figure 3. GAAS-80 stationary machine

Figure 5. Machine for aluminothermic welding

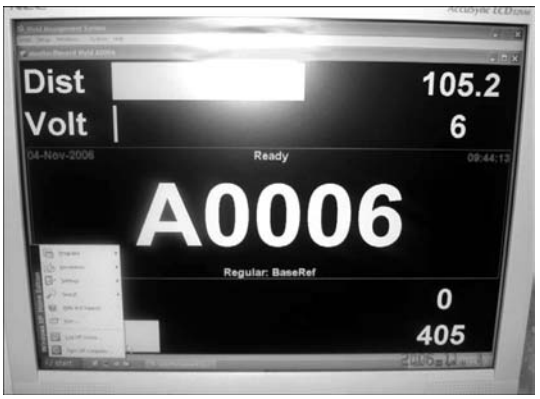

Figure 6. Interface of system for computer control of parameters and assessment of welding quality

Figure 7. Welding of rails using K-922 mobile complex

Let us estimate potential need in new rail-welding equipment for the period up to the year 2020, keeping in mind the following two positions:

- length of new trunk railways being built;
- need to replace worn rails in existing trunk railways. As it is known, average service life of the main track rails is 5 years, after which worn rails are subject to replacement for new ones.

Let us consider volume of welding operations relating to the first mentioned position. Within the period up to 2020 more than 28 thou km new railways will be built in China, for which purpose it will be necessary to lay 84 thou km single tracks, i.e. to produce 6 mln 72 thou welded joints.

As of 2007, general length of acting railways in China equaled 72 thou km, and by 2010 it should increase up to 90 thou km, and by 2020 — up to more than 100 thou km. For simplification of the calculations we assume that general length of serviced ways for the period from 2008 to 2020 (13 years) equals 90 thou km. As it was already noted, after 5 years of operation rails are subject to replacement. That's why in existing trunk railways it will be necessary to replace them 13:5 = 2.6 times.

So, within considered period of time 234 thou km of ways will be subject to replacement, which means 18 mln 720 thou welding operations. Altogether for fulfillment of two positions it will be necessary to produce within 13 years 25 mln 440 thou welded joints or annually 1 mln 957 thou joints. It should be noted once more that construction of new subway lines is not taken into account in the calculations. For convenience of further presentation we round off annual volume of welding works up to 2 mln welding operations.

In general volume of welding operations share of the stationary equipment participation constitutes about 90 % (or 1.8 mln operations for considered case), respectively the rest 10 % (0.2 mln) is the share of the mobile welding complexes. Annual productivity of one stationary machine is about 25 thou welding cycles at two-shift operation, and productivity of the mobile complex is approximately 3 thou welding cycles. Such difference is stipulated by significant time needed for ancillary operations, connected with preparation of the track for welding. So, for timely fulfillment of planned by the Program works 72 stationary machines and 67 mobile complexes will be needed.

According to data of the authors stock of stationary welding machines in China in 2008 numbered 22 GAAS-80 and 3 K-1000 machines (all together 25 pcs). Number of mobile complexes on basis of the K-922 machine is 12. Taking into account presented by the authors calculations, just now it is necessary to add 50 stationary machines and 55 mobile complexes to existing stock.

CONCLUSIONS

1. Experience of application of different technologies of welding of rails in construction of railways in China was considered.

2. Using preliminary technical-economic calculations, forecast of need in new equipment for welding of rails for the period up to 2020 was made.

WELDING OF BUTT JOINTS OF BRIDGE STRUCTURES AND PIPELINES USING FLUX-CORED WIRE AND EQUIPMENT FOR METAL TRANSFER CONTROL

M.V. KARASYOV[1], **D.N. RABOTINSKY**[1], **A.N. ALIMOV**[2], **V.G. GREBENCHUK**[3], **S.V. GOLOVIN**[4] and **R. ROSERT**[5]
[1]NPF «ITS Ltd.», St.-Petersburg, Russia
[2]«ARKSEL Ltd.», Donetsk, Ukraine
[3]OJSC CNIIS NITs «Mosty», Moscow, Russia
[4]«Institute VNIIST Ltd.», Moscow, Russia
[5]Company «Drahtzug Stein», Altleiningen, Germany

Results of development of the technology for butt welding of pipelines under field conditions are presented. Advantages of new types of flux-cored wires with the rutile type core, used with the VD-506DK rectifier, are shown. Recommendations for selection of shielding gas mixtures and welding conditions are given.

Keywords: *arc welding, seamless flux-cored wires, bridge structures, pipelines, welding technology, weld metal, mechanical properties*

In 2005 a group of the ITS enterprises in close cooperation with leading branch institutes of Russia (OJSC TsNIIS NITs «Mosty» and Institute VNIIST Ltd.) and developers and producers of flux-cored wires (the Drahtzug Stein company, Germany, and its Ukrainian partner ARKSEL Ltd.) started investigations and experiments on development of technology for welding of butt joints under field conditions for welding such objects as oil-and-gas complexes, construction of bridges, reservoirs, etc.

Taking into account more stringent requirements to reliability of the whole welding technology under different climatic conditions, seamless flux-cored wires and welding rectifiers of the VDU series, which demonstrated high reliability in welding in ship building and could meet requirements of the normative documentation in the mentioned branches, were selected as the base ones.

After the new welding installations started to be used and quality changes took place in stability of their operation in different modes, which previously were considered unfavorable because of technological reasons, the need appeared to develop welding materials, able to fully implement new possibilities of the equipment in automatic and semiautomatic welding. These possibilities included provision of more stable transition of alloying elements in the weld metal within wide range of welding conditions and respectively production of required structures and properties of the weld metals and control of the weld pool behavior in welding in different spatial positions.

In [1, 2] parameters of the mechanized welding modes in shielding gases using solid section wire with application of traditional welding rectifiers of the VDU-506, VDU-601, VDU-600, etc. types are described. This mainly concerns operation with the Sv-08G2S solid wire of 1.2–1.6 mm diameter in combination with the CO_2 shielding gas or mixture of Ar + 18 % CO_2 gases within the range of arc currents 140–150 A and arc voltage 17–34 V.

Disadvantage of using mentioned welding equipment and the solid wire for mechanized gas-shielded welding is complexity of control by the welder of the metal flow in the weld pool and its formation, especially in spatial positions, increased sputtering within range of currents 180–230 A, and insufficient stability and controllability of the welding arc. In case of using flux-cored wires stability of the process increases, but increase of the voltage is required (as a rule up to 27 V and more), which in combination with traditional welding rectifiers complicates welding of the butt joint root layer, causes overheating of the item being welded, and requires for application of additional technological gadgets (for example, ceramic backings) for formation of required edge penetration. For welding on ceramic backings one has to increase gap between the edges being welded, which causes excessive consumption of the filler metal and reduces productivity of welding. In addition, when welding pipe butts it is preferable to perform welding on one side, and application of backings in this case is problematic.

For work with flux-cored wires a group of the ITS enterprises suggested a new for Russia class of welding rectifiers, which ensure increased stability of the arcing in area of low voltages (14–21 V) and possibility of welding without backing with guaranteed penetration of edges and formation of a back bead of the weld with a favorable shape and smooth transition to the base metal. Difference of these sources from the traditional welding rectifiers consists in the fact that at short circuit of the arc gap or reduction of the acting arc voltage in process of growth of the drop feeding of the additional energy pulse into the arc gap from a separate built-in energy source occurs, whereby stabilization of arc voltage in the rectifier choke–arc welding circuit area takes place. Two kinds of such rectifiers are serially produced: VD-506DK (series 04), in which additional energy is formed at discharge

© M.V. KARASYOV, D.N. RABOTINSKY, A.N. ALIMOV, V.G. GREBENCHUK, S.V. GOLOVIN and R. ROSERT, 2008

of the inductive accumulator, and VDU-511, in which additional energy is formed at discharge of the battery of capacitors.

Application of mentioned rectifiers ensures serious technical and economical advantages before described above welding installations. In comparison with traditional rectifiers these advantages consist in the fact that new rectifiers stably operate within the whole range of arc currents that are needed by a welder for formation of a guaranteed penetration under different technological conditions, i.e. a welder may select conditions of welding proceeding from the conditions necessary for achieving maximum productivity of the process, which are admitted by the welded joint design. In addition, these rectifiers have high rate of response to dynamic processes in the circuit, in which passes welding current, which ensures efficient welding with application of flux-cored wires at currents up to 500 A and possibility of the arc voltage adjustment within wide range. All this makes it possible for a welder to perform welding of both root and filling layers of the weld without risk of the lack of fusion defect occurrence and with guarantee of favorable formation of the back bead in a one-sided welding without backing.

Combination of technological possibilities of the VD-506DK and VDU-511 rectifiers with peculiarities of transfer of the metal and formation of the weld when using flux-cored wires opened new possibilities for development of the technology for welding of butt joints of pipelines and bridge structures under field conditions with free formation.

As it is known, there is a big variety of types of section and technologies of shell formation of the flux-cored wires. For example, seamless flux-cored wires (Drahtzug Stein, FILEUR, Nittetsu), manufactured by rolling and drawing of welded in advance and filled with the powder pipe, have big number of technological conversions, that's why they are more expensive than wires with a non-leak-proof longitudinal seam. At the same time seamless flux-cored wires admit application on their surface of copper or other coatings, which improve electrical contact of the wire surface with a current-conducting tip and ensure low content of diffusively mobile hydrogen in metal of the welds, which is important in welding of special-purpose joints from steels of increased strength.

Technology of production of different types of wires affects specificity of their application. For welding of butt joints of pipelines and bridge structures under field conditions we have chosen a seamless flux-cored wire as the base one with two types of the flux filler — respectively a wire with the metal-powder and the rutile core.

The metal-flux-cored wire has a very small share of flux additives (up to 0.5 %) and does not leave on surface of the weld a flux crust in process of welding. This allows successful using it for welding without backing of a root of the butt joints with guaranteed penetration and excellent formation of back bead, welding the filling layers without slag removal in intervals between runs and minimizing risks of occurrence of slag inclusions in the root and the weld as a whole.

The POWER BRIDGE 50M and POWER BRIDGE 60M metal-flux-cored wires were developed by ITS Ltd (St.-Petersburg), the Drahtzug Stein company (Germany), and OJSC «Mosty» on basis of the MEGAFIL 710M serial metal-flux-cored wire specially for the gas-shielded mechanized welding under climatic conditions of Russia in combination with the VD-506DK and VDU-511 rectifiers. These rectifiers ensured three specific conditions of the electrode metal transfer — «short arc» (the process with forced short circuits), a «medium arc» (a chilled jet), and a «long arc» (jet transfer of the electrode metal) [1–3]. These wires are produced in Germany at the Drahtzug Stein company and differ from the MEGAFIL 710M prototype by additional alloying with titanium and nickel through the metal-powder core, optimization of manganese and silicon content and ratio between them, and limitation of sulfur and phosphorus content down to 0.01 %. During development of new wires peculiarities of transfer of the electrode drops in areas of a short welding arc, «a chilled» jet, and a «long arc» were taken into account [1].

In case of using the VD-506DK rectifiers and metal-flux-cored wire of the POWER BRIDGE type of 1.2 or 1.6 mm diameter, welding within range of currents 250–490 A at voltage 22–28 V is possible. Productivity of the process achieves 8 kg/h due to possibility of the welding current increase without worsening of the welded joint quality. Welding is possible both in a mixture of gases and in pure CO_2. The welding process is stable in all spatial positions, sputtering of the electrode metal is insignificant, and a welder easily controls flow of metal in the weld pool and formation of the weld.

Microalloying is a very important peculiarity of the metal-flux-cored wire. Microalloying in combination with optimum content of such traditional reducing agents in the weld pool as silicon and manganese allows ensuring at cooling of the weld pool presence of many crystallization centers, which disorients growth of dendrites and reduces their size. This causes formation of a favorable fine-grain structure of the weld and improves its operation characteristics, in particular ductility and impact toughness at temperatures up to –60 °C without reduction of strength.

Many elements (titanium, boron, vanadium, etc.) are used for microalloying. During development of the POWER BRIDGE wires titanium in combination with nickel were used for this purpose. Presence of a dozed amount of titanium enables formation of acicular ferrite inside the grain and suppresses precipitation of primary ferrite over the grain boundaries, whereby content of titanium in the weld metal should not exceed 0.05 %. Nuclei for formation of acicular ferrite inside the austenite grain are in this case the dispersed particles of titanium oxide.

In Figure 1 effect of the structure refining at application of the POWER BRIDGE 60M wire is shown.

An important factor for efficient action of the microalloying additions is ensuring of optimum dimen-

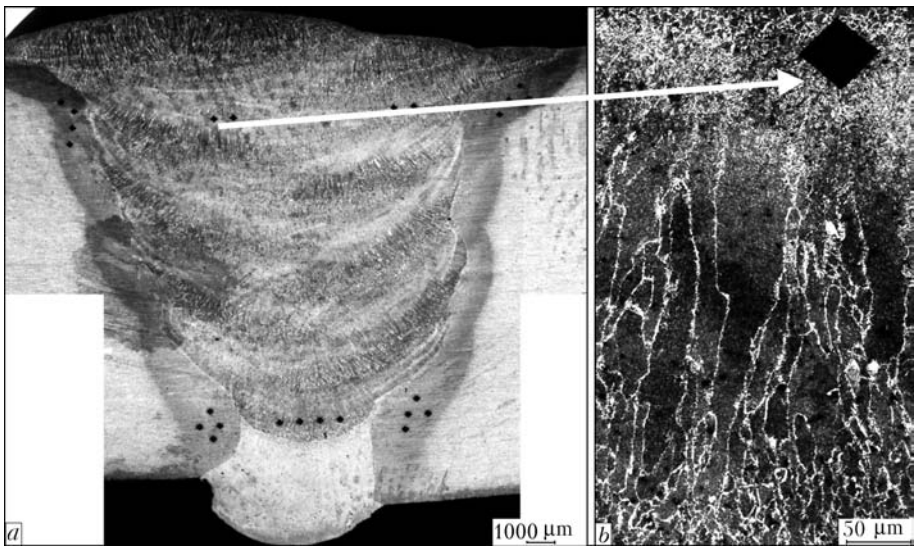

Figure 1. Macro- (*a*) and microsection (*b*) of multilayer welded joint produced using POWER BRIDGE 60M flux-cored wire (suppression of growth of crystallites at initial stage of their growth is observed)

sions of the weld pool by means of correct choice of arc voltage and character of transfer of the electrode metal drops. The VD-506DK and VDU-511 rectifiers in contrast to other power sources allow performing welding within a wide range of conditions with practically invariable size of the electrode metal drops, which ensures constancy of the deposited metal composition and its optimal microalloying. In Table 1 mechanical properties of metal of the welds, produced using the POWER BRIDGE 60M wire with application of different compositions of oxidizing shielding gases are shown. Obtained values of the properties meet requirements of technical documentation for welded bridge structures from the 15KhSND, 15KhSNDA and 10KhSNDA steels.

The POWER BRIDGE 50M wire is used for welding with free formation of vertical welds on reservoirs from the 09G2S steel under conditions of Far North, when it is necessary to ensure high impact toughness at temperatures up to −50 °C.

Application of metal-flux-cored wires is also efficient at orbital welding of position butts of the big thickness pipelines, when increase of impact toughness in root part of the weld is required.

Development of the POWER PIPE 60R and POWER PIPE 90R flux-cored wires of rutile type was carried out specially for gas-shielded automatic orbital welding of position butts of pipelines from pipe steels of the K54–K60 and K65 (X80) type with application of the PROTEUS complex [4]. These wires are also produced in Germany at the Drahtzug Stein company from a leak-proof seamless tube with a flux inside. They differ from the standard product by the fact that they ensure microalloying of the weld with titanium, boron and nickel, changed ratio of manganese and silicon, and limitation of sulfur and phosphorus content up to 0.01 %. During development of these wires compounding of the flux core slag component was corrected to exclude risk of formation of slag inclusions in the short arc and «chilled» jet welding [1].

Application of flux-cored wires with rutile type of the core and a non-leak-proof seam is frequently characterized by complicated formation of the weld at its free spatial formation in vertical and overhead positions.

During development of the POWER PIPE 60R and POWER PIPE 90R flux-cored wires share of the rutile quickly solidifying slag was increased up to the level, which ensured guaranteed favorable formation of a weld without sag and leakage of the weld pool over the whole length of a position butt of the pipe.

In case of using the VD-506DK rectifiers and the POWER PIPE 60R (90R) flux-cored wires of rutile type of 1.2 mm diameter in welding of position butts of pipes the welding current equaled 190–280 A at voltage 22–27 V. Productivity of the process achieved 7 kg/h. After welding of the weld root layer not later than in 10 min a hot run was carried out in direction from top downwards, which was performed with minimum running energy (0.5–0.6 kJ/mm^2) at high linear speed 40–45 cm/min and arc current 190–220 A. Then in direction from below upwards filling and facing runs were made. Depending upon thickness of the pipe walls and requirements to impact toughness of a welded joint, conditions of welding and scheme of arrangement of the beads were selected. When selecting conditions of welding, special attention was paid

Table 1. Mechanical properties of metal of welds produced with application of POWER BRIDGE 60M flux-cored wire

Composition of shielding gas	σ_t, MPa	σ_y, MPa	*KCV*, J/cm^2, at temperature, °C		
			−40	−50	−60
82 % Ar + 18 % CO_2	610–650	510–570	70–90	50–65	35–45
75 % Ar + 25 % CO_2	580–610	470–490	90–110	–	50–70
CO_2	570–600	470–490	90–100	–	50–70

Table 2. Mechanical properties of metal of welds produced using POWER PIPE 60R flux-cored wire

Grade of steel	Composition of shielding gas	σ_t, MPa	σ_y, MPa	δ, %	*KCV*, J/cm^2, at temperature, °C	
					−20	−40
K60, K56	82 % Ar + 18 % CO_2	600–620	490–520	25–27	120–160	90–120
K54	75 % Ar + 25 % CO_2	560–590	480–500	25–27	100–140	80–110
K65	82 % Ar + 18 % CO_2	650–700	570–600	21–22	–	90–110, root ≥ 60

that running energy did not exceed 1.5 kJ/mm^2 (Figure 2, *a*).

In welding of pipe steels of the K54 and K65 types important part plays choice of the mixture of shielding gases in case of application of single POWER PIPE 60R wire for welding of both root and filling layers. Insignificant change of oxidation capacity of the shielding gas may affect operation characteristics of the weld metal. In Table 2 results of mechanical tests of metal of the pipe position butt joints, welded with application of the PROTEUS complex and the POWER PIPE 60R flux-cored wire are presented as an example.

In conclusion it should be noted that development and commercial production of rectifiers of new generation of the VD-506DK and VDU-511 type, which ensure stable operation at different arc voltages and implement all known kinds of the electrode metal drop transfer, allowed passing over to development of new technologies of gas-shielded mechanized welding of multilayer butt welds in construction of bridges and laying of pipelines under field conditions.

New seamless POWER BRIDGE 50M and POWER BRIDGE 60M metal-flux-cored wires were developed for mechanized welding of structural steels of the 10KhSND, 15KhSND and 09G2S types, and flux-cored wire of rutile type POWER PIPE 60R and POWER PIPE 90R for gas-shielded automatic welding of pipe steels in all spatial positions.

Implementation of technological possibilities of new flux-cored wires using the VD-506DK and VDU-511 rectifiers ensures required operation characteristics of welded joints and allows significant increasing productivity of the butt joint welding process under field conditions.

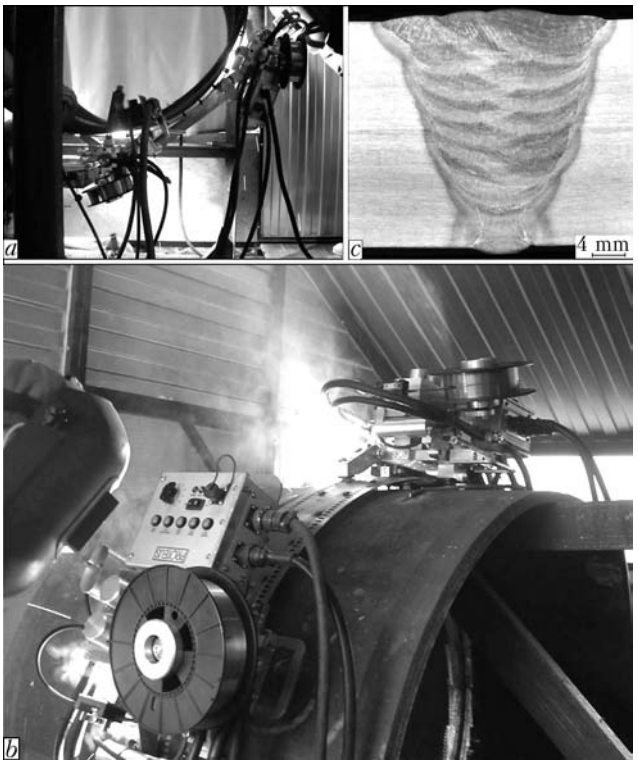

Figure 2. Beginning (*a*) and end (*b*) of automatic welding of position butt of pipelines using PROTEUS complex, and section of pipeline welded joint from K65 steel of 27.7 mm thickness (*c*)

1. Karasyov, M.V., Ladyzhansky, A.P., Golovin, S.V. et al. (2006) Examination of effect of conditions of semiautomatic welding in shielded gas mixtures and of type of electrode metal transfer on chemical composition and mechanical properties of welded joint. *Truboprovod. Transport. Teoriya i Praktika*, **1**, 48–53.
2. Karasyov, M.V., Rabotinsky, D.N., Pavlenko, G.V. et al. (2004) New developments of NPO SELMA-ITS for shielded-gas arc welding. *Avtomatich. Svarka*, **5**, 40–45.
3. Karasyov, M.V., Vyshemirsky, E.M., Bespalov, V.I. et al. (2004) Characteristics of modern units for mechanized GMA welding. *The Paton Welding J.*, **12**, 36–39.
4. Rabotinsky, D.N., Salnikov, M.Yu. (2008) Minimization of costs in performance of welding operations on pipelines. *Territoriya Neftegaz*, **6**, 134–135.

SERIES OF «CHAJKA» MACHINES FOR RESISTANCE BUTT WELDING OF BAND SAWS, WIRES AND RODS

V.G. CHAJKA, B.I. VOLOKHATYUK and **D.V. CHAJKA**
E.O. Paton Electric Welding Institute, NASU, Kiev, Ukraine

Peculiarities of existing technologies of resistance and flash butt welding of band saws, rods and wires are considered. Existing producers of the machines and drawbacks, peculiar of their application, are noted. Advantages of a new series of the «Chajka» machines are described.

Keywords: *resistance welding, flash butt welding, saws, band knives, rods, wires, disadvantages of machines, new series of machines, advantages*

At present the need exists to consider in scientific journals peculiarities of application of machines for resistance butt welding of band saws, wires, and rods. The need is stipulated by the fact that when proposing for sail the equipment, a seller does not present in necessary volume its characteristics, peculiarities, and differences of existing welding technologies. Because of this reason a consumer very often is not satisfied with results of its use. That's why the need exists to clarify these issues.

Butt welding includes heating of ends of the parts and their upset. Two methods of resistance butt welding exist that differ by kinds of heating — resistance and flash welding, which differ both by complexity of design of the welding machines, using which these technologies are implemented, and quality of produced joints [1]. In machines for resistance welding a mobile clamp is usually put in motion by force of a spring, while in machines for flash welding — using a special drive (electric, pneumatic, hydraulic, etc.), which contains the program of change of the speeds at flashing and upset.

In resistance welding parts are preliminarily compressed with an assigned force and then the welding transformer is turned on. Welding current flows through the parts and area of the butt gradually heats up to the temperature, close to melting point. Ends of the parts emolliate and under action of applied force of the spring their upset occurs. The parts are deformed in the butt, a physical contact is formed, and a joint is produced. Welding current is switched off in process of upset. Resistance heating of the parts, especially such as band saws, occurs very irregularly because of occasional arrangement of contacting areas, which is the main problem in resistance welding. It should be noted that uniformity of heating depends also upon design of secondary circuit of the welding machine; when clamps of the bands are arranged asymmetrically in relation to the welding machine axis, it worsens. Irregularity of heating increases by means of increase of width of the bands being welded, and it is impossible to ensure a distributed uniform contact along a butt of the bands of more than 20 mm width. In ends of the bands, installed into clamps of a welding machine, the contact is traditionally formed on one side of the butt. In process of welding the area of initial contact is subjected for a longer time to heat action and heated up to higher temperatures, which causes overheating of metal in this area with all proceeding from this consequences — growth of grains, precipitation of impurities over grain boundaries, etc. Plastic and strength properties of the metal of this zone reduce, and it is impossible to improve them by high-temperature tempering.

Ensuring of uniform heating and respective temperature field is just first condition for a successful welding process. Second condition includes formation of a welded joint in process of plastic strain of heated ends during upset. Decisive influence on process of a welded joint formation in butt welding exert oxide films on end surface of the parts, which hamper interatomic interaction and prevent from formation of strong metal bonds. In resistance welding in process of upset occur just partial destruction and removal of oxides, which determines relatively low ductility of produced joints.

Machines for resistance butt welding are rather widely distributed due to their simplicity and low cost. Their application is justified in those cases, when rigid requirements are not established for welded joints. On the market such machines as IDEAL BSS-016, BSS-025 (Germany), G20-40 GRIGGIO (Italy), SM-60 (China), etc. and their copies SAP-40, G-45 (Ukraine), SAKS-051, USL-50 (Russia) are offered for resistance welding of band saws. These are actually the same machines, which initially were designed for welding of saws having width up to 20 cm. Due to low demand for the machines because of limitation of width of the bands being welded, the suppliers reequip them for using clamps for welding of bands of 40, 50 and even 60 mm (unreasonably from the viewpoint of possibilities of the resistance welding technology and to the detriment of quality of welding).

In flash welding first voltage from a welding transformer is fed on the parts, and then they are pulled together at an assigned speed. As a result between the parts continuously occur and disappear electrical con-

© V.G. CHAJKA, B.I. VOLOKHATYUK and D.V. CHAJKA, 2008

tacts and the ends flash till production on them of a continuous layer of the molten metal. Then speed of pulling the parts together sharply increases, the ends connect, and as a result of upset a welded joint is formed [2]. Current is turned off during upset of the parts. Characteristic for the flashing process are high local densities of current in the contacts and small average density of current (significantly lower than in resistance welding). Mechanism of heating at flashing may be presented in the following way. In process of pulling the parts together between surface areas of the ends electric contacts are formed. Because of high density of currents metal of the contacts quickly heats and is explosively destroyed. Simultaneous and repeated formation and destruction of the contacts occurs over the whole cross section area of the butt, which ensures its uniform heating. In the process of subsequent upset occurs removal from the ends of oxides and formation of metal bonds in the joint zone. Mechanical properties of such joints are significantly higher than in resistance welding, although in this process also exist reserves for its improvement.

Increase of closing rate of the sparkle gap and upset rate will allow producing more fine-grain structure and additional reduction of content of oxides in the weld metal. The rate increases by means of the upset force increase and reduction of the mobile clamp mass. However, it is difficult to increase rate on existing equipment, because high forces of upset cause loss of stability of band ends, and mass of a mobile clamp may not be changed. Especially low is rate of upset in welding of cross-sections, which are minimal for the welding machine (because of small upset forces). In addition, increase of the rate is extremely desirable in welding of difficultly welded steels and alloys. To such steels relate spring and high-speed steels, from which are manufactured bimetal saws and on which, as it is known, it is difficult to obtain stable quality of welding on existing machines.

One of main characteristics of the flashing process is its stability, which is ensured by 3–5-fold reserve of electric power of the machine [3]. At high power even short-term interruption of flashing with transition to resistance heating (short-term short circuit) causes sharp increase of current and overheating of the metal in the joint zone. That's why development of welding machines with lower reserve of electric power, which ensure high and stable quality of joints, is rather actual.

Offered on the market machines for resistance butt and flash welding IDEAL BAS-050, BAS-060, etc. (Germany), FULGOR FW400 (Italy), FL50 (Russia) are made according to a traditional scheme of the same type and mainly differ from each other by power and appearance. Machines of Ukrainian producers G-22 and its copy MS4, having better appearance but worse rigidity of the structure, are heavy, unreliable, and do not meet requirements of today.

Most widely are used machines of the IDEAL company (Germany), because they ensure stable quality of welding. The machines are available on market, because they are serially produced; they may be completed with pyrometers for automatic maintenance of temperature in heat treatment, which is often an argument in favor of their choice, although, in our opinion, this is an erroneous argument because of the following reason. As far as automatic system of heat treatment that includes a pyrometer measures and maintains temperature in a point (approximately in area 1 mm^2), it is necessary that temperature of the metal in heat treatment over width of the band be equal. In practice uniform heating and respectively satisfactory work of automatic system of heat treatment depend upon quality of feeding of electric current, which is preserved just for a limited number of welding operations. That's why the producer recommends to dismantle current-leading jaws from the machine and carry out their grinding on a grinding machine each 10–20 welding operations (depending upon width of the band being welded). By means of increase of the number of welding operations the current lead gets inadmissibly soiled and uniformity of the band heating worsens (irregularity of heating may achieve 120 °C) (Figure 1). In this case the machine will carry out heat treatment of a joint according to the pyrometer measurements for 540 °C, whereby real distribution of temperature in the weld will not correspond to readings of the pyrometer, and this will affect quality of the joint. That's why, in our opinion, manual heat treatment with visual assessment of averaged temperature of the joint is the most rational method. Depending upon non-uniformity of heating, a welder may adjust both temperature and duration of heating. Irregularity of heating should not be too high and it is necessary to grind current leads, but with higher periodicity. According to our observations, in process of training a welder achieves an acceptable skill within the first day of training.

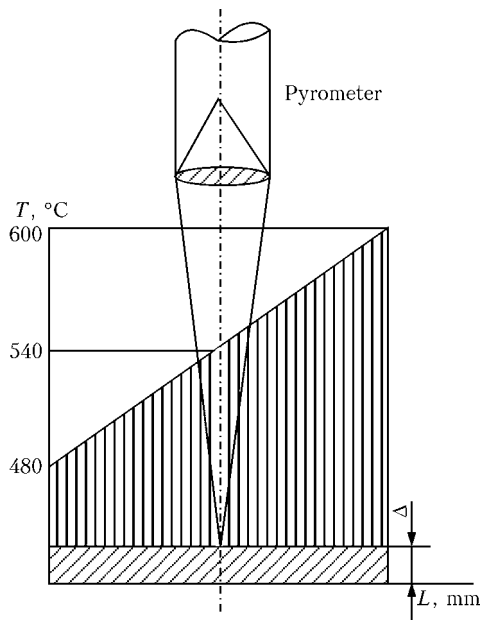

Figure 1. Schemes of distribution of temperatures along weld in heat treatment (L, Δ — width and thickness of blade, mm)

Technical characteristics of «Chajka» machines for resistance flash butt welding*

Machine	Maximum primary current (in welding), A	Width/thickness of welded blades, mm	Diameters of welded wires and rods from low-carbon steels, mm	Number of welding operations (bands) per hour	Welding time, s	Welding voltage, V	Force of upset, N	Mass, kg
MKSSO-40BU	10	$\frac{10-40}{0.6-1.3}$	1.0–8.0	30–40	0.9–2.0	2.8–3.2	200–400	105
MKSSO-60	15	$\frac{20-60}{0.7-1.3}$	1.5–9.0	30–40	1.0–2.0	2.8–3.4	200–700	105
MKSSO-60B	15	$\frac{10-60}{0.6-1.3}$	1.5–9.0	30–40	1.0–2.2	2.8–3.4	200–700	105
MKSSO-80	20	$\frac{30-80}{0.8-1.2}$	3.5–12.0	10–40	1.5–2.5	2.9–3.8	400–1200	125

*All presented machines had primary voltage of main network 380 V, independent water cooling, smooth adjustment of heat treatment, and overall dimensions 280 × 540 × 430 mm.

Figure 2. MKSSO-60B machine for welding of band saws

Existing resistance machines for resistance and flash welding have exhausted their technological possibilities for improvement of welding quality of band saws and have the following disadvantages:

• ensuring of flashing stability by increasing reserve of electric power at interruption of flashing and short-term short circuits causes sharp increase of the welding current and overheating of the metal in the joint zone;

• asymmetric in relation to axis of the welding transformer arrangement of clamps of the parts being welded does not ensure uniform heating of bands in heat treatment (the electromagnetic field of the transformer shifts lines of current);

• big masses of movable clamps stipulated low rates of upset in welding of bands of smaller sections and respectively low quality of welding;

• the flashing process is accompanied by release of big number of the metal particles in the form of sputter and aerosol. That's why in all welding machines bearings of the moving clamp carriage and surfaces of the copper current-carrying jaws are extraordinary vulnerable. To grind current leads it is necessary to dismantle them from the welding machine.

Taking into account all listed shortcomings, a series of machines for flash butt welding were developed and introduced into production [4]. The developed machines have following main peculiarities:

• the flashing drive is of a spring-hydraulic (without a hydroelectric station) type. The upset drive is of a spring type with dynamic adjustment of force directly in the process of upset;

• maximum (envisaged by the design) speed at closing of the spark gap and in process of upset in welding of all sections in all welding modes;

• carriage of the movable clamp has no rubbing parts (has no bearings) and does not require for special servicing in process of the machine operation;

• clamps of bands are opened in such way, that they ensure full access to current-leading jaws for their cleaning after each welding;

• cocking of the force spring, the welding cycle control, and regulation of temperature in heat treatment, i.e. full control of the machine is performed by a single lever (absence of control buttons);

• the transformer is designed, taking into account ensuring of a stable flashing at minimum reserve of power; losses of power from magnetic flows of dissipation are brought to minimum.

Technical characteristics of the «Chajka» machines for flash butt welding are given in the Table, appearance of the MKSSO-60B machine is given in Figure 2. The developed equipment is patented and certified, has high reliability, and ensured stable quality of welded joints of both rods and wires and band saws. It was established in the process of its operation that percentage of refuse in welding of the bimetal saws of the FENES, BAHCO and EBERLE companies in comparison with welding on the BAS-050 machine reduced four times and equaled 0.5 %.

1. Orlov, B.D., Chakalev, A.A., Dmitriev, A.L. (1986) *Technology and equipment for resistance welding*: Manual. Ed. by B.D. Orlov. Moscow: Mashinostroenie.
2. Kuchuk-Yatsenko, S.I., Lebedev, V.K. (1976) *Continuous flash-butt welding*. Kiev: Naukova Dumka.
3. Paton, B.E., Lebedev, V.K. (1969) *Electric equipment for resistance welding. Theory elements.* Moscow: Mashinostroenie.
4. Chajka, V.G. *Machine for flash-butt welding*. Pat. 77255. Publ. 15.02.2006.

NEWS

VERSATILE POWER UNIT — WELDING RECTIFIER VDU-601S

Open Joint Stock Company «Electric Machine Building Factory «SELMA» has mastered production of versatile power unit VDU-601S, which is intended for semi-automatic arc welding devices and devices for manual covered-electrode arc welding (MMA mode).

The rectifier in a set with a semi-automatic device is meant for DC gas-shielded metal electrode wire welding (MIG/MAG mode).

VDU-601S can be used as a welding voltage source for mechanised welding, and can be integrated with automatic welding devices, robots, etc.

Main advantages of the rectifier are as follows:

- 100 % duty cycle;
- smooth regulation of the welding current in the MMA mode, and welding voltage in the MIG/MAG mode;
- versatility provided by the presence of two external characteristics: constant and drooping;
- easy arc ignition and stable arcing;
- remote control of welding parameters from a panel (optional);
- insulation class N;
- quick-release safe current connectors;
- simple maintenance and repair;
- by request of customers, the rectifiers can be supplied with a set of wheels to provide their easy movement.

Specifications

Mains voltage, V	3 × 380
Mains frequency, Hz	50
Rated welding current, A (at duty cycle, %)	630 (100 %) (MMA) 620 (100 %) (MIG/MAG)
Welding current regulation range, A	45–630 (MMA) 60–630 (MIG/MAG)
Welding voltage regulation range, V	22–50 (MMA) 17–52 (MIG/MAG)
Rated working voltage, V	44 (MMA) 51 (MIG/MAG)
Open circuit voltage, V, not more than	80
Power consumption at rated current, kVA, not more than	50
Electrode diameter, mm	2–8 (MMA)
Weight, kg, not more than	260
Dimensions, mm, not more than	895 × 05 × 835

ACTUAL PROBLEMS OF WELDING CONSUMABLE PRODUCTION (ACCORDING TO RESULTS OF BROADENED MEETING OF «ELECTRODE» ASSOCIATION OF CIS COUNTRIES)

Within 3–5 of June 2008 the «Electrode» association of enterprises of CIS countries held jointly with OJSC «Mezhgosmetiz-Mtsensk» in Mtsensk meeting of the association with discussion of actual problems of production of welding materials at CIS enterprises. Managers and chief specialists of state and joint-stock enterprises, known scientists, technologists, designers, and other specialists, working in the area of production and consumption of welding materials, participated in work of the conference. Fifty two participants represented 33 enterprises and organizations.

Below main reports, voiced at the meeting, are briefly presented.

V.P. Kostyuchenko (director-general of OJSC «Mezhgosmetiz-Mtsensk») first noted actuality and usefulness of the meetings, which are periodically organized by the association, and need in collective discussion and development of recommendations for increase of the production efficiency. Then he dwelled upon state of production of welding materials at his enterprise, which will be 10 years in 2009. It produces about 250 t electrodes per month. The nomenclature includes about 100 grades, including electrodes of general designation, high-alloy surfacing ones, those for welding of non-ferrous metals, etc. Since 1999 the enterprise annually has been doubling volumes of production (in 2007 volume of manufactured products amounted to 600 mln roubles). Demand for the products grows and production will increase and its quality improved. Good prospects of the electrode consumption growth exist in power engineering. However, main share of production at present constitutes a welding coppered wire.

In recent two years production of wires of big diameter (Italian lines) was mastered. Wires of 4 and 5 mm diameter consume machine building plants and pipe-welding enterprises. «Mezhgosmetiz» supplies wire to all pipe-welding plants of Russia. This is a prestigious and at the same time responsible task, because it requires for ensuring of the highest quality of the wires. The enterprise pays constant attention to this aspect. Since 2002 production of welding materials was certified according to ISO 9000. NAKS, Ukrseproz, Belarus, River and Marine register certificates are also available. A number of wires have DNW and Lloyd-register certificates.

In 2008 production of the wire with a polished surface (a non-coppered one) was mastered, which earlier was offered for the market by ESAB, whereby rolled wire of Moldavian production is used. It allows producing wires according to state-of-the-art technology (without heat treatment and etching for removal of the scale). It is planned to master in future production of ceramic fluxes for pipe industry and pro-

The Conference participants

duction of flux-cored wires, to buy lines of the Western companies. Parallel with development of the production it is necessary to try to ensure its profitability. For this purpose purchase of new Italian lines was continued in order to double in 2008–2009 production of the coppered wire. New directions in relation to fluxes and flux-cored wires will develop as soon as in 2009, expanding range of our presence on market of welding materials.

I.V. Ignatchenko (executive director of the «Electrode» association, Kiev) noted that at present one of the main directions of the association activity is production of competitive welding materials, corresponding to the WTO requirements. Only in this way it will be possible to protect our market against intrusion of products from foreign countries, whereby the WTO requirements will concern not just welding materials, but also suppliers of the raw material components. Then results of production of welding materials in 2007 were analyzed. Volumes of production of the materials annually increase and their growth depends upon industrial production of steel and rolled stock in Russia and Ukraine, which is proved by the following data.

In 2007 metallurgists of Russia and Ukraine produced 113.9 mln t of steel and 94.49 mln t of rolled stock, from which 72.39 mln t of steel and 59.63 mln t of rolled stock were produced in Russia. Increase in comparison with the year 2006 of steel production constituted 2 and of rolled stock — 2.8 %. Ukraine produced 41.61 mln t of steel and 34.86 mln t of rolled stock. Increase of steel production constituted 1.5 and of rolled stock production — 2.5 %. General volume of production of the coated welding electrodes in CIS countries in 2007 constituted 345 thou t, of which 77.3 % were produced at enterprises of Russian Federation, 17.1 % in Ukraine, and 5.6 % in the rest CIS countries. Last year general volume of the electrode production increased in comparison with 2006 by 6.6 %, including in Russian Federation by 4.3 % and in Ukraine by 10 %. Volume of production of electrodes with rutile-ilmenite coating equaled 203.8 thou t and with basic coating — 119.3 thou t. Production of electrodes of special designation for welding of high-alloy steels and non-ferrous metals constituted 21.73 thou t. In Russian Federation 266.6 thou t of electrodes were produced, including 149.2 thou t with rutile-ilmenite coating, and 20.8 thou t with basic coating. In Ukraine 52.2 thou t of electrodes were produced, including 37.8 thou t of those with rutile-ilmenite coating, 20.6 thou t with basic coating, and 0.845 thou t of special electrodes. Positive trend in increase of production of electrodes of small and medium diameter from 2.0 to 4.0 mm has outlined. Their total production constituted 304.4 thou t, increase in comparison with the year 2009 equaled 9 %. Volume of production of electrodes of 5.0 and 6.0 mm diameter constituted respectively 40.6 and 0.8 thou t. As a result 9.1 % electrodes up to 5.0 mm diameter were produced.

General volume of production of alloyed welding wire of up to 2.0 mm diameter for gas-shielded mechanized welding equaled 53.2 thou t, from which 18.8 thou t of 0.8–1.4 mm diameter wire.

In Russian Federation 39.6 thou t of welding wire were produced, from which 18.8 thou t of 0.8–1.4 mm diameter, and in Ukraine — 13.6 thou t, of which 5.8 thou t of 0.8–1.4 mm diameter.

General volume of the welding wire production increased in comparison with the year 2006 by 14 % — in Russian Federation by 11.3 and in Ukraine by 20 %. Especially should be emphasized positive growth of the welding coppered wire production, which corresponds to the world standards and is supplied in necessary amount on spools and coils with row winding, having mass from 3 to 15 kg. Main suppliers of such wire are member-enterprises of the association: OJSC «Mezhgosmetiz-Mtsensk», Cherepovets, Oryol and Volgograd plants, OJSC «Severstalmetiz» and OJSC «MMK-Metiz». Welding and surfacing flux-cored wires were produced in 2007 in amount 4823.7 t, of which 2299.6 t of welding wire and 2500.2 t of surfacing wire, excluding 1500 t of wire for out-of-furnace treatment. Increase of the flux-cored wire production in Russia in comparison with the year 2006 made up 32 %, while in Ukraine on the opposite, it reduced by 23 %.

Production of welding fluxes in the year 2007 constituted 37.817 thou t, including 8.6 thou t in Russian Federation, 7300 t of which was ceramic flux; in Ukraine 29.154 thou t of welding flux were produced.

General volume of the welding flux production in comparison with the year 2006 reduced by 2.3 %.

Volume of the welding flux production in Russia reduced in comparison with the year 2006 by 1 %, while in Ukraine it increased by 3 %.

In the year 2007 general volume of production of welding materials constituted 440.8 thou t, including 113.7 thou t for mechanized welding. Share of production of welding materials for mechanized welding constituted 26 % of general production.

So, as before main share of welding works in CIS countries is performed using coated electrodes, but despite existing level of mechanized welding situation started to change to the better. At present our countries have sufficient capacities for production of welding materials for both manual and mechanized welding. However, as before available capacities are not loaded because of slow growth of industrial production. Unfortunately, new electrode-producing enterprises continue to be established without considering if there is need in them.

Z.A. Sidlin (technical director of the «Tekhprom» Ltd, Moscow) dwelled upon peculiarities of production and supply of raw materials. Situation with quality, prices, and volumes of supply he considered at regional and international levels. World reserves of raw materials and deposits, which earlier were considered the leading ones, get exhausted. Strategy of producers of raw materials has changed. Earlier main

emphasis was placed on extraction of the target product, while associated materials remained in tailings, refuse dumps, and wastes. Now they started to extract from them associated materials. It is known that the same material of different deposits behaves differently in technology of electrode production and effects quality of the final product. Requirements of the welding material producers to the raw materials are significantly more rigid, while volumes of consumption are sizably lower than in other branches of industry. Today a new discipline appeared in the metallurgical higher educational institutions — raw material base of metallurgical production and its influence on properties of the metal. Nowadays supplies and prices on manganese increased, and secondary produced materials got more expensive. According to confirmed data, reserves of manganese ores in Russia constitute only 2.8 % of world reserves at average content of manganese in the ore about 20 %. In Ukraine 42.6 % of world reserves of manganese ores are concentrated. Content of manganese in Gabon's ore is about 50 % and its reserves constitute about 4.5 % of the world ones. Chinese manganese ore constitutes 2.5 % of confirmed reserves with 50 % content of manganese in the ore.

If one analyses figures of leading countries, where reserves of manganese constitute more than 2.5 %, today in Ukraine main deposits are concentrated. However, they are already exhausted to a significant degree and require for big capital investments, but today only the wish to skim immediately the cream exists. That's why one should not expect that difficulties with ferromanganese, ferromanganese silicon, and metal manganese, which exist today, will be less crucial tomorrow. These are objective reasons. Another issue that price policy of the suppliers is different.

If to speak about raw material dependence of the country upon other suppliers concerning the whole number of materials, Russian plants, for example, significantly depend today not just upon Ukraine, but also upon a number of other countries, including countries of near abroad, which earlier were part of the USSR. Today materials from far abroad are already supplied in really meaningful volumes on market of Russia — from Brasilia and China. This trend will continue, as prices for them approach those existing now in our market.

Another problem consists in the fact that introduction of a new material is not just a time consuming process, but it also required significant energy of people, who deal with their introduction. One should not expect quick introduction, development, and use of new deposits, whereby volumes, which have producers of electrodes (and these volumes against background of application of the same kinds of raw materials let's say in big metallurgy) are insignificant for the supplier, while our requirements as consumers are sufficiently stringent. If we look at demand for fluorite, the volume, which is needed for production of welding materials, equals about 4 thou t per year — this is a scanty figure in comparison with application of fluorite, let's say, in big metallurgy and other fields. Need in ferromanganese equals 5 thou t, rutile and ilmenite — in total about 16 thou t, marble — about 11 thou t. These are very small volumes from the viewpoint of suppliers.

As far as rather stringent requirements are established, one may not hope that the suppliers will reduce the price. That's why the only possibility is to create a competitive environment for suppliers of the materials. Introduction of new materials has to be started at the very ore mines. Let's take, for example fluorite, which was already mentioned. At present a real offer exists for supplies from Tajikistan from Takobsky deposit, former Sredmashevsky deposit, that was frozen about 15 years ago. Today real possibility exists to receive the material from there. But it is necessary, in addition to other operations, to test this material, and it is necessary that the organizations did this. At first stage this material may be more expensive, but it has significantly higher quality in regard to content of harmful impurities and subsequently, taking into account situation with labor force in Tajikistan, it should be, of no doubt, cheaper than the material, used at present.

In Appatity a special sphene site, adjusted for requirements of producers of electrodes, was organized. Experimental installations were developed and manufactured, on which sphene was commercially produced. Within a number of years several thousand tons of electrodes were produced using sphene concentrate, which is a substitute of ilmenite and application of which allowed restraining growth of prices on ilmenite concentrate. However, the price, which was initially fixed, was first advantageous for producers of electrodes, but than one of the electrode plants, competing with other plants, agreed for a higher price in order to get competitive advantage and due to the volumes started to get sphene concentrate at a higher price. This allowed the supplier assuming that the electrode plants really could use this material. Later the price was increased and all consumers refused from this sphene concentrate exactly because of the price, but the sphene concentrate producer did not agree to reduce the price — it was purely a managerial decision. So, the material, into which were applied great efforts, connected with checking, testing, development of experimental electrodes, and marketing, practically is not supplied at present. As far as new materials, such as rutile and ilmenite of Kazakhstan production are concerned, again investments are necessary into the enterprise itself and subsequent expenses in order to check the material and receive agreement of manufacturers of the welding materials. All this requires for investments. Application of such material from Kazakhstan may change situation with rutile on internal market of both Russia and Ukraine, whereby it will affect at the same time suppliers from Volnogorsk, which carefully track possibilities and prices,

at which the supplies are performed at present. And sometimes even a small motion is sufficient in regard to the raw material, cost of which is decisive for cost of the materials and will call respective interest of the consumer to the products. And here prices may play a decisive part.

M.I. Kucherova (head of technical department of CJSC ELZ) dwelled upon new kinds of raw materials, which were tested within recent years at the enterprise — a milled Koelgin marble that has good granulometric composition. The material is supplied in big bags. Transition to milled marble was connected with reconstruction of the enterprise, and it was calculated that it would be more advantageous to pass over to the milled marble than organize anew its processing.

A.V. Zholus (director-general of CJSC «Shelf») touched issues of potash supply on Russian market. In 2005 Pikalevsky alum earth plant stopped its production. At present potash is supplied from China. Unfortunately, its price continuous to grow.

S.A. Doroshenko (chief engineer of the PWI Pilot Plant of Welding Consumables) made offer to protect corporative interest of the enterprises, which enter into the association. For this purpose one has to address on its behalf with recommendatory letters to enterprises-suppliers of the raw materials in order they operatively took into account interests of the enterprises, producing electrodes.

V.A. Zyskin (deputy director-general of OJSC «Dorogobushkotlomash») covered issues of production of ferrotitanium, used in electrode production. In particular, he noted difficulties in ensuring its heterogeneity. At the enterprise technology for production of ferrotitanium using plasma melting at subcritical temperatures was developed. This allowed sharp increase of heterogeneity of the ingots. A workshop, having capacity 100 t of ferrotitanium per month, was built. This ensured stable supply of 9 plants.

A.V. Baranov (deputy director-general of FSUE CR&DI of Structural Materials «Prometej») briefly described activity of the institute and dwelled in greater detail upon issues, connected with application of different kinds of raw materials for production of welding materials. In particular, of interest for the participants was information about new approaches to assessment of fitness of the raw materials, which took into account interaction of the components with liquid glass, especially application of quartz sands, quartzite, and fluorite.

I.N. Vornovitsky (scientist of SPA TsNIITMash) dwelled upon the need to improve methodologies for quality assessment of the coated electrodes. TsNIITMash has been involved in these issues for a number of years and today about 15–18 parameters of quality are offered, divided into three groups.

Many presentations caused brisk discussion of the participants. After exchange of opinions a joint decision was made, which contained practical recommendations for achievement of higher efficiency of work of the enterprises in the field of production of electrodes.

Eng. P.V. Ignatchenko, PWI

DIFFUSION BONDING AND BRAZING OF DISSIMILAR MATERIALS

Technological processes of diffusion bonding in vacuum of ceramics, graphite and also these materials with metals have been developed. Technologies of bonding ceramics on the base of aluminium oxide, silicon nitride, silicon carbide, piezoceramics and others are offered. Technologies of bonding of ceramics and graphite with titanium, copper, steel, refractory and heat-resistant alloys have been developed for multi-component systems with and without use of interlayers. Technological processes and designed equipment guarantee the high quality of the joints.

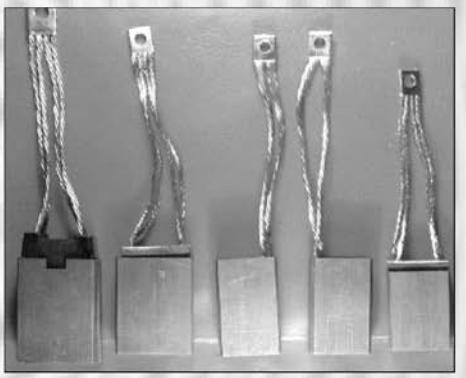

Purpose and application. Technological processes are designed for welding and brazing of products made from ceramics, graphite, including different combinations with metals. They are used in instrument industry, radio electronics, electrophysical equipment, power engineering and others.

Status and level of development. Technology and equipment for welding cermet sectioned tubes of electron accelerators are implemented at NIIEFA (St.-Petersburg, therefore).

Proposals for co-operation. Signing of contract is possible.

Main developers and performers: Prof. Yushchenko K.A., Dr. Nesmikh V.S., Lead. Eng. Kushnaryova T.N.

Contacts: Prof. Yushchenko K.A.
Tel./fax: (38044) 289 2202

61st ANNUAL ASSEMBLY OF INTERNATIONAL INSTITUTE OF WELDING

From 6 to 11 of July 2008 in Graz (Austria) was held 61st Annual Assembly of International Institute of Welding (IIW). Central Institute of Welding Equipment (SZA), Austrian Society of Welders, and Technological University of Graz acted as organizations-organizers. In work of the Assembly participated about 500 delegates from 47 countries. From 51 member-countries of IIW at the Assembly delegations of Argentina, Greece, Indonesia, Israel, Lebanon, Libya and Malaysia were absent. At the same in the assembly participated on rights of observers countries, which filed applications for joining IIW: Lithuania, United Arab Emirates and Turkey. Traditionally the biggest delegations were sent from Japan (77 persons), Germany (56 persons) and USA (36 persons) — the practice, which has been existing within last 15–20 years. Then according to the number of delegates follow Sweden (30), France (25), Slovakia (18), Canada (17), England (16), Finland (16), Australia (13), Italy (13), Holland (10), Korea (10), Russia (10), and Ukraine (10). Delegations of the rest countries consisted of several representatives. From the organizer-country 35 persons participated in the Assembly.

At present in IIW function more than 20 commissions and other structural subunits in the following fields: high- and low-temperature brazing, thermal cutting and processes of gas-flame processing; arc welding and welding consumables; resistance and cold welding, as well as related processes of joining of materials; beam methods of welding; control and quality ensuring of welded structures; terminology; labor protection; behavior of materials in welding; welded structures; failure prevention; pressure vessels, boilers and pipes; arc welding processes and technologies; fatigue strength of welded assemblies and structures; education and training; designing, analysis, and production of welded structures; welding of polymers and adhesion technology; training and certification; introduction and accreditation; permanent joints for new materials and coatings for aircraft construction; automotive transport; environment; quality control in welding and related technologies; standardization; underwater welding; welding physics; strategy of investigations in welding and cooperation. As a whole they rather fully cover fields of welding in all its many-sided nature, including stages of investigation, training, practical application, standardization, cooperation, etc.

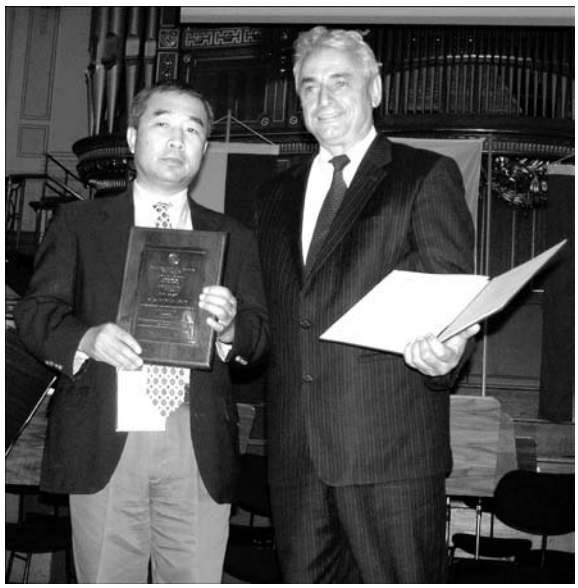

Handing the Evgeny Paton prize

Participation of national delegations in work of the IIW assembly is very useful, because at the forum of this kind exists possibility to familiarize oneself with present situation in different fields of welding, especially in those, in which in one's country works are not carried out because of different reasons, whereby an interesting regularity is observed, which consists in the fact that countries with a developed welding production and science send to the IIW assemblies the most numerous delegations (Japan, Germany, USA). This may be explained by the fact that participation in work of the IIW assemblies allows maintaining and further increasing achieved level of the welding production and science development in one's own country.

During ceremonial opening of the assembly handing of international prizes to a number of scientists for the most prominent works in the field of welding and related technologies took place. These year Dr. Pingsha Dong (USA) was awarded international Evgeny Paton prize. On behalf of IIW and National Committee for Welding of Ukraine the prize was handed by academician of the NAS of Ukraine K.A. Yushchenko.

First three days of work of the 61st IIW Assembly were devoted to meetings of the commissions, working groups, and other subunits. Representatives of Ukraine participated in work of 13 commissions of Council for standardization, Council for international skill and certification of the personnel and welding production, and in work of the research group SG-212.

Main issues, which were discussed at meetings of working groups for education, training and certification, introduction and accreditation, concerned problems of optimization of organizational documents of international system of certification of welding production and international system of certification of the welding production personnel, which are at present being developed by IIW. Similar systems have been functioning within framework of European Welding Federation (EWF) since 1991, but area of their propa-

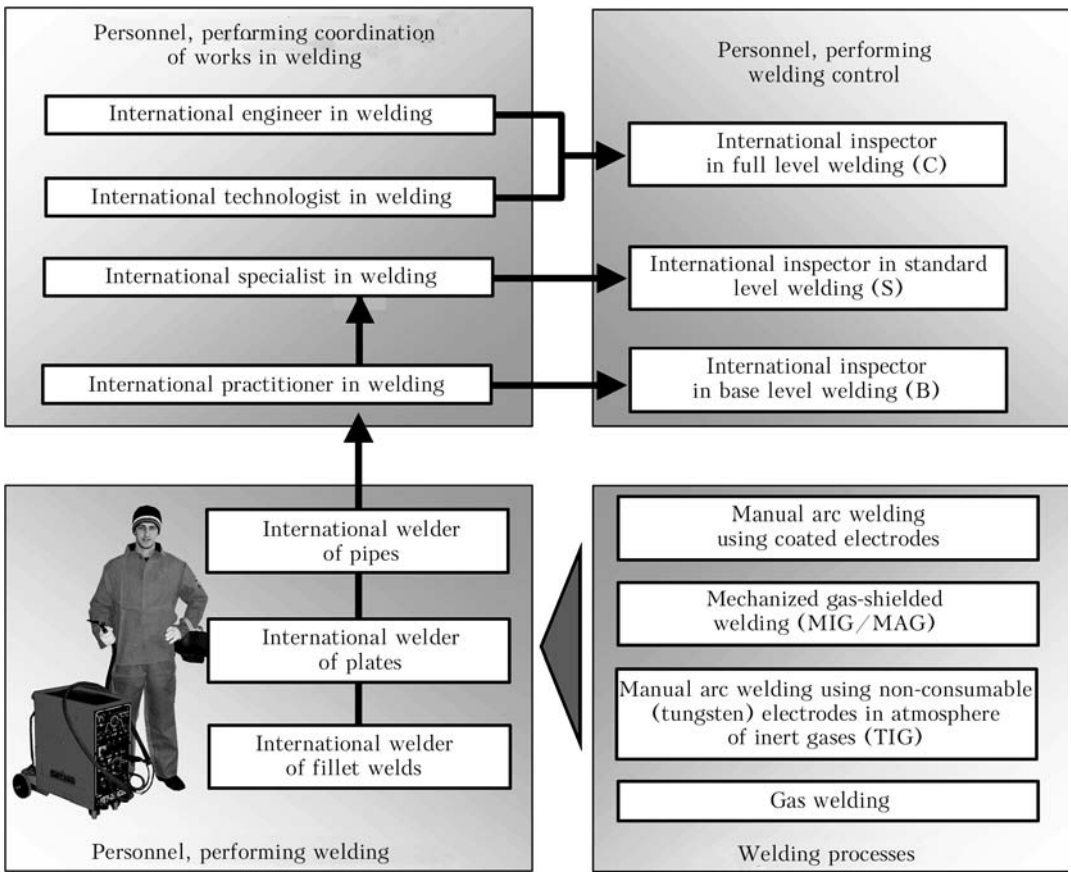

Scheme of international system for training of welding production personnel

gation is, naturally, limited just by Europe. After these systems start functioning establishment of first comprehensive system of training and certification of the welding production personnel and certification of the welding production itself will be over. It is assumed that systems of certification of the personnel and welding production itself under auspices of IIW will start functioning as soon as from the year 2009.

Basic standard of this system will be the ISO 3834 standard, which regulates requirements to the fusion welding quality and is introduced in the form of a harmonized national standard of Ukraine. In particular, it is specially emphasized in this standard that the producer should have respective personnel, which perform supervision over fulfillment of welding and should have sufficient authority and bear full responsibility for ensuring quality of welding.

At meetings of working groups also issues of improvement of efficiency of international system of the welding production personnel training, which is used already in 36 countries, including Ukraine, were considered. This is presented above schematically.

Authorized national body, which is accredited by IIW for carrying out this activity in territory of Ukraine, is Inter-Industry Training-Attestatation Center of the E.O. Paton EWI. The Center received accreditation for training of all presented in the above scheme international specialists of welding production.

In 2008 expired three-year term of stay of Chris Smallbone (Australia) in position of president of IIW. He was replaced by doctor-engineer Ulrich Dilthey (Germany) who occupied prior to this various positions in management of IIW.

During work of 61st Assembly of IIW also annual Assembly of ESF and meeting of its technical committees were held. This is already a common practice in recent years, caused by two reasons. First one is wish to reduce extra financial expenses of national committees for welding, and second, the main, one consists in the fact that after the system of harmonized training of the welding production personnel was transferred under management of IIW and in connection with carried out at present transfer to IIW of the welding production certification system as well area of exclusive activity of ESF significantly reduced (under management of ESF remained practically only 10 programs of the welding production personnel training, which for a time being are not covered by IIW, in particular courses for training of a European specialist in thermal spraying, a European welder of plastics materials, operators of installations for heat treatment of welded joints, etc.

After termination of work of 61st Assembly of IIW the International Conference «Safety and reliability of welded structures in power engineering and processing industry» was held (10–11 of July 2008) at which about 100 reports were presented.

Next in turn 62nd Assembly of IIW will be held on 6–11 July 2009 in Singapore. In 2010 honorable mission of organizer of the IIW assembly will be granted to Ukraine.

Dr. V.E. Ponomarev, PWI

SUBSCRIPTION
FOR «THE PATON WELDING JOURNAL»

If You are interested in making subscription directly via Editorial Board, fill, please, the coupon and send application by fax or e-mail.

The cost of annual subscription via Editorial Board is $324.

Telephones and faxes of Editorial Board of «The Paton Welding Journal»:

Tel.: (38044) 287 6302, 271 2403, 529 2623

Fax: (38044) 528 3484, 528 0486, 529 2623.

«The Paton Welding Journal» can be also subscribed worldwide from catalogues of subscription agency EBSCO.

SUBSCRIPTION COUPON
Address for journal delivery

Term of subscription since _____ **200** **till** _____ **200**
Name, initials _____
Affiliation _____
Position _____
Tel., Fax, E-mail _____

ADVERTISEMENT IN «THE PATON WELDING JOURNAL»
(DISTRIBUTED ALL OVER THE WORLD)

«AVTOMATICHESKAYA SVARKA»
RUSSIAN VERSION OF «THE PATON WELDING JOURNAL»
(DISTRIBUTED IN UKRAINE, RUSSIA AND OTHER CIS COUNTRIES)

External cover, fully-colored:
First page of cover (190×190 mm) – $700
Second page of cover (200×290 mm) – $550
Third page of cover (200×290 mm) – $500
Fourth page of cover (200×290 mm) – $600

Internal cover, fully-colored:
First page of cover (200×290 mm) – $400
Second page of cover (200×290 mm) – $400
Third page of cover (200×290 mm) – $400
Fourth page of cover (200×290 mm) – $400

Internal insert:
Fully-colored (200×290 mm) – $340
Fully-colored (double page A3) (400×290 mm) – $570
Fully-colored (200×145 mm) – $170

- Article in the form of advertising is 50 % of the cost of advertising area
- When the sum of advertising contracts exceeds $1000, a flexible system of discounts is envisaged

Technical requirement for the advertising materials:
- Size of journal after cutting is 200×290 mm
- In advertising layouts, the texts, logotypes and other elements should be located 5 mm from the module edge to prevent the loss of a part of information

All files in format IBM PC:
- Corell Draw, version up to 10.0
- Adobe Photoshop, version up to 7.0
- Quark, version up to 5.0
- Representations in format TIFF, color model CMYK, resolution 300 dpi
- Files should be added with a printed copy (makeups in WORD for are not accepted)